Using Thermal Infrared Spectroscopy to Reveal Feldspars Mineralogy and Chemistry

Asyari Ismail Wardhana

March, 2009

Using Thermal Infrared Spectroscopy to Reveal Feldspars Mineralogy and Chemistry

by

Asyari Ismail Wardhana

Thesis submitted to the International Institute for Geo-information Science and Earth Observation in partial fulfilment of the requirements for the degree of Master of Science in Geo-information Science and Earth Observation, Specialisation: Earth Resource Exploration

Thesis Assessment Board

Prof. Dr. F. D. Van der Meer (Chair)
Dr. Paul Van Dijk (External examiner)
C.A. Hecker, M.Sc (1st Supervisor)
Dr. F. J. A. van Ruitenbeek (2nd Supervisor)

Observer:
Drs. T.M. Loran (Course Director AES)

INTERNATIONAL INSTITUTE FOR GEO-INFORMATION SCIENCE AND EARTH OBSERVATION
ENSCHEDE, THE NETHERLANDS

Disclaimer

This document describes work undertaken as part of a programme of study at the International Institute for Geo-information Science and Earth Observation. All views and opinions expressed therein remain the sole responsibility of the author, and do not necessarily represent those of the institute.

Abstract

Mapping feldspar composition and mineralogy is important in identifying alteration zones. Conventional analysis techniques such as XRD and microprobe could yield the mineral composition and mineral chemistry of feldspars. How ever, these techniques have a limitation; they are very time consuming and require high cost for the analysis. The thermal infrared (TIR or 8-12µm) has great potential for remote mineral mapping.

The main objective of this research is to develop a methodology to determine feldspar composition and mineralogy from thermal infrared spectra, to assist alteration mapping on airborne TIR data. The study was conduct in the Yerington area, Nevada, USA. The area is approximately 250,000 m^2. Yerington area especially Mc Arthur mine site, where post ore-tilting during extreme crustal extension in Late Tertiary rotated the Jurassic porphyry copper deposit. This condition creates the exposure from various alteration zones on the surface of the study area and Tertiary volcanic rocks.

The methods that conducted in this research were divided into two categories in order to answer the specific problems, they are 1. Determining the diagnostic wavelength region in TIR for feldspars identification using USGS spectral library and 2. Rock samples TIR measurement in laboratory. The result shows the important wavelength for feldspar identification occurs in the range of 8- 10 µm. Plagioclase feldspar was influenced by percentage of anorthite. From the USGS spectral library analysis, the feldspar members that are idecntified are albite, oligoclase, andesine, labradorite, bytownite, microcline, sanidine and orthoclase. It was shown in the TIR data, the alkali feldspar group, could be analyzed using band depth absorption calculation. The results showing the decreasing of spectral absorption band depth from Ca rich feldspar to K-rich feldspar in alkali feldspars group. Analysis of field samples reveals classification of mineralogy in the study area. There are three members of feldspar was resulted from 51 samples that were measured in TIR wavelengths. Those feldspar members are albite, andesine and sanidine. The variations of feldspars member were present in the various alteration zones.

Key words: Remote Sensing, Thermal Infrared, Feldspar, Mineralogy

Acknowledgements

Above all, always and forever I want to thank to Allah SWT for being so merciful and as a light in my life,

I would to thank my parents and my family for all the prayer, love and supports especially during my study period in ITC.

I am grateful to C.A. Hecker,M.Sc. as my first supervisor and Dr. F.J.A van Ruitenbeek as my second supervisor for scientific comments, advices, suggestions and kindly guided me for this thesis.

I would like to thank to Drs. Boudewijn de Smeth, as my student advisor who always supports, advising during my study period and assistance during the laboratory work at ITC.

I would like to thanks to Nugroho, Dita and Fuad for last minute helps and always available for helping my work.

My deep appreciation goes to my classmates Kerice, Marco, Ghere, Henry, Yassin, Regina, Atta, Savior, Elahi, Tasfaye, last but ot least Gyanta who always supporting me in knowledge and discussion.

I would to thank my ITC Indonesian fellow Daeng Wawan, Bang Oi, Mas Sigit, Mas Bhe, teh Evy, Ketut, Suhatt , Lely and especially Bang Nas for discussion and suggestion during thesis work.

I would like to express my gratitude to Farah, Adit, Hera and Gery for support and sharing times that helps me passing my tough time. For all Indonesian fellows in Enschede, thank you all for the friendship during this period.

Table of contents

List of figures

List of tables

List of Acronyms

TIR	Thermal Infrared
SWIR	Short Wave Infrared
V-SWIR	Visible Short Wave Infrared
MIR	Mid Infrared

1. Introduction

1.1. Background

The thermal infrared (TIR or 8-12µm) has great potential for remote mineral mapping. Instruments that are sensitive to TIR wavelength can measure known spectral features that are related to the fundamental vibrational frequencies of inter-atomic bonds within common rock-forming minerals. Commonly feldspars do not have characteristic spectral features in SWIR wavelength. However, they do have spectral features in TIR wavelength.

The members of the feldspar mineral group are the most abundant constituents of igneous rocks. The ubiquity of feldspars, together with their wide range in composition, has led inevitably to their use as the primary tool in classification of igneous rocks (Deer et al., 2001). Although the feldspars are susceptible to alteration and weathering, they are useful classifying clastic sediment as well.

The majority of feldspars may be classified chemically as member of the ternary system NaAlSi3O8 (albite, Ab)- KAlSi3O8 (K-feldspar, Or)- CaAl2Si2O8 (anorthite, An). Composition between NaAlSi3O8 and KAlSi3O8 are referred as alkali feldspar and those between NaAlSi3O8 and CaAl2Si2O8 referred as plagioclase feldspar (Deer et al., 2001) (Figure 2-1). However, with the same chemical composition feldspars can have different mineralogy. This condition is caused by the structural state that was formed at different temperature.

(Cudahy et al., submitted) explains the member of feldspar mineral composition is potentially useful as a geobarometer and as an indicator for metasomatism with many styles of gold and base metal deposit, such as porphyry copper, skarn. (Cudahy et al., 2001a) explains as well that mapping albite (Na plagioclase) is important in defining the magmatic alteration and zonation associated with the low grade high tonnage Cu deposits. He also stated Ca-plagioclase maps the alteration associated with invasion of Ca-rich brines from the adjacent sedimentary wall rocks. Hence, it is important to know the feldspars composition and mineralogy. If we are successful to map feldspars in a spatial manner then can be use for alteration mapping and as vector to ore.

Various works that has been conducted for studying feldspars spectral properties in TIR region, alkali and plagioclase feldspars have diagnostic spectral behaviour, especially in the 8 to 11 µm wavelength region there exists changes in the number and position of the reststrahlen features. All feldspars show a diagnostic reflectance high near 8.5 µm and reflectance low between 9.0 µm and 9.3 µm. Sanidine and orthoclase show a single asymmetric peak near 9.5 µm whereas microcline has peak at 9.5 µm and 9.8 µm and albite have peaks at 9.6 and 10.0 µm (Cudahy et al., 2001b) (Figure 2-2).

There has been information from airborne system for geological purposes in TIR wavelength region. Although it was fewer in TIR airborne system information compared than the information that was build in V-SWIR wavelength. However, hyperspectral TIR system such as SEBASS enabled the

measurement of specific silicate minerals, and in some cases their chemical compositions (e.g. garnets and feldspars) (Cudahy et al., 2001b).

1.2. Research Problem

As explained in the background, mapping feldspar composition and mineralogy is important. Several studies have conducted on studying feldspar minerals. One of the most popular methods is conventional analysis techniques (e.g. XRD and microprobe). The result of the conventional analysis techniques could yield the mineral composition and mineral chemistry of feldspars. How ever, these techniques have a limitation; they are very time consuming and require high cost for the analysis

Nowadays, remote sensing data offered many advantages in mineral mapping. It is have a good spatial and temporal resolution. Recently several researchers have been developing new methods by combining conventional analysis with remote sensing data/spectral information. First attempts on combining conventional analysis with spectral work have been done by Cudahy et al. (2001).They used TIR for plagioclase feldspars mineral mapping, including an estimation of their Na-Ca content. How ever, the usage of this new method on studying alkali feldspar has not been done yet in this study area. In this research the work will be extended not just for plagioclase feldspar, it's for the alkali feldspars as well.

1.3. Objectives

The main objective of this research is to develop a methodology to determine feldspar composition and mineralogy from thermal infrared spectra, to assist alteration mapping on airborne TIR data.
The specific objectives of this research are:

- To identify feldspars spectral characteristic in TIR wavelength region with USGS TIR spectral library
- To interpret feldspar mineralogy from the field samples using USGS TIR spectral library in the study area

1.4. Research Question

Questions to be answer by the research are:

- Which wavelengths do diagnostic absorption features in feldspar TIR spectra?
- Can feldspars mineralogy of field samples of Yerington area be determined using TIR spectroscopy?

1.5. Hypothesis

- TIR wavelength region is suitable for studying spectral characteristic in feldspar minerals.
- The interpretation of TIR spectra information from the field samples will lead to information in mineralogy that can be use to classify feldspar in the study area.

1.6. Scope and Limitations

This research was aimed to determine the ability of mineral spectral for mineral mapping. The main objective was to developed new method in mineral mapping. The idea was combining technology of remote sensing with existing alteration map to produce a new enhanced alteration mineral map. Due to time limitation, the main objective was not well achieved. The final result of this research was only until mapping distribution mineral based on alteration map. Therefore, the development of new method on mineral mapping was not achieved. Due to time limitation, the process on calibration and validation on new mineral map has not done yet. This stage supposed to be done after new map was produced. Since the new map base on the new method is not yet finish, this stage was removed.

2. Literature Review

2.1. Feldspars Mineral

This sub chapter is summarized from (Deer et al., 2001)
Approximately 63% of earth crust is formed by framework silicates minerals also known as tectosilicates (mainly 12% quartz and 51% feldspar). This sub group of mineral have a structure wherein all of the 4 oxygen of SiO_4^{4-} tetrahedra are shared with other tetrahedra. The ratio of Si to O is thus 1:2.

The majority of feldspars may be classified chemically as member of the ternary system NaAlSi3O8 (albite, Ab) - KAlSi3O8 (K-feldspar, Or) - CaAl2Si2O8 (anorthite, An). Composition between NaAlSi3O8 and KAlSi3O8 are referred as Alkali feldspar and those between NaAlSi3O8 and CaAl2Si2O8 referred as Plagioclase feldspar (Deer et al., 2001)(Figure 2-1). Alkali feldspar could contain maximum 10% of Ca and Plagioclase feldspar could content maximum of 10 % K.
As the alkali feldspar experienced cooling from high temperature to lower temperature, the crystal structure changes from sanidine, which is monoclinic, through orthoclase, also monoclinic but with different crystal structure then sanidine, to microcline, which is triclinic. This transformation is order-disorder transformation.

Sanidine generally occurs with an equant habit (almost square) and shows perfect $\{001\}$ and $\{010\}$ cleavages, which readily distinguish from quartz. Sanidine rarely shows twinning, however when it does, its usually simple twinning. Orthoclase is common alkali feldspar in granitic rocks an K-Al rich metamorphic rocks. It often shows perfect $\{001\}$ and $\{010\}$ cleavage. Microcline is the lowest temperature form of the alkali feldspar. Upon cooling, orthoclase must rearrange its structure from monoclinic to triclinic. When it is happen, it resulting a twinning. The twinning characteristic of microcline is a combination of albite twinning and pericline twinning. This result in a crosshatched pattern (often called tartan twinning) that is the most distinguishing characteristic of microcline.

At high temperatures, KAlSi3O8 and NaAlSi3O8 form a continuous solid solution series (end-members high sanidine and high albite) with highly disordered (Si, Al) distribution. When the temperature cooled relatively slowly unmixing take place and the gap in solid solution widens with decreasing temperature. Thus the majorities of natural occurring alkali feldspar consists of two phases and are referred to as cryptoperthite, macroperthite or perthite, in order to increasing coarseness of the intergrowth texture.

Plagioclase feldspar is the most common feldspar. It forms initially by crystallization from magma. The plagioclase solid solution series is coupled solid solution where substitution is:

$$Na^{+1}Si^{+4} \Leftrightarrow Ca^{+2}Al^{+3}$$

Thus, the general chemical formula can be written as:

$$Ca_xNa_{1-x}Al_{1+x}Si_{3-x}O_8$$

Where x is between 0 and 1.
Plagioclase compositions are usually expressed in terms of the two end-members albite and anorthite, Ab_x An_{100-x}. The series is divided arbitrary into albite, oligoclase, andesine, labradorite, bytownite and anorthite at An mole percentages of 0-10, 10-30, 30-50, 50-70, 70-90 and 90-100, respectively.

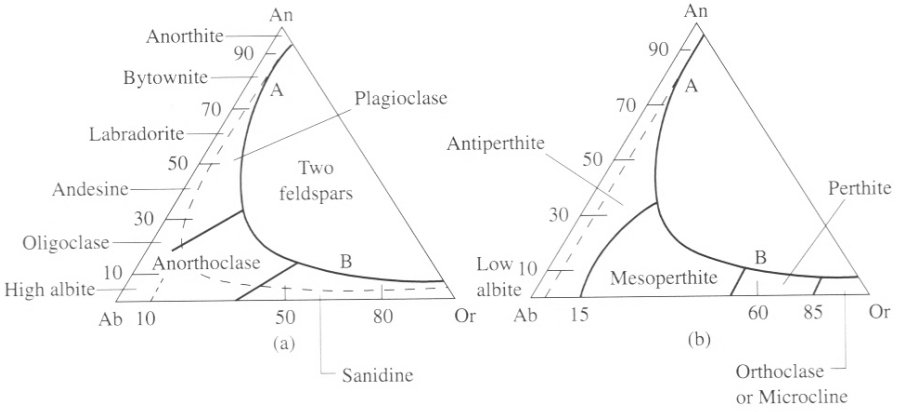

Figure 2-1 Feldspar nomenclature for (a) disordered ternary feldspar; (b) ordered ternary feldspars in which phase separation is at or below the resolution of microscope. Composition in mole%. Cuve A-B, limit of ternary solid solution. (Source: (Deer et al., 2001))

(Deer et al., 1966)discuss about distinguishing features of plagioclase and alkali feldspar. Alkali feldspar can be distinguished from the plagioclase feldspar members by the absence (except microcline) of lamellar twinning, by the lower specific gravity and the presence of cryptoperthitic or perthitic textures: from quartz by twinning, lower refractive indicies and biaxial characther.

Orthoclase can be distinguished from sanidine by its higher optic axial angle and the presence of microperthitic texture, and from high sanidine by orientation of the high optic axial plane. Orthoclase is distinguished from microcline by the straight extinction in the zones [010] and the absence of multiple twinning.

Their low relief, lack of colour, low birefringence, and the biaxial character of their interference figure may distinguish for plagioclase feldspar. The albite twinning giving rise to lamella of different birefringence Si characteristic; in its absence, or in a section approaching the pararellism to (010). The presence of good cleavage may distinguish plagioclase from the potassium feldspars.

2.2. Infrared Spectroscopy of Feldspars

The silicates group such as feldspars has difficulty to be analyzed in SWIR region; however, their typical features are seen in the TIR region. These spectra will be the guidance for distinguishing different group or member of feldspar.

Various works has been done for measuring the TIR spectral properties of Feldspar minerals. Alkali and plagioclase feldspars have diagnostic spectral behaviour, especially in the 8 to 11 µm wavelength region where there exist changes in the number and position of reststrahlen features (Figure 2-2).

These are related to fundamentals stretches and bends of the feldspar Si-O bonds that influenced by the feldspar crystal structure and its cation chemistry (Na, Ca, K) (Cudahy et al., 2001b).

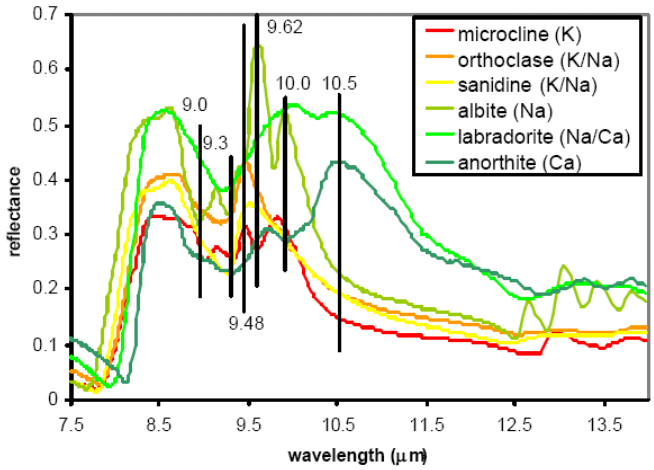

Figure 2-2 Directional hemispherical reflectance spectra of selected feldspar mineral, source:(Cudahy et al., 2001b)

All feldspars show a diagnostic reflectance high near 8.5 μm and reflectance low between 9.0 μm and 9.3 μm. Sanidine and orthoclase show a single asymmetric peak near 9.5 μm whereas microcline has peak at 9.5 μm and 9.8 μm and albite has peaks at 9.6 and 10.0 μm.

In the paper of (Nash and Salisbury, 1991)they analyzed the changes in the plagioclase feldspar due to the changes in the percentages of anorthite using the powdered crystallized plagioclase feldspar. They make a distinction between albite rich and anorthite-rich plagioclase feldspars (Figure2-3). The results also influenced by the many overtoned and combination tones of the internal molecular vibrations (stretching and bending of the Si-O and Al-O bonds).

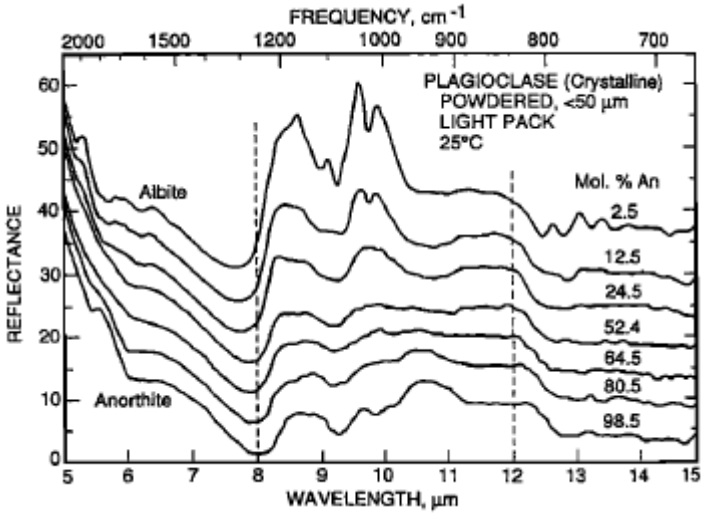

Figure 2-3 Plagioclase group spectra (source:(Nash and Salisbury, 1991))

(Smith and Brown, 1988) explain about the influence of order and disorder Al-Si bond in to spectral characteristic in feldspar mineral. By observing the alkali feldspar groups with the transmission spectra, it resulting the influence of order and disorder feldspar was appear on a broadening peaks in strong disorder feldspar spectrum (Figure 2-4).

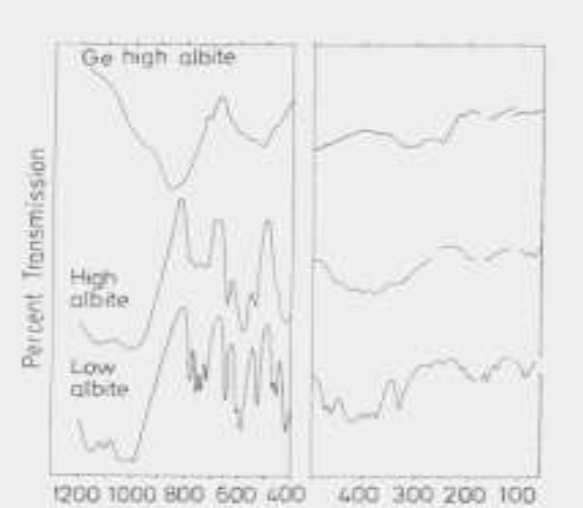

Figure 2-4 Transmission spectra of albite mineral (source: (Smith and Brown, 1988))

2.3. USGS Spectral Library

This spectral library are used in this research were downloaded from the world wide web of USGS (http://speclab.cr.usgs.gov) (Clark et al., 2007). The spectral library that is use in this research is the USGS spectral library 2006. This spectral library contains more than 1300 spectra including the spectra from the year 2005. This spectral library provide the spectral information from various materials, such as minerals, plants, rocks, soils, artificial mixture and also for man made materials. The USGS also provide the spectral information from the UV - MIR (0.2 – 150 microns). In this research is only using the mineral spectral library, especially in the TIR wavelength region (7- 16 microns). Based on the information from the USGS spectral library website, all the spectral data for mineral groups obtained from pure minerals. The spectral library data in the TIR wavelength was measure using Nicolet Fourier Transform Infra-Red (FTIR) Interferometer Spectrometer. The spectral data that measured was covering the range from about 1.3 to 150 µm.

2.4. FTIR

Fourier-Transform Infrared Spectrometer (FTIR) is based on the idea of the interference of radiation between two beams to yield an *interferogram*. The latter is a signal produced as a function of changes pathlength between the two beams. The two domains of distance and frequency are interconvertible by the mathematical method of *Fourier-Transformation* (Stuart, 2004).

3. The Study Area

3.1. General

The study area is located in the Yerington area, Nevada, USA (Figure 3-1). It is confined by latitude of 38° 18’ 26” N to 39° 9’ 61”N and a longitude of 119° 76’ 75”W to 119° 59’ 44” W. it has an area of approximately 250,000 m^2.

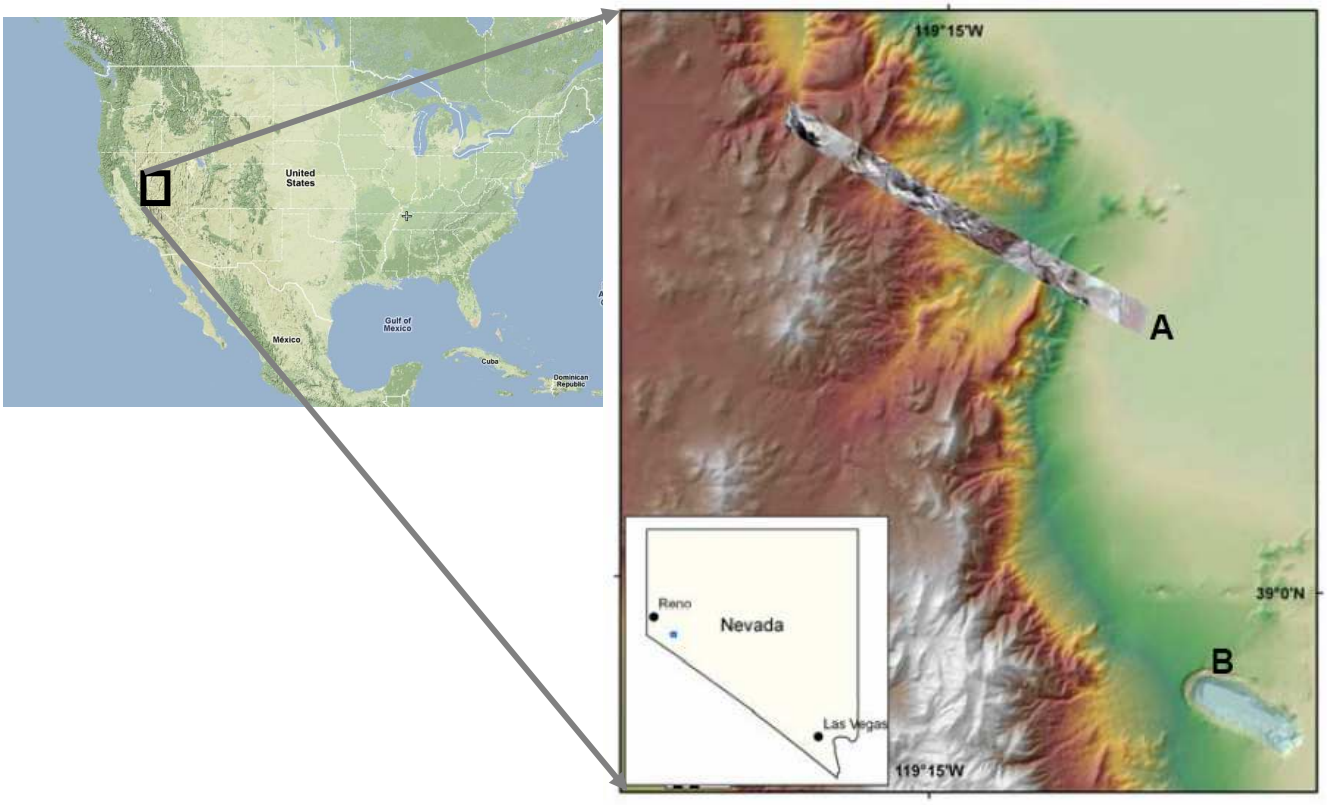

Figure 3-1 Study area modified from (Hecker, 2006)
A) McArthur SEBASS strip with McArthur open-pit mine and study area;
B) Yerington open-pit mine

3.2. Geology and Alteration Zones

The study site was selected based according to the extent of the SEBASS TIR data scene and the spatial distribution of rock samples (Figure 3-4). The information about this sub chapter for the study area was summarized from (Dilles et al., 2001) and (Enaudi, 1994):

Based on(Pirajno, 1992) There are three general type of Porphyry copper deposit type. The types are namely plutons types, Classic types and volcanic types. For plutonic types occur in batholithic setting, with mineralization principally occurring in one or more phases of plutonic host rock. The “classic” types occur with high-level post orogenic stocks that intrude unrelated host rocks. In this types,

mineralization may occur entirely within the stock , within the country rock or occur in both. The last types or volcanics types, presence in roots of volcanoes and with mineralization in volcanic rocks and in associated co-magmatic plutons. Related to the study area the types may be combining between plutonic types and volcanic types. The schematic are presented in the Figure 3.3.

In this study area, there exist several deposits, such as porphyry copper (molybdenum), Copper skarn, Fe oxide, and copper sulphide ores in metasediments rocks, and shallow batholith-hosted Cu-Au-Fe oxides lodes. In cumulative, the geologic resources and the production of Yerington district includes 6 Mt Cu in sulphides ores and more than 100 Mt of Fe in oxides ore. All these production are directly associated with the Jurassic Yerington batholith, which serves as either host rock or as a source rock for heat and material that produced contact metasomatism in the aureole to the batholith.

The Yerington district is located in the western edge of the present day Basin and Range province in the former site of a subduction-related magmatic arc that developed along the western margin of North America in Jurassic period. Mesozoic crystalline rocks, Cenozoic volcanic rocks, and Quartenarry alluvial deposits are present in the Yerington district. The late Triassic or older intermediate and silicic volcanic rocks intruded by middle to late Triassic age plutons, these are the sequence of the oldest rock in this area.

The Artesia Lake Volcanics are thought to represent the early, extrusive part of magmatic system that developed into the Yerington batholith. Thus, the Yerington batholith is emplaced into the base of the Artesia Lake Volcanics. The batholith consists of three major equigranular intrusions, each progressively smaller in volume, more deeply emplaced, and more silicic in composition. The batholith was emplaced and crystallized in about 1 million years a go. based on the U/Pb zircon ages of 169.4 Ma for early McLeod hill quartz monzodiorite and 168.5 Ma for a late, mineralized granite porphyry dike. A series of sub areal intermediate- to silicic- composition lavas, domes, ignimbrites, and volcaniclastic sedimentary rocks that form the Fulstone Spring Volcanics were deposited following the emplacement of the Yerington batholith.

Following a long period of erosion or nondeposition, a series of Oligocene and early Miocene ignimbrites and some lava flows covered the Yerington district (0.5-2 km thick). These rocks are overlain by middle Miocene-age andesitic lavas. During andesitic magmatism, rapid extension via closely spaced, east-dipping normal faults began and terminated about a million years later. These oldest rocks are cut and offset by two sets of east-dipping normal faults, the younger of which include the two active fault system bounding the modern basins and ranges in the area. As a consequence of the down-to-the east normal faulting, the pre-Miocene rocks, including the mineralized Mesozoic rocks, were tilted approximately 60 to 90 W.

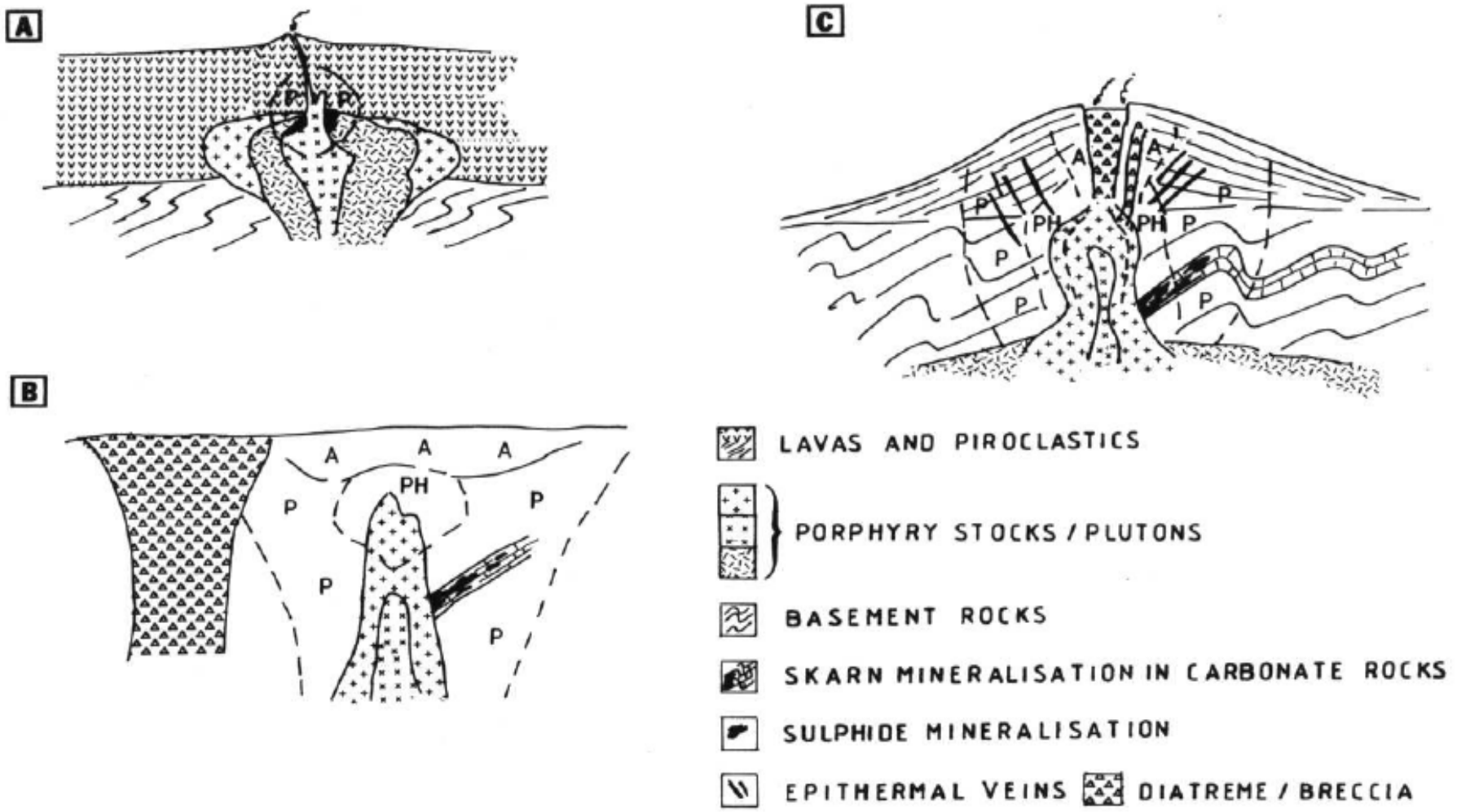

Figure 3-2 Schematic models of types of porphyry copper deposits: (a) plutonic type; (b) “classic type”; and (c) volcanic type. (From Pirajno, 1992). A = argillic; P = potassic; PH = phyllic

Based on the alteration zones map, we can see the alteration zones variation in this area (Figure 3-3). The variations of alteration zones are Potassic, sodic-calcic, prophylitic and sericitic. This variation also occurs on feldspar mineral changes. Most of the copper was deposited in potassic alteration, consisting of plogophite (magnetite-rutile) form after hornblende and rutile, potassium feldspar was form after plagioclase and very rich quartz-sulfide veinlets.

Sodic-calcic alteration occurred at depth and laterally along the margins of granite cupolas, however the sodic-calcic alteration overlapped upward and centrally with potassic alteration. Sodic-calcic assemblages are characterized by actinolite after hornblende and biotite, oligoclase after K- feldspar, abundant sphene, local epidote, local tourmaline, and absence of biotite, magnetite and sulfides. Veinlets contain oligoclase-quartz-(actinolite) locally with patchy chalcopyrite-pyrite where superimposed on potassic ore. The most intense sodic-calcic alteration yielded an oligoclase-quartz-sphene rock with halos of oligoclase-quartz- sphene-actinolite-(epidote). Weak sodic-calcic was transitional to propylitic alteration assemblages. Sodic alteration was superimposed on all porphyry dikes and on potassic and propylitic zones.

Propylitic alteration is characterize by addition of actinolite, epidote, chlorite, minor calcite, hematite, sulfide and magnetite in mafic mineral sites and by weak alteration of plagioclase to epidote, fine grain white micas and clays and minority of K- feldspar. Veins are dominated by epidote along fractures similar to deeper sodic-calcic assemblages.

The Youngest sericitic alteration consisting of cericite-quartz with 2 to 10% volume, pyrite formed as well defined halos on though-going pyritic fractures and pebble breccias with steep Jurassic dips. Sericite-quartz-pyrite related to the porphyry copper coalesces into a regional zone of pervasive sericite. This zone shows no indication of the remaining feldspar mineral.

Table 3-1. Cross table of alteration zones and mineral changes in study area simplified from (Enaudi, 1994).

Alteration Zones	**Important Mineral changes**
Potassic	• Hornblende and biotite→ Plogophyte • **Plagioclase→ K-feldspar**
sodic-calcic	• Hornblende & biotite → Actinolite • **K-Feldspar → oligoclase**
Propylitic	• **Oligoclase, K-Feldspar**, Hornblende, biotite, Magnetite and sphene are remain • New mineral occur are actinolite, biotite, **albite**, epidote, Hematite, sericite , rutile, Pyrite, Tourmaline (chalcopyrite).
Sericite	• Chalcopyrite is remain • Sericitic and quartz • **No feldspar**

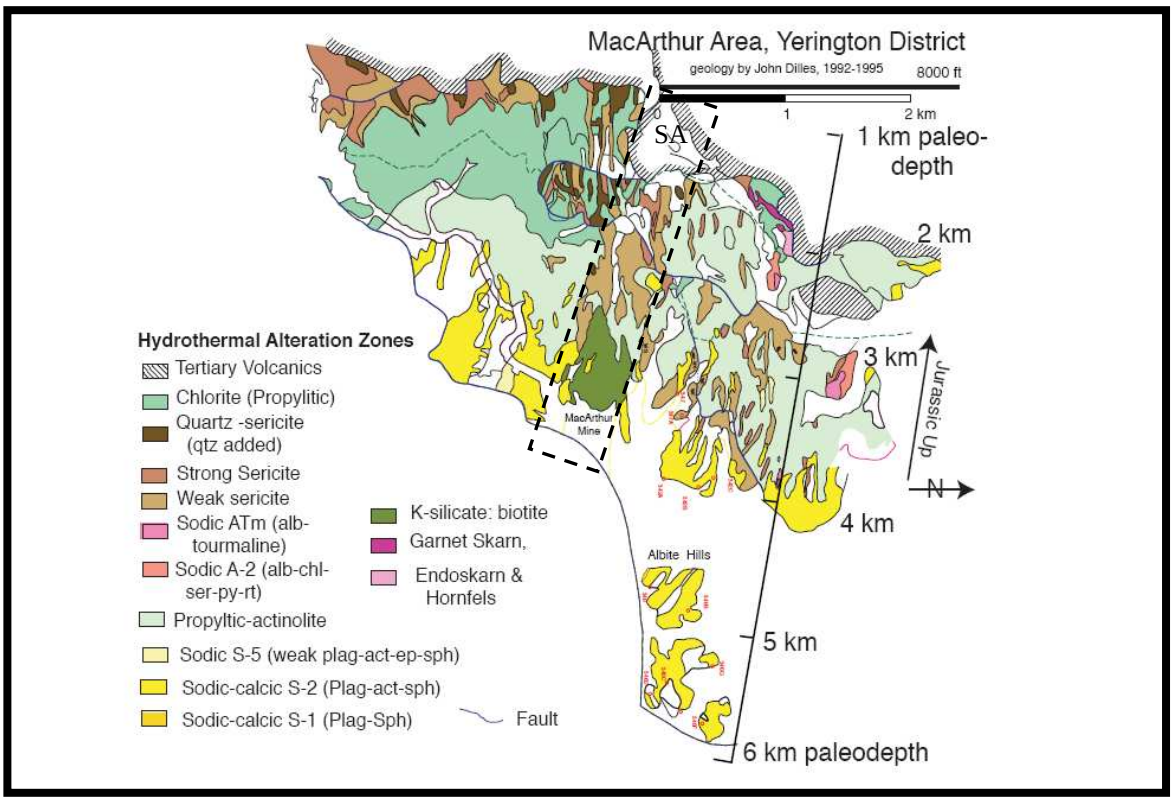

Figure 3-3 Hydrothermal alteration zones by John Dilles (1995)

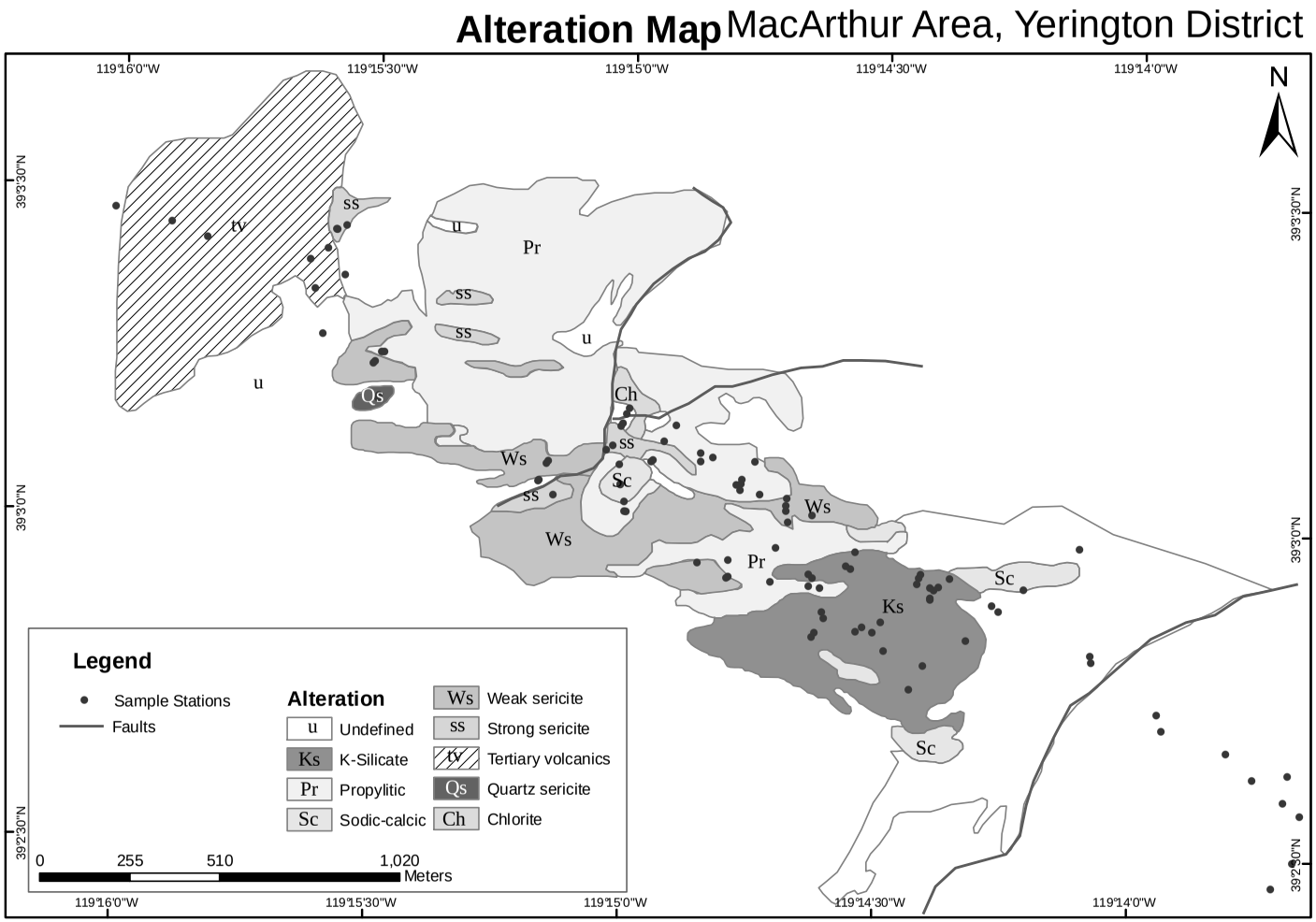

Figure 3-4 Rock sampling points covering the alteration maps that modified from Dilles, 1995 (Zoomed from Fig.3-3, SA)

4. Methodology

4.1. Introduction

The methods conducted in this research were divided into four categories or stages in order to adress the specific problems. Each stage is summarized by means of a flowchart starting from determining the important wavelengths region in TIR for feldspars-classification until the analysis of results (Figure 4-1).

The first stage is to determinate the TIR wv regions which are most suitable for feldspars identification. In this stage, TIR spectra for feldspars were studied and related to the mineralogy, changes in the chemical composition and the influence of the crystal lattice. The analysis was using the existing data from USGS spectral library collection.

The next stage was conducted in the ITC spectrometer laboratory. In this stage the available altered rocks samples were measured to obtain TIR reflectance using Bruker FTIR spectrometer. The measured samples were analyzed by visualizing the rock samples spectra in ENVI software with the reference from the USGS mineral TIR spectral library. The aim of this method is to interpret the altered rocks TIR spectra from the study area, especially in the feldspar minerals. The last stage is to validate rock samples TIR measurement with the existing data such as alterations zones maps and field samples point maps.

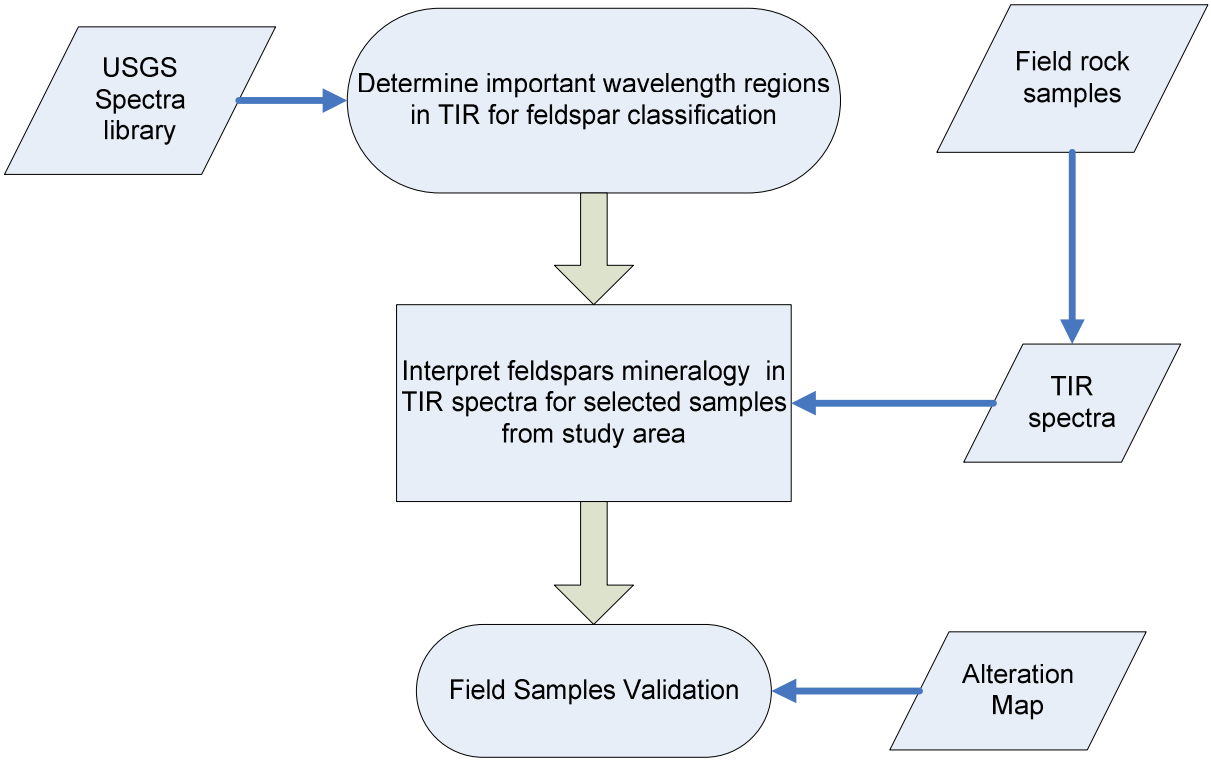

Figure 4-1 Methodology flowchart

4.2. Materials

The following materials were used for this research:

4.2.1. Data

The data available for this research are:

- 51 Rock samples from study area
- TIR rock spectra obtained from FT-IR spectra measurement
- USGS TIR mineral Spectral library
- Alteration map 1: 550 from previous researcher
- Hyperspectral SEBASS imagery

4.2.2. Software

Applications for image processing, mapping, interpretations, and data integrating to get expected output are ENVI were used. In addition office software (Microsoft words, excel, visio, etc.) were used for reporting.

4.2.3. Instruments

The Bruker Vertex 70 FTIR spectrometer was used in this research for measuring the field samples spectra (TIR).

4.3. Field Samples Preparation

There are 51 rock samples from the Yerington study area. The samples were taken in the area covered by the SEBASS strip. Even though, the SEBASS data was not used in this The main purpose from collected samples was to collect representative samples of feldspars mineral, in order to do laboratory spectra measurement as well as mineralogical description.

Before conducting the spectral measurement, all rock samples were photographed in order to mark the position for their measuring. The set of samples were put into sample bags. Several samples bags were containing different rocks. For not making confusion in differentiate the rock samples in the same sample bags. It was re-label it with sample code+number, in example 06 CH 012 and 06 CH 012-1. Several samples were measured several times, first at the certain side and afterwards at the opposite side considering the rock physical appearance (figure 4-2). Photographs of the samples are shown in the appendices of this report.

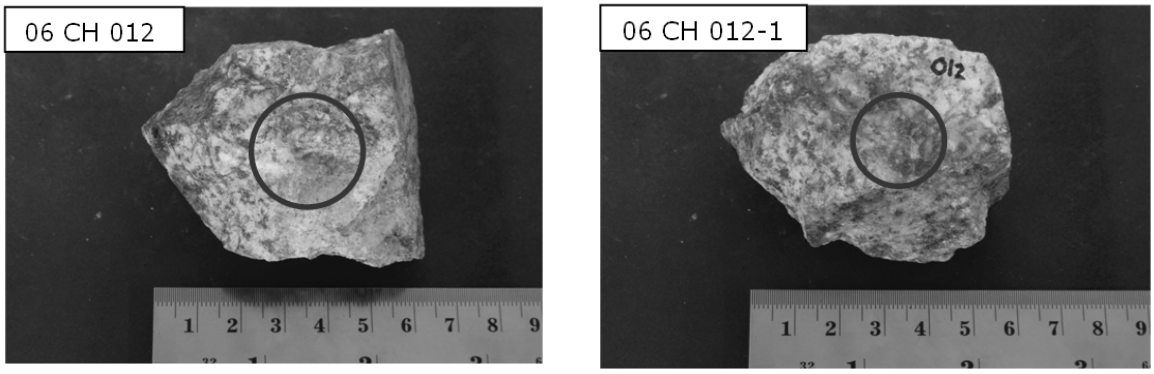

Figure 4-2 Rock samples photograph

4.3. Spectral measurements (Bruker Vertex 70)

In this research, the fourier transform infrared (FT-IR) lab spectrometer from Bruker Optics B.V. were selected for spectral measurement (figure 4-3). This measurement was performed in the ITC laboratory environment. The instrument can measure in the range of SWIR- MIR wavelengths. To accommodate the needs of earth sciences, the instrument was modified with integrated sphere. The aim of this modification is to help on measuring samples with the dimension, such as rock samples.

Before measuring, the basic instrument needs a warming up session in order to prepare the internal lamp. For the internal lamp, the instrument needs to be tuned on at least 30 minute before the measurement. Due to the over heating of the external MIR sensor, this instrument needs to be cooled. Liquid nitrogen is chosen to prevent he system from over heating . Care is needed here, as if the sensors are not in the right temperatures the spectral results will contain errors.

As mentioned in the sub chapter 4.3 of samples preparation, field sample that already marked for the measurement is placed under the integrated sphere. Below the integrated sphere there is a laboratory jack for adjusting the distance between the samples and the integrated sphere. For analysis reason, the distance between samples and sphere need to be adjusted as closed as possible. In this part we have to be careful for adjusting the distance of the sample, taking into account the role of fine grains contaminating the sphere from the samples.

This instrument was supported by additional software to produce the result from the measurement. The software is called OPUS. In this software we can adjust the measurement setting depending to the requirement of the samples measurement. Basic settings that were used in the measurement for this research are listed as follow:

- Spectral resolution: 8 cm^{-1} (wave number)
- Background scan : 4096 scans
- Sample scan : 4096 scans
- Saved data from : 7000 cm^{-1} to 500 cm^{-1}
- Result spectrum : reflectance

The complete descriptions for the measurement setting in this instrument are inserted in the appendices 1.

To understand the principle of the spectral measurement mechanism, the reflectance ratio was obtained from simplified equation (equation 1). The measurements are taking into two parts. The first measurement is the reference spectra, known as the background scan (RSC), and the second part is sample measurement, known as the samples scan (SSC).

$$\text{Reflectance} = \frac{SSC}{RSC} \quad \text{.....(1)}$$

Where:
SSC = Sample Single Channel, the results from the sample measurement in the sphere
RSC = Reflectance Single Channel, the result from the background measurement in the sphere

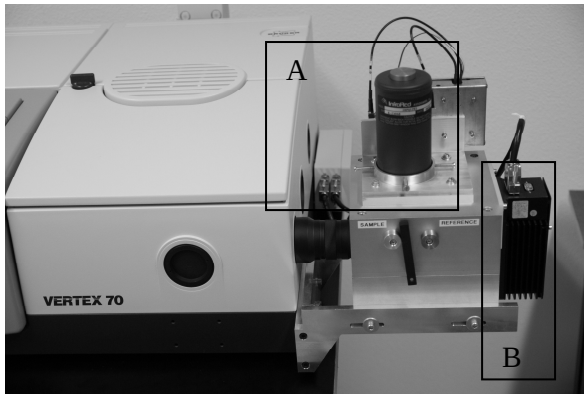

Figure 4-3 External sphere on vertex 70 with connecting funnel, MCT detector (A) and InGaAs detector (B)

4.3.1. Sphere design

The sphere was used to help on hand specimen size sample measurement. The sphere of 150mm diameter was made from aluminium. First, the surface was blasted with glass pearls, then a gold coat was added through galvanization (i.e. electroplating) to a thickness of about 3 microns to create a highly diffuse reflecting surface. The Optosol coating is reportedly about 97% reflecting and 95% diffuse (oral comm. Michael Koehl, Optosol). For wavelengths larger than 25µm, the coating apparently does not behave diffusely anymore (not measured here).

The incident beam coming from the spectrometer is slightly convergent at an angle of 3-4°. The incidence angle on the sample surface is around 10-12° (Figure 4-4). In order to prevent the specularly reflected part from escaping through the entrance hole, the measured sample area is about 25 mm in diameter.

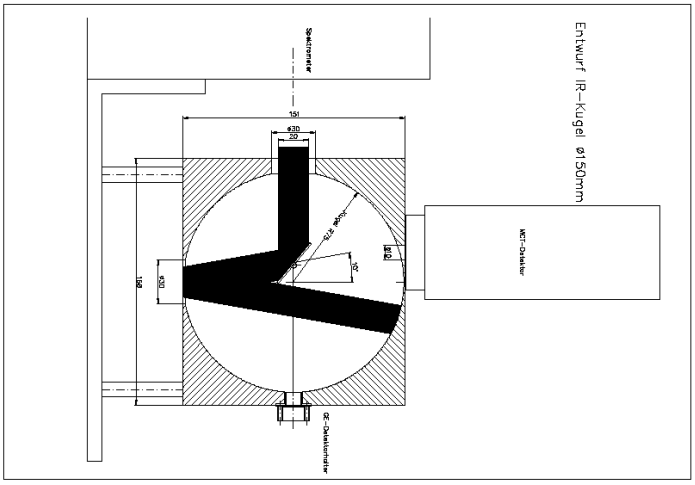

Figure 4-4 Design of integrating sphere

There are four ports on the sphere:

- 30mm diameter entrance port at the equator
- 30mm diameter sample port at the bottom pole
- 5 mm diameter detector port near the top pole for the down-looking MCT detector
- 8 mm diameter detector port near the back equator for the InGaAs detector

The MCT detector port is not on the pole of the sphere but slightly closer to the entry port. This allows the folding mirror to block the first reflection of the sample and of the calibration spot in reference position. No further baffles are needed.

The sample has to be placed at the opening at the bottom of the sphere. The incident beam (opening 30mm) is deflected onto the sample opening by a centre-mounted mirror. This mirror acts as baffle for the directly reflected beams, when the detectors are placed on top (MCT) and the rear side of the sphere (InGaAs). The illustration of the mechanism from the instrument is presented in the Figure 4-5.

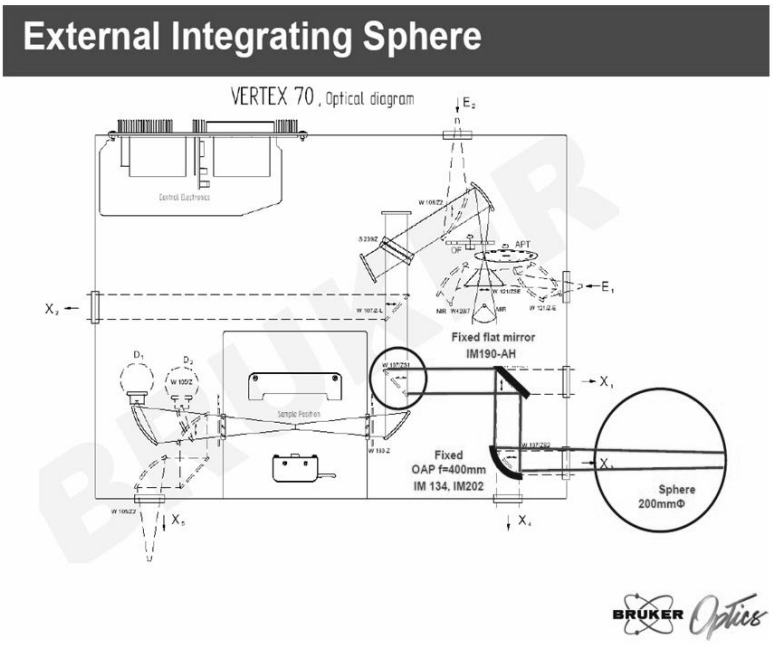

Figure 4-5 Simple diagram showing the optical path going into the integrating sphere.

4.4. Spectral Characterization

Spectral characterization from the rock samples in the study area and the USGS spectral library was determined using the wavelength position of the absorption and reflectance features as well as the shapes. The spectral results in this research shown in single range, 7- 16 μm.

5. Results

5.1. Introduction

This chapter addresses the results of the research. It starts from the result of analysing spectral characteristic of feldspars in TIR wavelengths region using USGS spectral library. The results from this first stage are use for spectral analysis of the Yerington rock samples. In this stage, the Yerington spectral data was processed using ENVI software and visually compared with the USGS spectral library as the spectral reference.

5.2. Analysis of feldspars spectra from USGS spectral library

In this section, the source of the spectral data is derived from USGS spectral library. Analyses of the spectra in the feldspar group were conduct to understand the best discriminating wavelength to classify the feldspar group. This analysis is performed for two general feldspar groups; namely plagioclase feldspar and alkali feldspar.

5.2.1. Plagioclase Feldspars

For this feldspar group, the analyzed mineral had six members. The members are albite, oligoclase, andesine, labradorite, bytownite and anorthite. The spectral characterization was applied to this feldspar group in order to examine the spectral responses. It was influenced by the changes in the composition of the percentage anorthite.

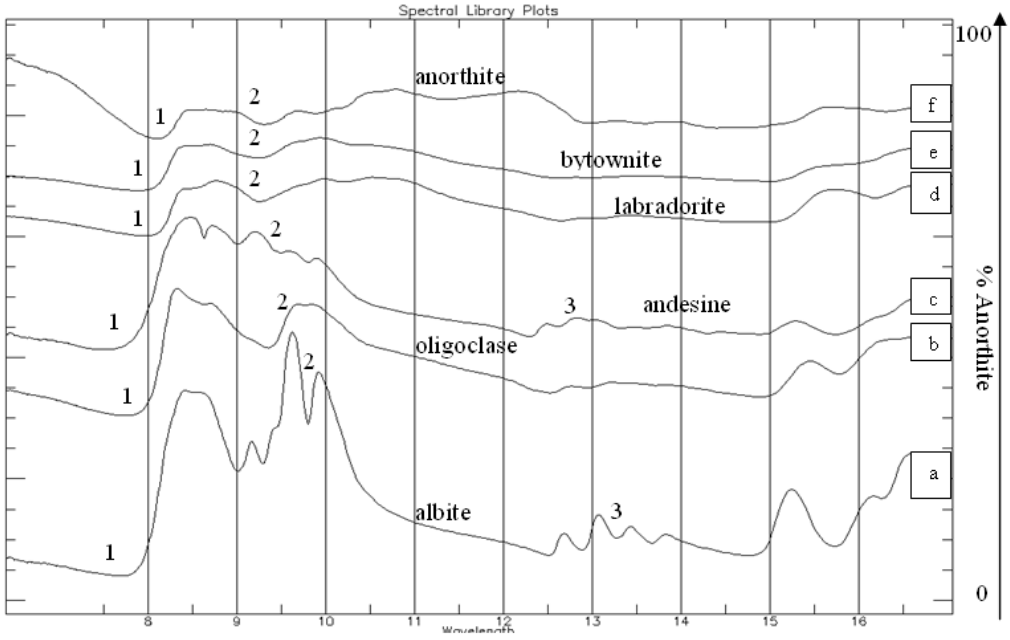

Figure 5-1 Plagioclase feldspars spectra plot in offsets for clarity (a) albite, (b) oligoclase (c) andesine (d) labradorite (e) bytownite (f) anorthite.

In this group, the spectra characteristic were varying from albite to anorthite (Figure 5-1). Generally, the variations are concentrated between 8 to 10.5 µm. For this region absorption, bands occur basically due to silicon-oxygen stretching. For albite to andesine, the variation also occurs between 12 to 16 µm (Figure 5-1a3 and Figure 5-1c3).

Regarding the albite spectra, the reflectance minima is shown near the 7.7 µm (Figure 5-1a1). The diagnostic spectral features for albite are shown in two distinctive peaks. These two diagnostic peaks are shown at the near 9.6 µm and near 10 µm (Figure 5-1a2). The peaks are showing high reflectance in the spectral characteristic of albite.

The oligoclase spectra contains the most prominent features between 8 and 10.25 µm (Figure 5-1b). The reflectance value steadily decreases and flattens above 10µm. The distinctive feature of oligoclase spectra are shown at 8.3 and 9.3 µm (Figure 5-1b2).

For andesine, the spectral characterization was shown between the reststrahlen bands. The spectral characteristic of this mineral exhibits a wavy pattern. It is has a relatively same height or depth on the diagnostic spectral features. The variations are shown in between near 8.25 µm and near 10 µm (Figure 5-1c2).

Labradorite has a general pattern with a low reflectance value. Variation with high value of reflectance is visible at 8 to 10.25 µm and afterwards the values decrease. The variations of peak and valley are characterized at 8.7 and 9.2 µm wavelength (Figure 5-1d2).

Bytownite is a rare member in plagioclase series. The general pattern of this spectrum shows small variation in peaks or valleys. From the plot 5-1e, we see that the shape of the spectra is relatively flat. However, this mineral has diagnostic spectra position at 8.6 and 9.9 µm wavelength (Figure 5-1e2).

The last member in this group is anorthite. This plagioclase member has several diagnostic position spectra at 9.6; 9.8; 10.8 and 12.2 µm wavelength (Figure 5-1f2). This diagnostic position on the spectra was showing the high reflectance in this mineral. Even thought the percentage of reflectance is not as high as the other mineral in this group, for example albite.

5.2.2. Calculating the plagioclase feldspars spectra differences

To analyze the changes in the plagioclase groups, an analysis was perform to calculate the changes due to the spectral band depth, area, spectral width and reflectance minima position (Christiansen frequency) of the spectra versus the composition changes. In this analysis, two approaches were followed. The first one uses the reflectance spectra for analyzing the reflectance minima position of plagioclase; and afterwards converting the percentage reflectance into emissivity reflectance. In the second approach the aim is to calculate the spectral band depth, spectral area and spectral width calculation in DISPEC. DISPEC is a third party extension in ENVI software. This extension assists calculating the spectral depth, width and the area (Figure 5-. 2).

The calculations in the DISPEC were in the range of 7-9 µm wavelengths. This range was chosen because of the similarity of the spectral shape, showing a peak and considered easy to compare between each member. The results are summarized in table 5-1. The analysis continued by analysing the value of the band depth, with and area against the percentage of anorthite by plotting it in a spreadsheet. The result from absorption band depth and spectral area calculation shows the changes from albite to anorthite related to the mineral compositions changes. From the plots Figure 5-3, it is presented that the values were decreasing in the band depth position. The plot explains that the parameter of changes is influenced by the changes in the increasing percentage of anorthite composition.

There are interesting results from the calculation of band depth absorption and spectral area calculations. The interesting part from these plots is the plot of the albite groups which seems to be divided into two groups. This may be link to the forming of order and disorder of albite group. The albite group that have a high value or more depth is categorized into disordered albite (Figure 5-3a and 5-5a) then the other group was classified as order albite (Figure 5-3b and 5-5b). This analysis related with the different shape from albite group spectra that were plotted in the Figure 5-6.

From the spectral width calculation against composition (Figure 5-4), the plot does not show any pattern that could help to distinguish between plagioclase feldspar members. The value of spectral width is in the range 0.4 – 0.8.

Table 5-1 Plagioclase feldspars spectral absorption band depth, width, area and reflectance minima position calculation table

feldspars	depth	width	area	Minima (µm)	% An
albite_gds30.359	0.11	0.71	0.07	7.73	10
albite_hs143.524	0.12	0.63	0.07	7.80	10
albite_hs324.3b.414	0.24	0.67	0.16	7.72	10
albite_hs66.3b.469	0.28	0.67	0.18	7.70	10
oligoclase_hs110.16239	0.17	0.62	0.10	7.76	30
Andesine_hs142.2101	0.14	0.70	0.09	7.50	50
labradorite_hs17.12449	0.05	0.63	0.03	7.97	70
bytownite_hs105.4014	0.05	0.60	0.03	7.90	90
bytownite_hs106.4071	0.04	0.71	0.02	8.01	90
anorthite_gds28.2570	0.02	0.44	0.01	8.10	100
anorthite_hs201.2625	0.03	0.49	0.02	8.10	100
anorthite_hs349.2680	0.05	0.55	0.03	8.08	100

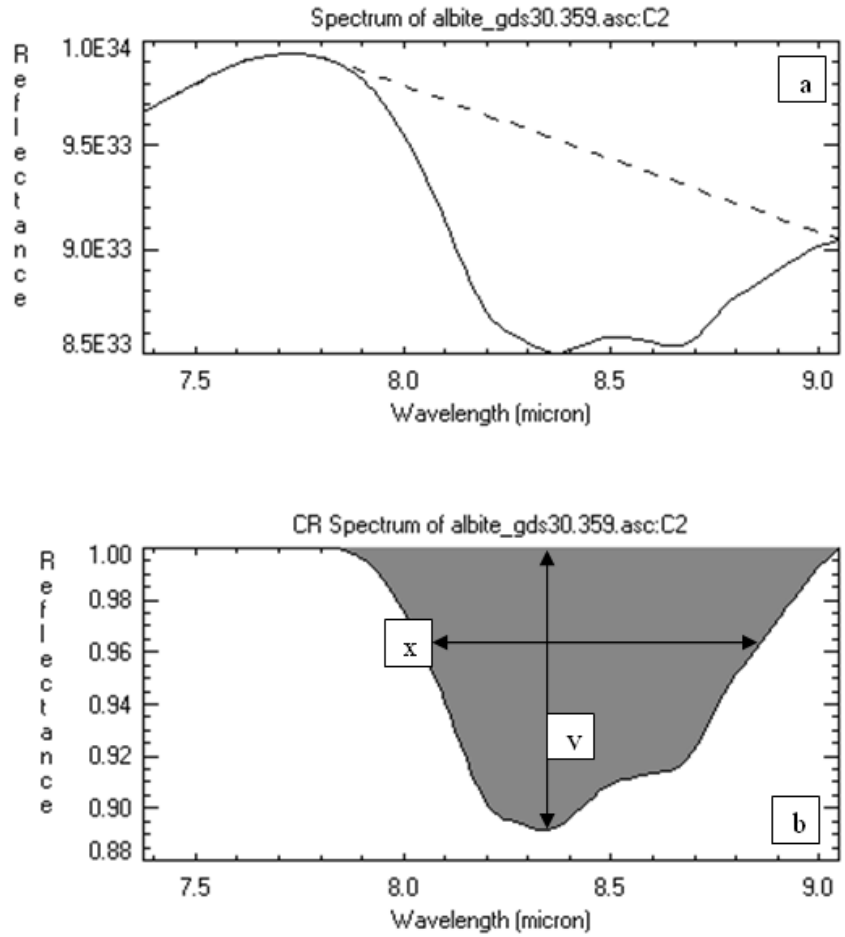

Figure 5-2 Analysis for spectrum of albite using DISPEC(a)real spectrum, (b) calculated spectrum (x) width of the spectral absorption, (y) depth of the spectral absorption

.

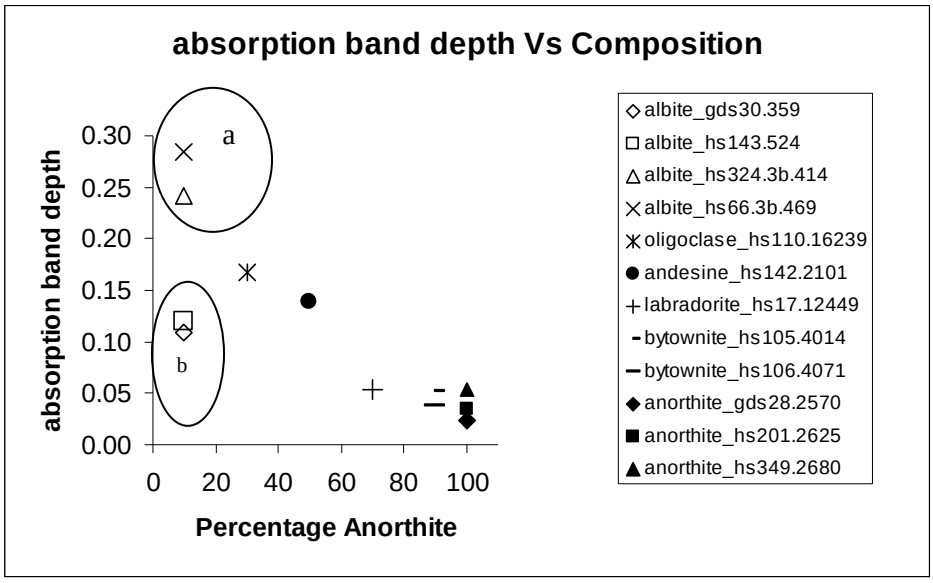

Figure 5-3 Plot of absorption band depth position Vs composition for plagioclase feldspar (a) disordered albite group (b) ordered albite group.

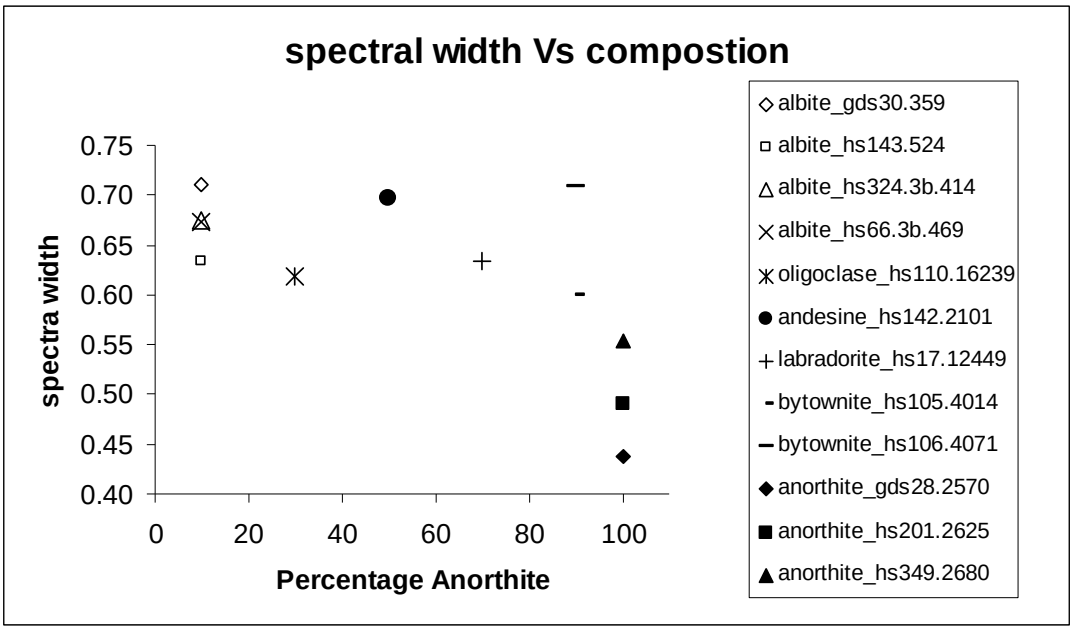

Figure 5-4 Plagioclase feldspars spectral width calculation plot

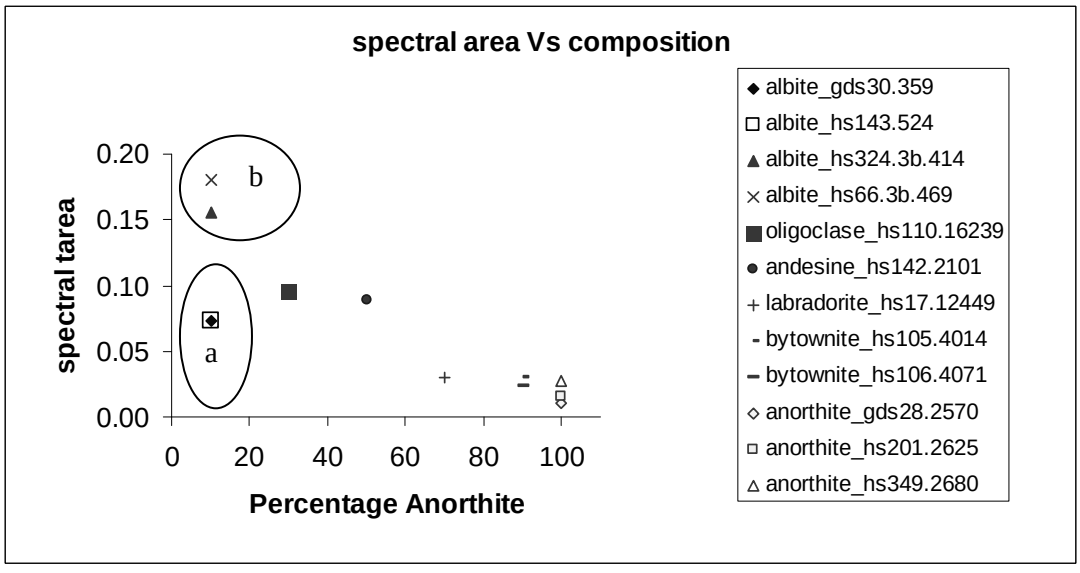

Figure 5-5 Plagioclase feldspars spectral area width calculation plot (a) disordered albite group (b) ordered albite group.

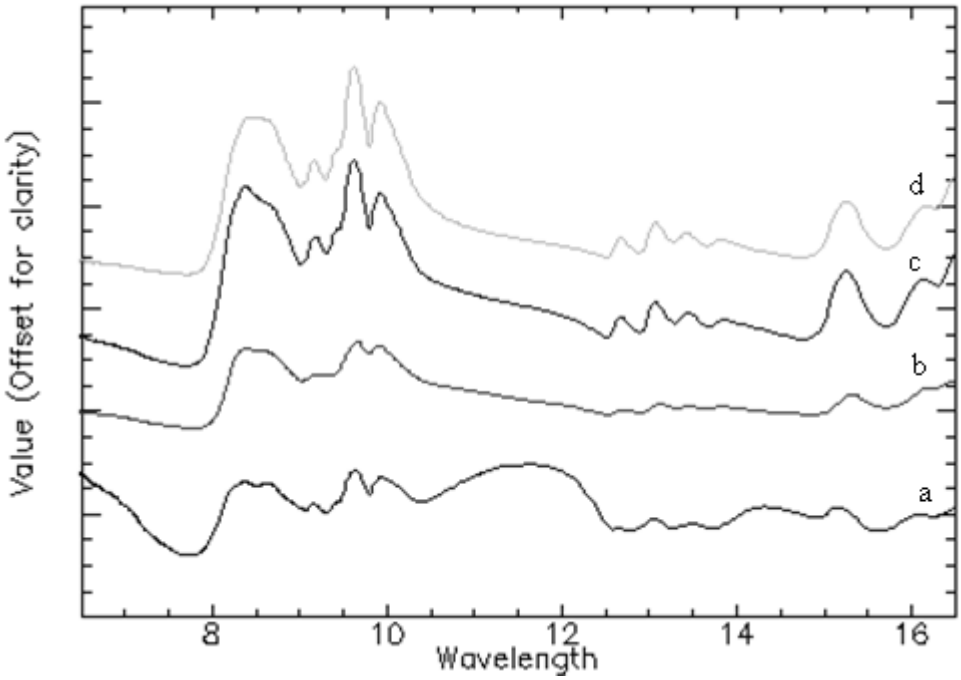

Figure 5-6 Reflectance spectra of albite group (a) albite_gds30.359, (B) albite_hs143.524, (c) albite_hs66.3b.469, (d) albite_hs324.3b.414;

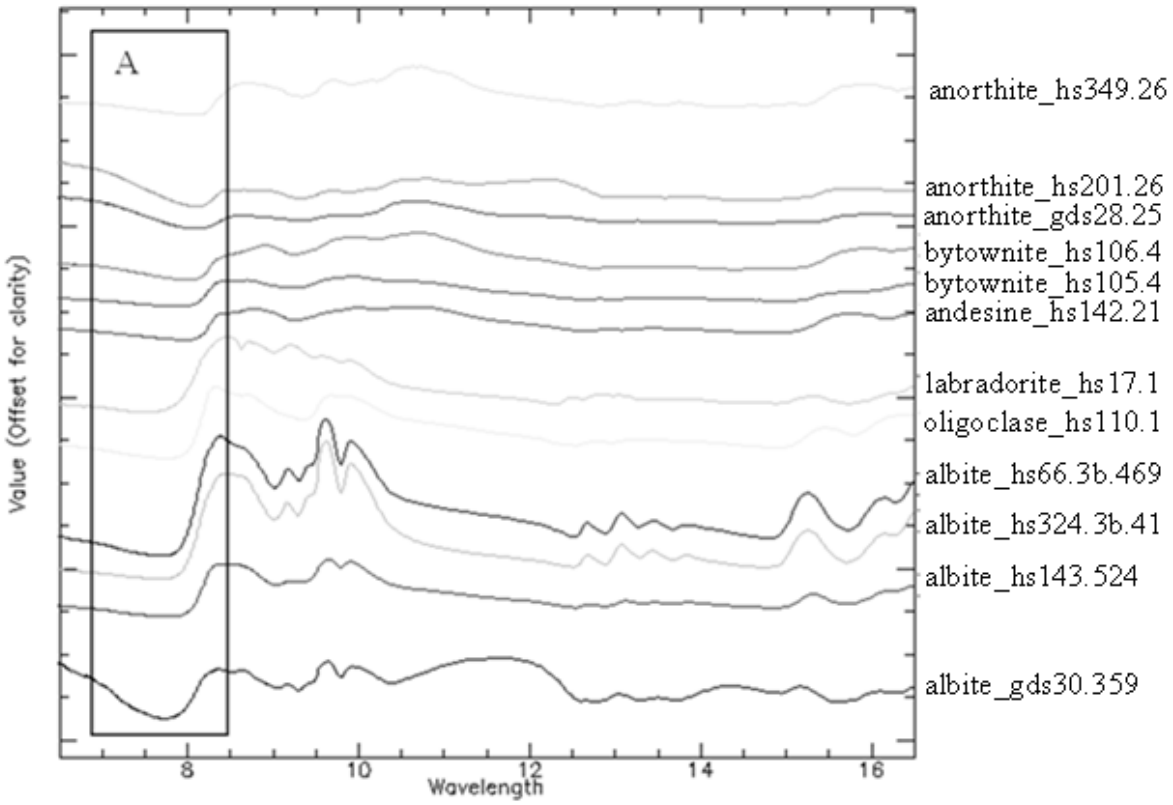

Figure 5-7 Plagioclase group spectra plot (A) reflectance minima area of observation

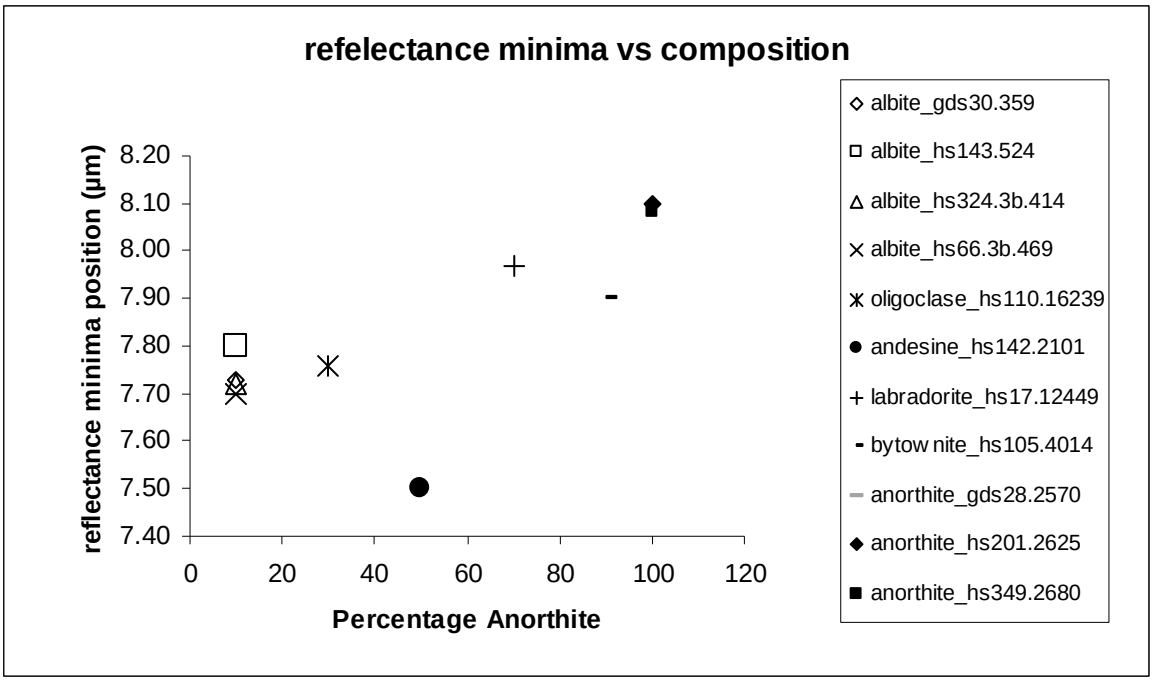

Figure 5-8 Reflectance minima analysis plot for plagioclase groups

From Figure 5-7 the spectra of plagioclase minerals studied for the position changes in the reflectance minima were determined. From these spectra the position against the percentage of anorthite was calculated. The result (Figure 5-8) shows that changes occur generally into systematically pattern; except for the andesine, which was showing anomaly in the graph. This could be caused by the different sampling source of andesine.

5.2.3. Alkali Feldspars

The result of this spectral library is also obtained from the USGS spectral library. In this sub group, four mineral are observed. They are albite, microcline, sanidine and orthoclase. This observation will carry out the important wavelength on classifying the alkali feldspar member.

Albite is also a member in this sub groups (Figure 5-9a). The reflectance for albite is located at 7.7 µm (Figure 5-9a1). Moving towards the longer wavelength it shows the distinctive spectral features of this mineral. The double peaks occur about 9.6 and 10 µm (Figure 5-9a2). As well as in the plagioclase group, this is the prominent features in the albite mineral spectra.

From the USGS spectral library, the sanidine spectrum is analyzed (Figure 5-9b). In this mineral, the reflectance spectral minima were located at near 7.5 µm (Figure 5-9b1). The prominent feature for this mineral is the single peak shown at 9 to 10 µm wavelength range. From the Figure 5-9b, we can clearly see that shape for the peak of this mineral is broad. The ordering of the Al and Si atoms might cause this. The effect of this ordering is broadening. Sanidine shown the spectral characteristic in the shorter wavelength compared to the other mineral members in this sub group.

The prominent features in the microcline spectra are shown with the reflectance spectral minima at near 8 µm (Figure 5-9c1). Moving towards the longer wavelengths, the prominent features characterized with triple peak shapes occur at the range of 9 to 10 µm. The shape of the peak in this mineral has less height compared to the albite spectra at the same wavelength range. The peaks are located at near 9.25; 9.5 and 10 µm (Figure 5-9c2).

Orthoclase is placed in the last order of this observation in the feldspars sub groups (Figure 5-9d). This mineral has spectral reflectance minima at 8 µm (Figure 5-9d1). For orthoclase, the prominent features occur also in the longer wavelength, between 9 and10 µm. Orthoclase is characterized with triple peak spectral features. The wavelength positions of the peak occur at near 9.25; 9.5 and 10 µm (Figure 5-9d2). The difference of orthoclase prominent spectral features is the peaks are less pronounced compared to those of albite and microcline.

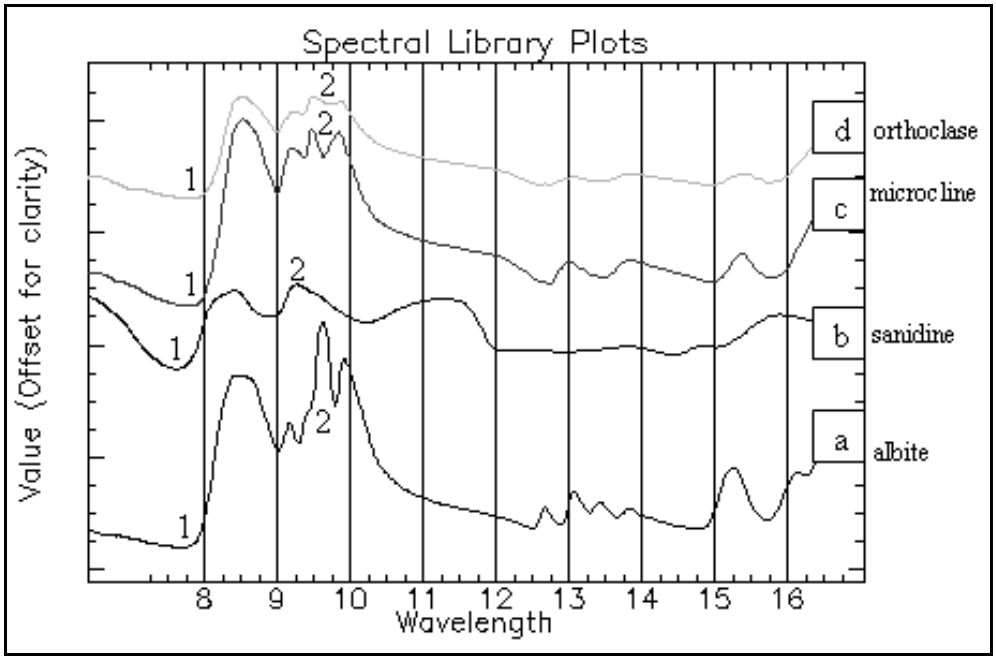

Figure 5-9 Alkali feldspars spectra plot in offsets for clarity (a) albite, (b) sanidine (c) microcline (d) orthoclase

5.2.4. Calculating the alkali feldspars spectra differences

As well as in the plagioclase groups, the alkali feldspar spectra was examined for their spectral differences, in order to observe if there is any pattern that can show the differences between the spectra in the alkali groups. The used parameters are: reflectance spectra minima position changes; absorption band depth calculation; spectra width calculation and spectra area calculation. The reflectance spectra minima were analyzed manually with ENVI Software. For the absorption band depth calculation, spectra width calculation and spectra area calculation were extracted using the third party extension in ENVI software called DISPEC. For calculating the spectral differences in alkali feldspar is using the same method that used in plagioclase feldspar spectra differences calculation.

The first observation was using the wavelength position on the lowest percentage reflectance value for each spectrum in this group, known as in the Christensen frequencies. The observation was done with spectral library viewer in ENVI software. This observation is done in the reflectance spectra. The second part of observation uses the DISPEC (Figure 5-11), the reflectance spectra was converted into emissivity spectra. This approach was used as well when we calculated spectra differences in the plagioclase groups. The calculations were done in the range of 7-9 µm wavelengths. The reason for using this wavelength range is due to the similarity in the spectral shape for calculations and comparison. The results are summarize in Table 5-2 as follow:

Table 5-2 Alkali feldspars spectral absorption band depth, width, area and reflectance minima position calculation table

alkali group	minima	depth	width	Area
albite_gds30.359	7.73	0.10	0.69	0.07
albite_hs143.524	7.80	0.11	0.63	0.07
albite_hs324.3b.414	7.72	0.24	0.67	0.15
albite_hs66.3b.469	7.70	0.28	0.67	0.17
microcline_hs103	7.84	0.14	0.57	0.08
microcline_hs107	7.89	0.06	0.57	0.04
microcline_hs_108.13761	7.74	0.25	0.57	0.13
microcline_hs108.13816	7.87	0.16	0.54	0.09
microcline_hs82	7.84	0.24	0.59	0.14
microcline_nmnh135231	7.80	0.10	0.58	0.06
sanidine_gds19	7.85	0.10	0.58	0.06
sanidine_nmnh103200	7.63	0.09	0.67	0.06
orthoclase_hs13	7.80	0.12	0.54	0.07
orthoclase_nmnh142137	7.85	0.05	0.58	0.03

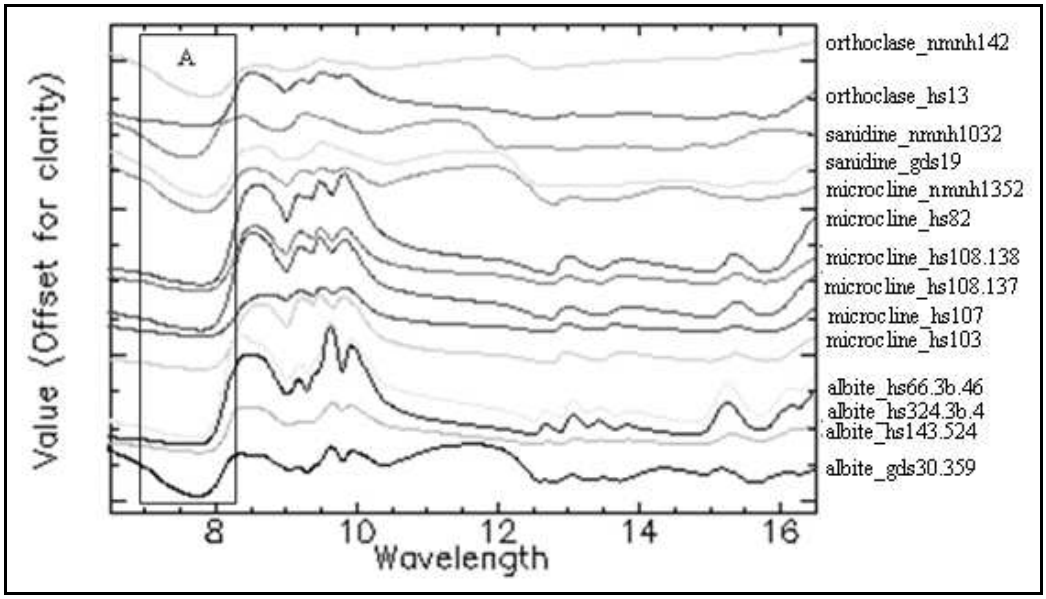

Figure 5-10 Alkali group spectra plot (A) reflectance minima area of observation

From Figure 5-10 the alkali feldspar group spectra were observed for changes in position of the reflectance minima of its members. The reflectance minima position was located near 8 µm. The aim of this analysis is also to observe if there any influence of reflectance minima position changes for determining alkali feldspar member. The result is plotted as a graph in the figure 5-15.

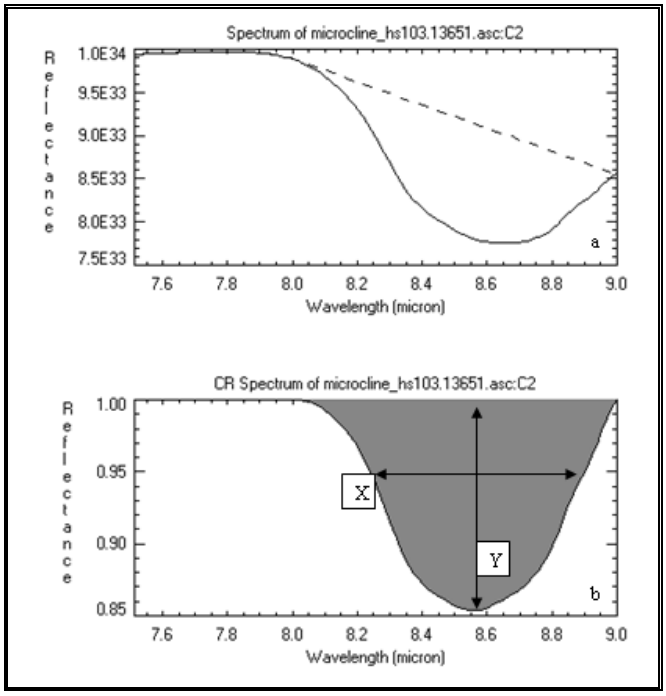

Figure 5-11 Analysis for spectrum of microcline using DISPEC(a)real spectrum, (b) calculated spectrum (x) width of the spectral absorption, (y) depth of the spectral absorption.

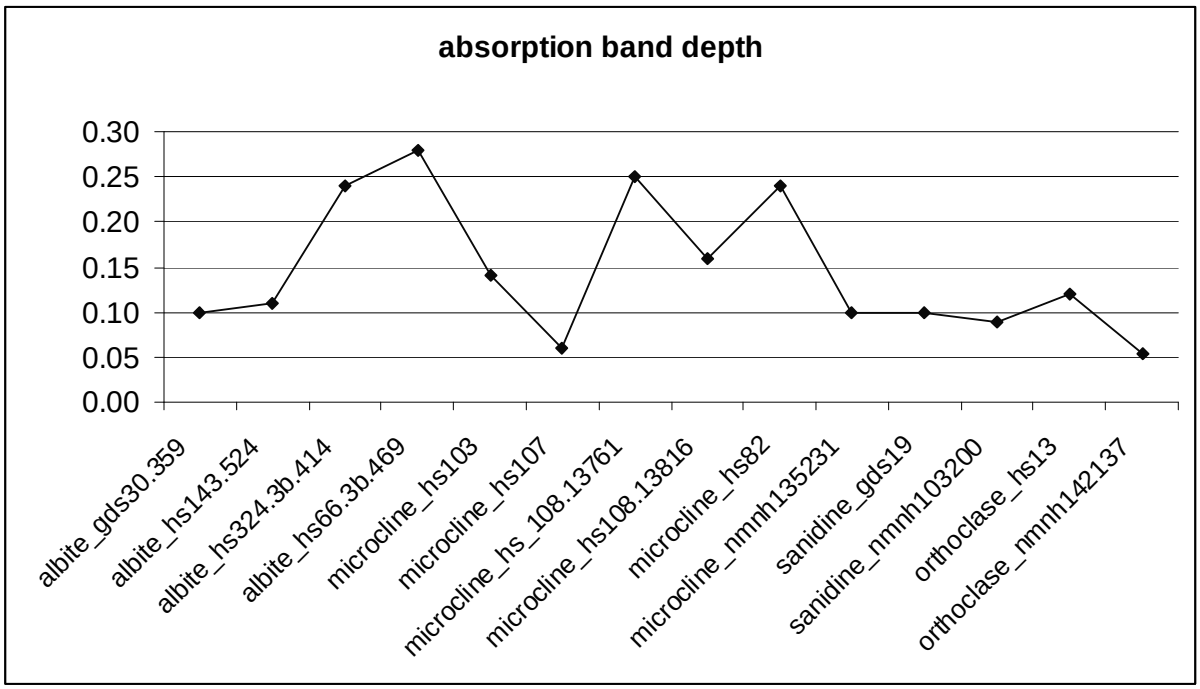

Figure 5-12 Absorption band depth calculation plot for alkali feldspars

In Figure 5-12, the absorption band was calculated for each alkali feldspar member. The value varies in the range of 0.05-0.30 and for albite group it is distributed value in the range of 0.10-0.27. Albite group shows the highest value in the absorption band depth. In the next group is microcline, this mineral showing a variation with the lowest value of near 0.06 and highest value of 0.25. The third group shown in the plot is sanidine. Sanidine shows in the moderate value of absorption band depth. There are two sanidine spectra which have been calculated, with their values near 0.07 and 0.10. The last mineral in the alkali feldspar spectra was analysed is orthoclase. This mineral has a variation between 0.05-0.12. Orthoclase shows one of the samples has the lowest band depth absorption calculation value in the alkali feldspar. In this analysis the result value were vary, the plots has not show any pattern that could help on determining the member of alkali feldspar.

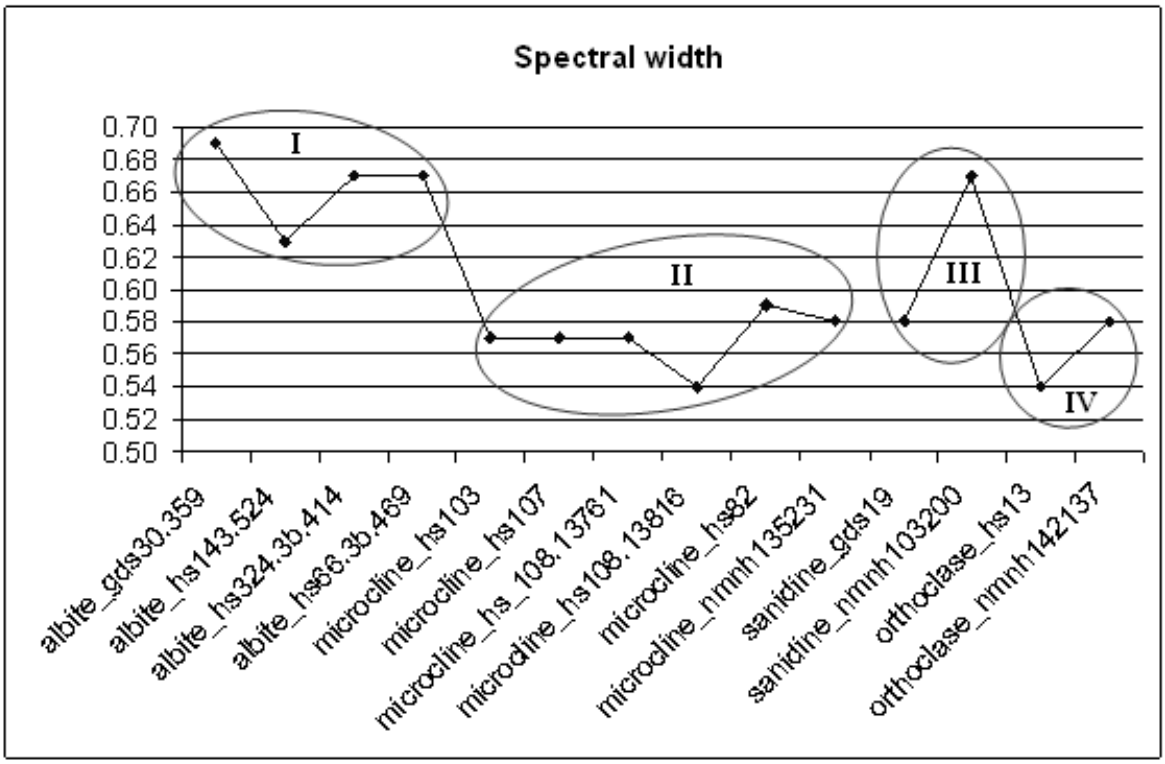

Figure 5-13 Spectral width calculation plot for alkali feldspar (I) albite group; (II) microcline group; (III) sanidine group and (IV) orthoclase group

In Figure 5-13, the graphs were grouped for each member to enhance the systematic changes that occur in this analysis. The albite group varies between 0.63 and 0.69. The microcline group shows decreasing values in the range of 0.54-0.59. The third group or microcline are in the range of 0.58-0.67, however there is anomaly for sanidine_nmnh103200. This anomaly could be caused by different source of sampling locations in this group. The last group or orthoclase shows the value of spectral width in the range 0.54-0.58. This could help on determining the alkali group member spectra. The general pattern of this parameter is that every member has a decreasing trend in its spectral depth.

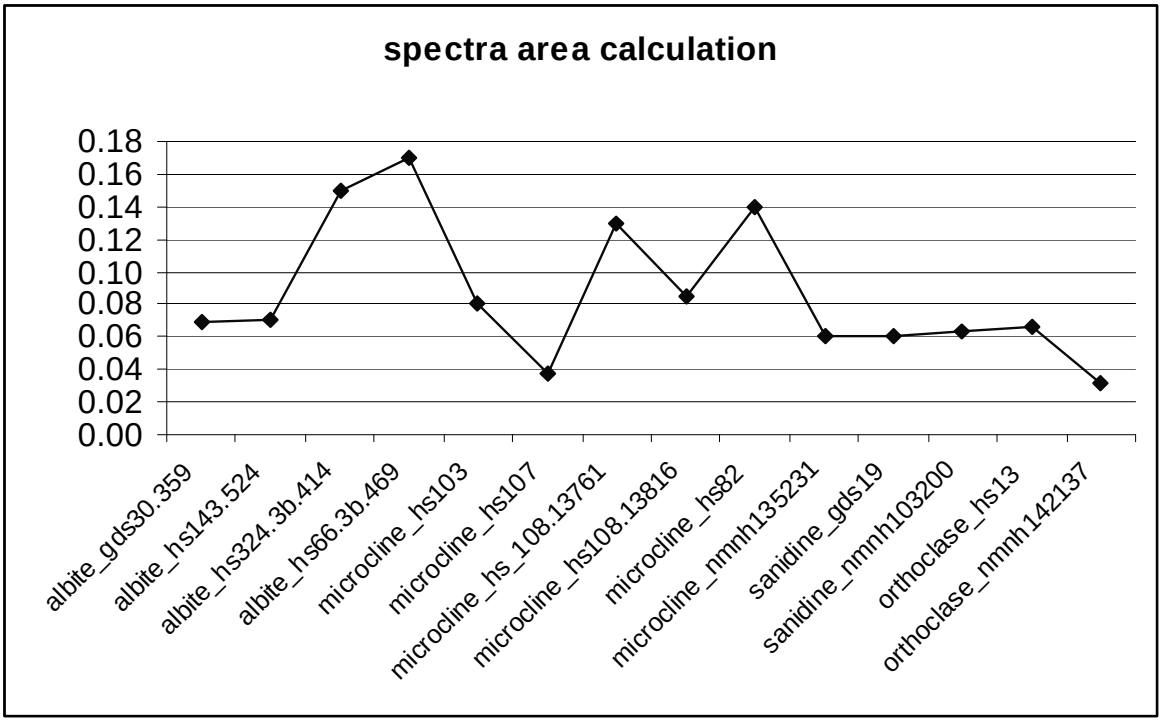

Figure 5-14 Spectral area calculation plot for alkali feldspar

Spectra area was calculated and this result is plotted in Figure 5-14. The values of the area calculation are in the range of 0.03-0.17. For each mineral in this calculation there is a strong variation. Albite has values in the range of 0.07-0.7. albite_hs66 shows the highest value in spectra area calculation of alkali feldspar. The next mineral is microcline, which has six calculated sample spectra. This mineral has values in the range of near 0.04 to 0.14. Microcline continued by sanidine mineral, for sanidine was showing the values that very close. The plot values for two samples of sanidine are 0.6 and approximately 0.7. The last mineral in this calculation is orthoclase; this mineral shows a decreasing value between their samples. The values are near 0.75 and near 0.35. The values of sanidine_gds19 and microcline_nmnh135231 are the same. Thus, the differentiation between sanidine and microcline spectra it is difficult by this calculation.

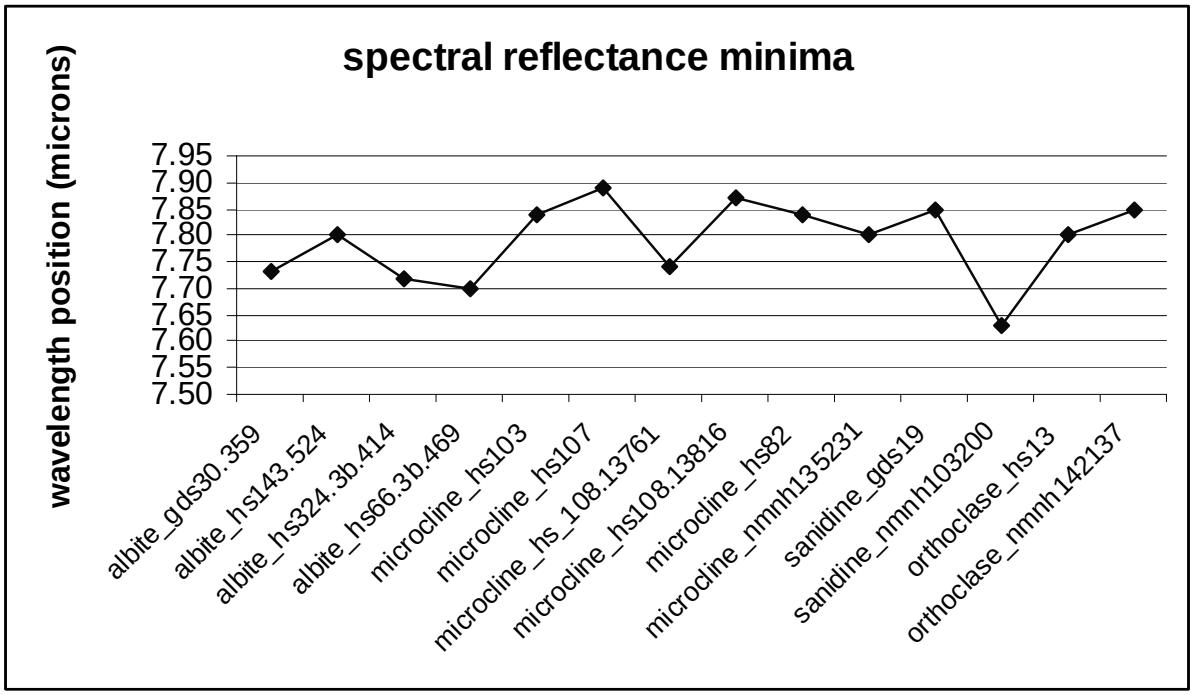

Figure 5-15 Reflectance spectra minima position plot for alkali feldspars

The last analysis is changes in position of spectral reflectance minima. as shown in Figure 5-15. There is no systematic changes in the result of this analysis. The analysis shows a r minima reflectance lying in the range of 7.65 to 7.9 µm. According to this result, we are not able to distinguish the member of alkali feldspar spectra.

From the previous analyses, the results do not seem very promising. As shown from the figures 5-12, 14 and 15 there is not a systematic pattern of changes in the group members. The analyses were done on the absorption band depth; spectral area calculation and the spectral reflectance minima position observation. However, a systematic pattern was shown in spectral width calculation analysis plot. In this observation, the result was not perfect; there is an anomaly on the sanidine_nmnh103200 member.

5.3. Yerington rock samples spectra

These samples were taken from study area. 51 rock samples have been analyzed in the spectrometer laboratory. Most of the samples are in fresh condition. The dimensions of the samples are enough in size to be measured by bruker FT-IR spectrometer. The samples were analyzed in the TIR and SWIR region. Even though the SWIR region result contains noise spectra, the aim for measuring in this region was to know the possible minerals present in the rock samples.

The sample that was taken from the study area was measured with the FT-IR spectrometer. The entire sample was analyzed with visual comparison between the rock sample spectra and the spectral reference from the USGS 2006 mineral spectral library using help from the ENVI software, they are shown in figures 5-17 to 5-32. The results also summarized as a table below in the appendices.

Several samples are not available for comparison with the spectral library is defined as unknown mineral. The location of the samples is visualized by displaying them in the alteration map (Figure 5-16).

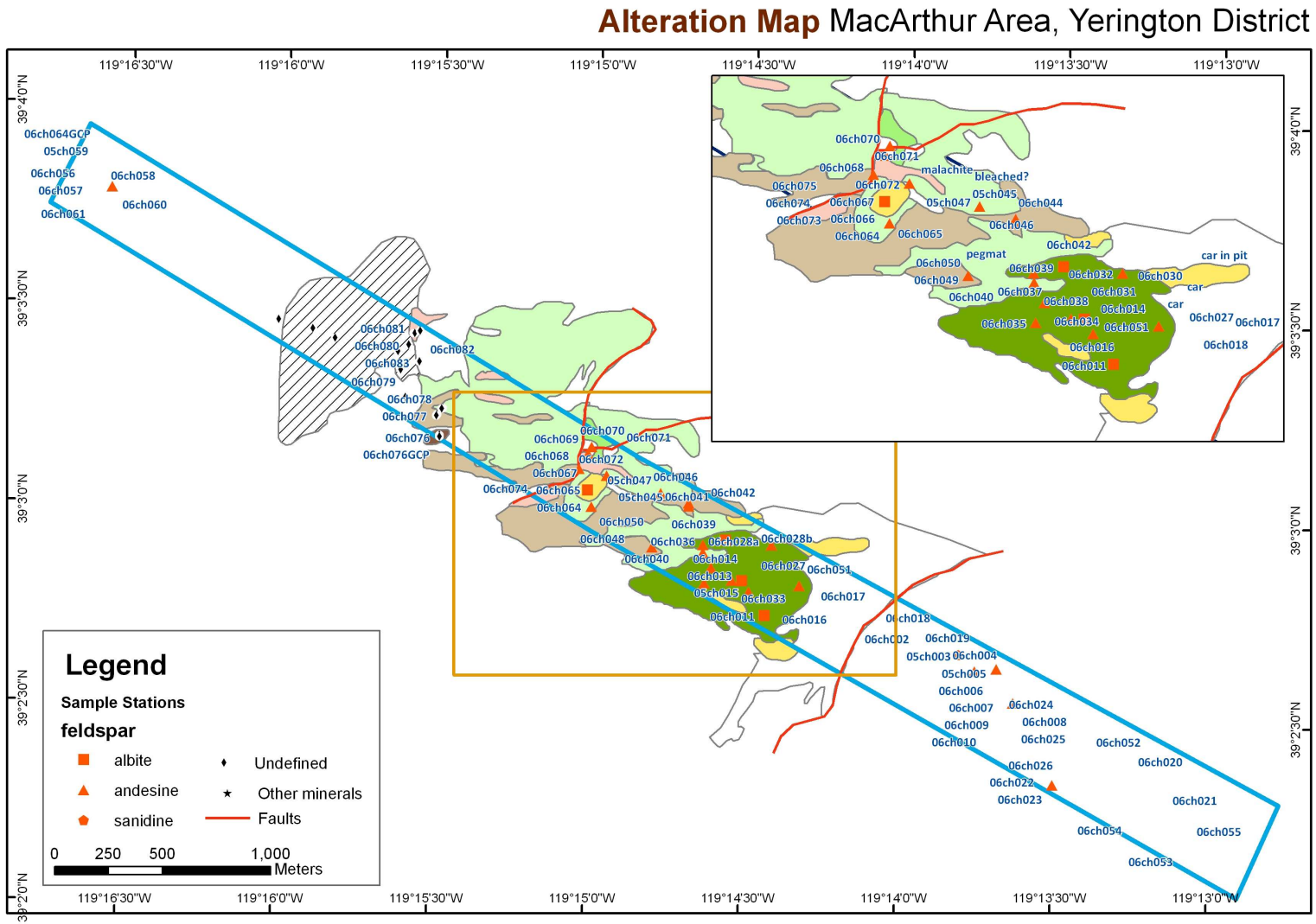

Figure 5-16 Field samples distribution overlay on alteration map

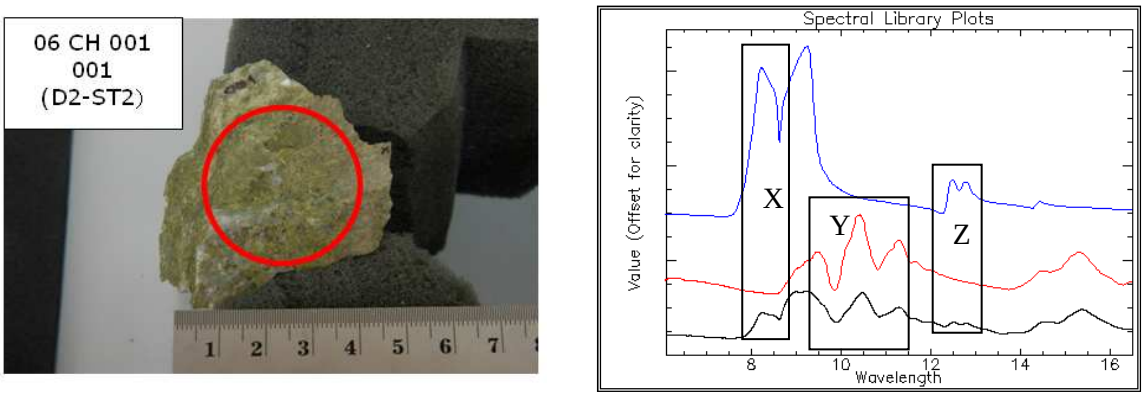

a b

Figure 5-17 (a) Rock sample 06 CH 001 photograph with red circle indicating the measurement boundary, (b) spectral analysis 06 CH 001 (black) matched with spectral reference, quartz (blue) and epidote (red).

The spectral measurement from rock sample 06 CH 001 matched with spectral reference from epidote and quartz minerals (Figure 5-17b). It has a good match between the sample 001 and the spectral reference. We can see from the figure, that in the range 8.5- 11 µm wavelengths, the rock sample spectrum was matched with the epidote spectral feature (Figure 5-17Y). For the longer wavelength, in the range of 12-13.5 µm, the sample spectra matched with the reference spectra from quartz mineral (Figure 5-17 X and Z).

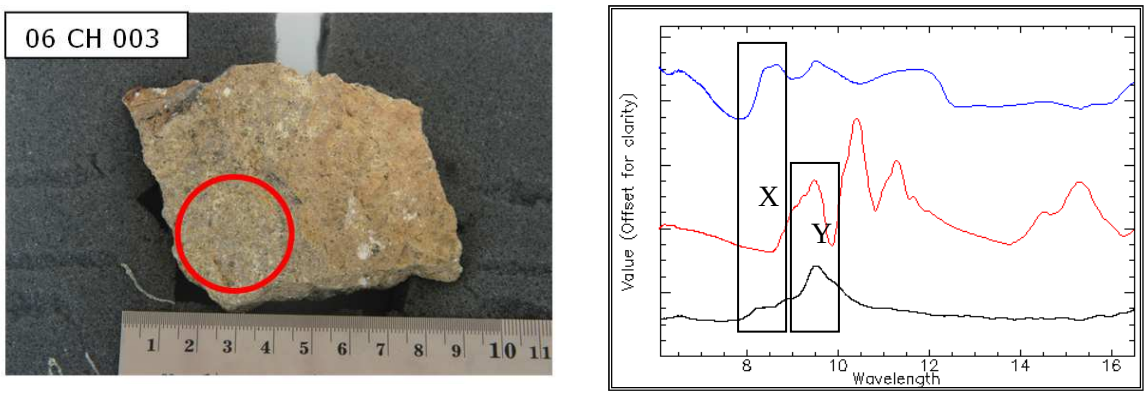

a b

Figure 5-18 (a) Rock sample 06 CH 003 photograph with red circle indicating the measurement boundary (b) spectral analysis of 06 CH 003 (black) matched with spectra of epidote (red) and sanidine (blue)

Figure 5-18b, shows the spectral measurement from rock sample 06 CH 003, the sample spectra matched with a moderate matching results with spectral reference from mineral sanidine and epidote minerals. In the range near 8- 9.5 µm wavelengths, the rock sample spectra matched with the sanidine spectral feature (Figure 5-18X). Moving to the longer wavelength, in the range of 9-10 µm, the peak on the sample spectra was matched with the reference spectra from epidote mineral (Figure 5-18Y).

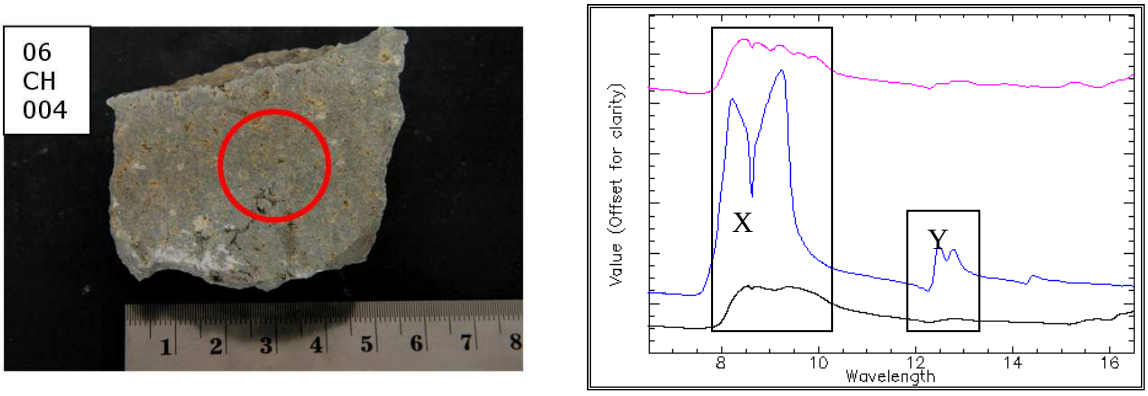

a b

Figure 5-19 (a) Rock sample 06 CH 004 photograph with red circle indicating the measurement boundary, (b) spectral analysis of 06 CH 004, matched with andesine (purple) and quartz (blue)

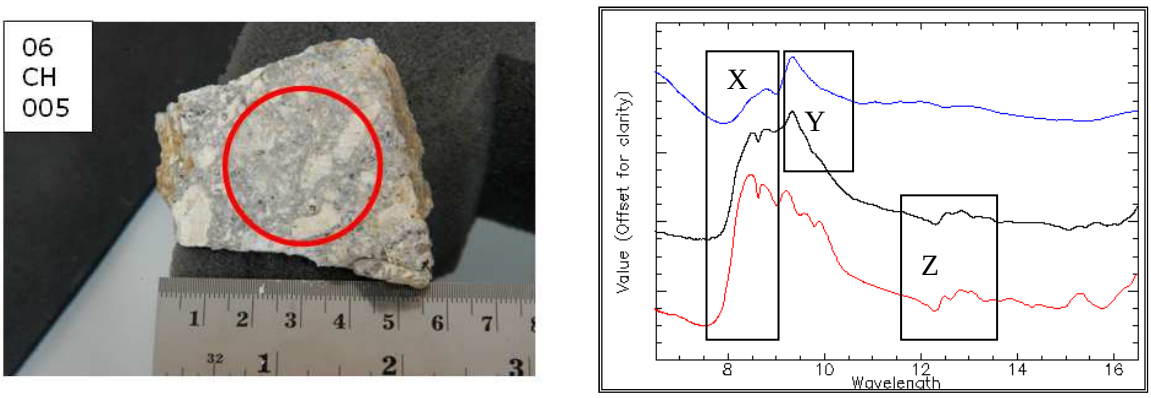

a b

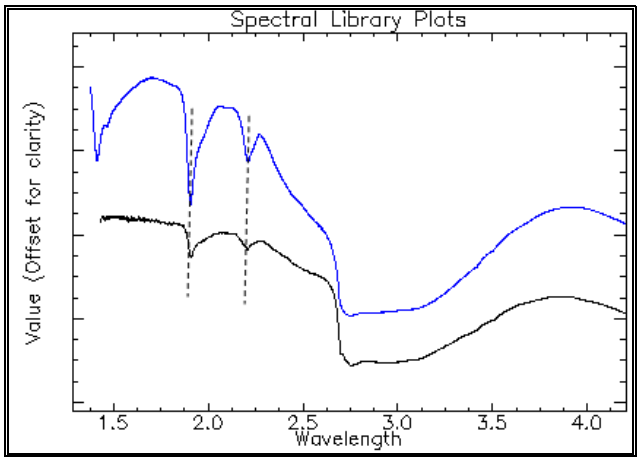

c

Figure 5-20 (a) Rock sample 06 CH 005 photograph with red circle indicating the measurement boundary (b) apectral measurement of 06 CH 005 (black) matched with spectra of andesine (red) and montmorilonite (blue). (c) rock sample 06 CH 005 and montmorilonite mineral spectra in SWIR wavelength range

The spectral measurement from rock sample 06 CH 004 has a good matching result with spectral reference from andesine and quartz minerals (Figure 5-19b). We can see from the figure that in the range 8.5- 11 µm wavelengths, the rock sample spectrum was matched with the andesine spectral feature (Figure 5-19X). For the longer wavelength, in the range of 12-13.5 µm, the sample spectra was matched with the reference spectra from quartz mineral (Figure 5-19Y).

Figure 5-21b, shows the spectral measurement from rock sample 06 CH 005, the sample spectra matched with good matching results with spectral reference from andesine and montmorilonite minerals. In the 7.5-9 range µm wavelengths, the rock sample spectrum was matched with the andesine spectral feature (Figure 5-20X). Moving to the longer wavelength, in the range of 9.5-10.5 µm, the sample spectra peak was matched with the reference spectra peak from montmorilonite mineral (Figure 5-20Y). In the range of 12-13.5 µm, the spectral features matched with the andesine spectral features (Figure 5-20Z). In the Figure 5-20c, it is shown that the sample was compared in the SWIR wavelength region with a good result between the samples and montmorilonite spectra absorption features.

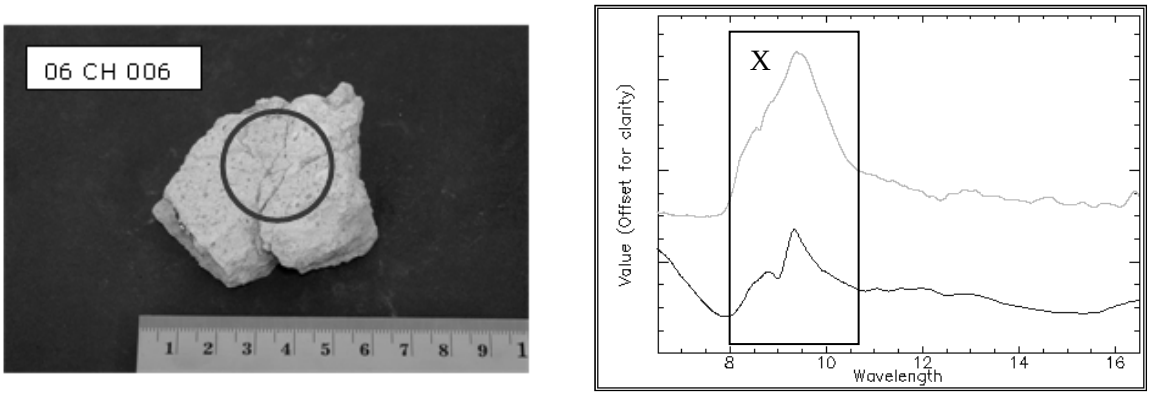

a b

Figure 5-21 (a) Rock sample 06 CH 006 photograph with red circle indicating the measurement boundary, (b) spectral measurement of 06 CH 006 (grey) matched with spectral reference of montmorilonite (b).

The spectral measurement from rock sample 06 CH 006 was matched visually with spectral reference from montmorilonite minerals (Figure 5-21b). We can see from the figure, that in the range 8.5- 10.5 µm wavelength, the rock sample spectrum matched with the montmorilonite spectral feature (Figure 5-21X).

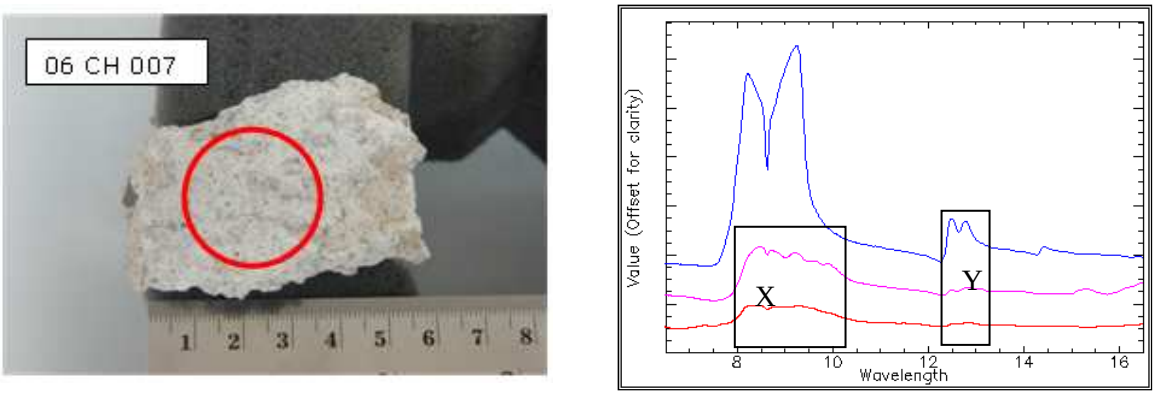

a b

Figure 5-22 (a) Rock sample 06 CH 007 photograph with red circle indicating the measurement boundary, (b) spectral measurement of 06 CH 007 (red) matched with spectral reference of andesine (purple) and quartz (blue)

Figure 5-23b shows the spectral measurement from rock sample 06 CH 007, the sample spectra matched with a moderate matching results with spectral reference from andesine and quartz minerals. In the range 8- 10 µm wavelength, the rock sample spectrum was matched with the andesine spectral feature (Figure 5-23X). Moving to the longer wavelength, in the range of 12.5-13 µm, the sample spectra features were matched with the reference spectra features from quartz mineral (figure 5-23Y). In the samples spectra was showing a low value of reflectance. Therefore, in this sample the result was analyzed base on the match position of the features.

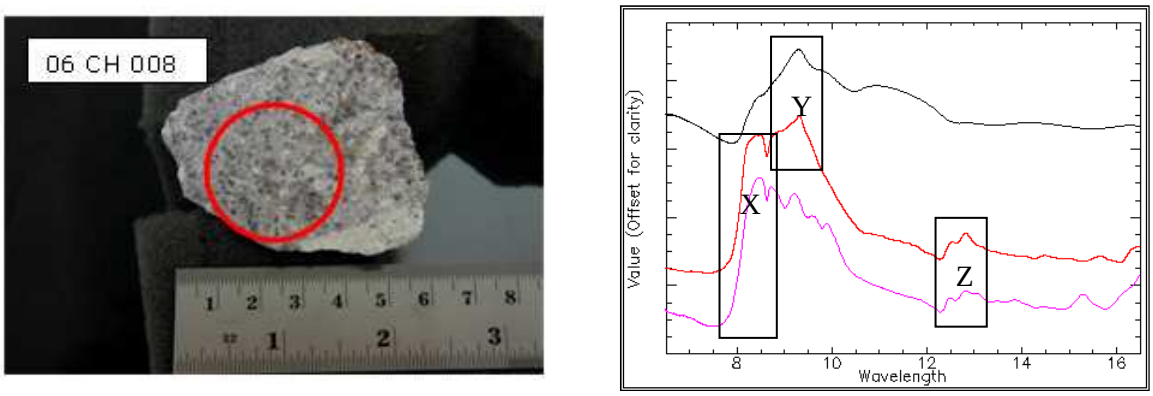

a b

Figure 5-23 (a) Rock sample 06 CH 008 photograph with red circle indicating the measurement boundary, (b) spectral measurement of 06 CH 008 (red) matched with spectral reference of heulandite (black) and andesine (purple)

Figure 5-23b shows the spectral measurement from rock sample 06 CH 008. As it is seen, the sample spectra matched the spectral reference from andesine and heulandite mineral. In the range 7.5- 9 µm wavelength, the rock sample spectrum was matched with the andesine spectral feature (Figure 5-23X). Moving to the longer wavelength, in the range of 9.5-10.5 µm, the sample spectra peak was matched with the reference spectra peak from heulandite mineral (Figure 5-23Y). In the range of 12.25-13.5 µm, the spectral features matched with the andesine spectral features (Figure 5-23Z).

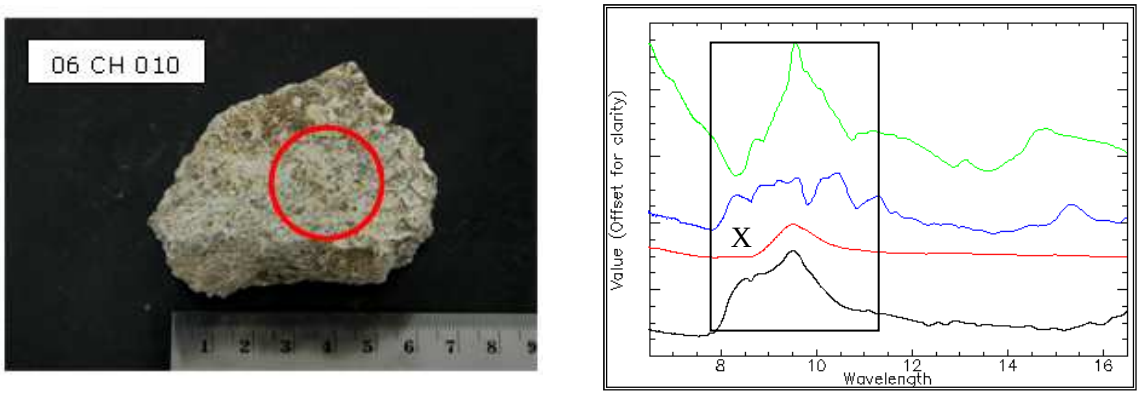

a b

Figure 5-24 (a) Rock sample 06 CH 010 photograph with red circle indicating the measurement boundary, (b) spectral measurement of 06 CH 010 (black) matched with spectral reference of antigorite (green); chrysocolla(red) and epidote(blue)

The spectral measurement from rock sample 06 CH 010 matched with spectral reference from antigorite, chrysocolla and epidote minerals (Figure 5-24b). We can see from the figure, that in the range 8- 11.5 µm wavelength, the rock sample spectrum was matched with peak and absorption features from the three minerals spectral feature (Figure 5-24X).

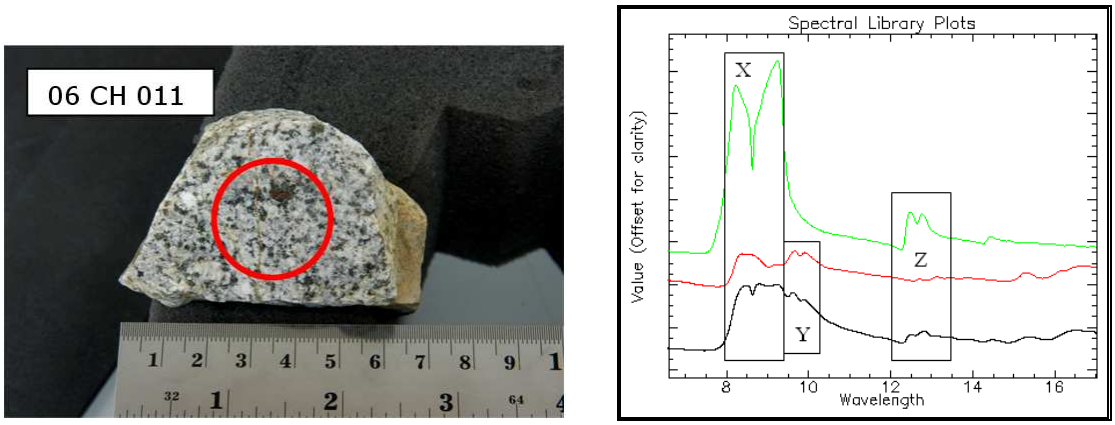

a **b**

Figure 5-25 (a) Rock sample 06 CH 011 photograph with red circle indicating the measurement boundary (b) Rock samples 06 CH 011 spectra analysis, where red is rock sample spectra, green is albite spectra reference and blue is quartz spectra reference (x) matched with albite reference (y)matched with quartz reference.

From Figure 5-25b it is seen the spectral measurement from rock sample 06 CH 011, the sample spectra matched with spectral reference from mineral albite and quartz minerals. In the range 8- 10 µm wavelength, the rock sample spectrum was matched with the albite spectral feature (Figure 5-25X). Moving towards the longer wavelength, in the range of 11.5-13.5 µm, the sample spectra was matched with the reference spectra from quartz mineral (Figure 5-25Y).

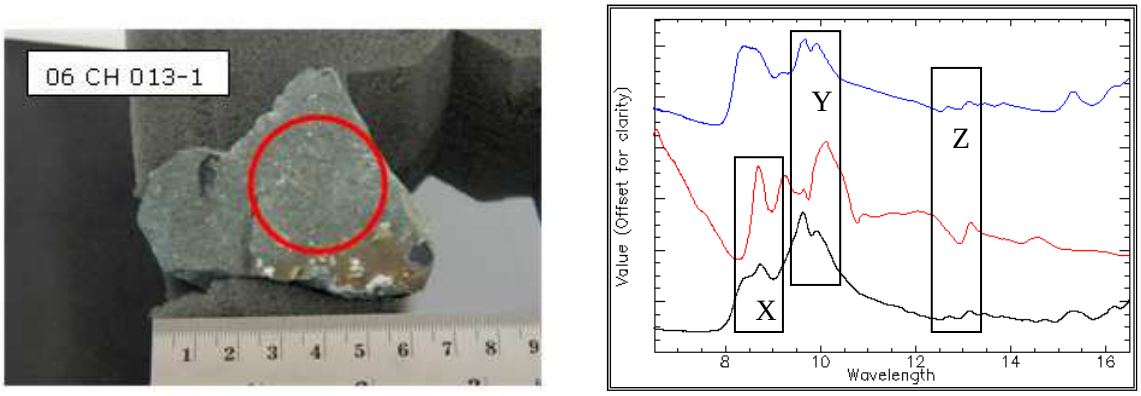

a b

Figure 5-26 (a) Rock sample 06 CH 013-1 photograph with red circle indicating the measurement boundary, (b) spectral measurement of 06 CH 013-1 (black) matched with spectral reference of albite (blue) and amphibole (red)

Figure 5-26b shows the spectral measurement from rock sample 06 CH 013-1 and the sample spectra matched with a good matching result with spectral reference from albite and amphibole minerals. In the range 7.5- 9 µm wavelength, the rock sample spectrum was matched with the amphibole spectral feature (Figure 5-26X). Moving to the longer wavelength, in the range of 9.5-10.5 µm, the sample spectra peak was matched with the reference spectra peak from albite mineral (Figure 5-26y) and in the range of 12.25-13.5 µm, respectively (Figure 5-26z).

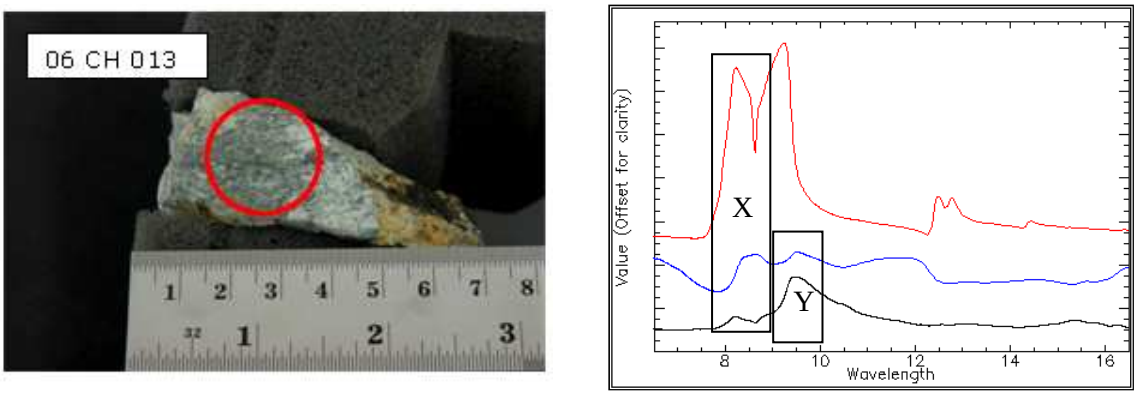

a b

Figure 5-27 (a) Rock sample 06 CH 013 photograph with red circle indicating the measurement boundary, (b) spectral measurement of 06 CH 013 (black) matched with spectral reference of quartz (red) and sanidine (blue).

The spectral measurement from rock sample 06 CH 013 matched with a spectral reference of sanidine and quartz minerals (Figure 5-28b). We can see from the figure, that in the range 7.5- 9.5 µm wavelength, the rock sample spectrum matches with peak and absorption features from the quartz mineral spectral feature (Figure 5-28x). In the range of 7.5- 9.5 µm the rock sample spectral peak matches with the peak from sanidine peak feature (Figure 5-28y).

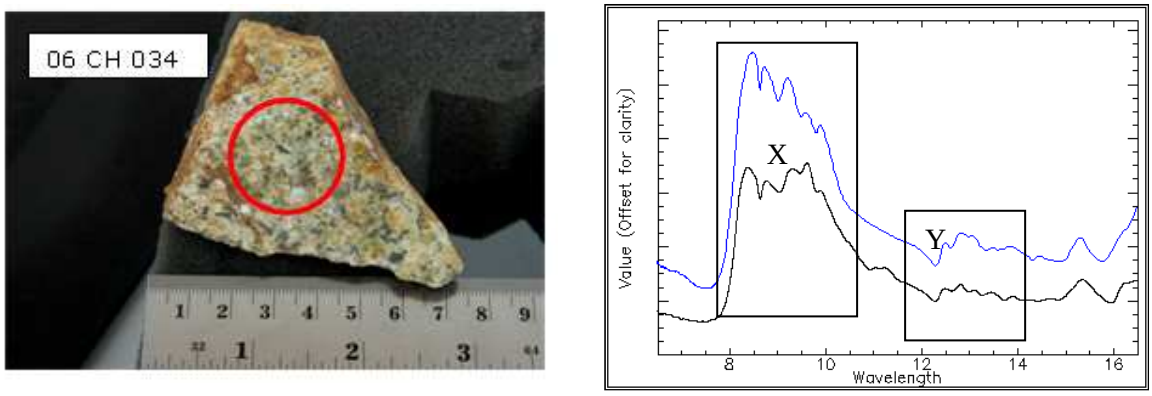

a b

Figure 5-28 (a) Rock sample 06 CH 034 photograph with red circle indicating the measurement boundary, (b) spectral measurement of 06 CH 034 (black) matched with spectral reference of andesine (blue)

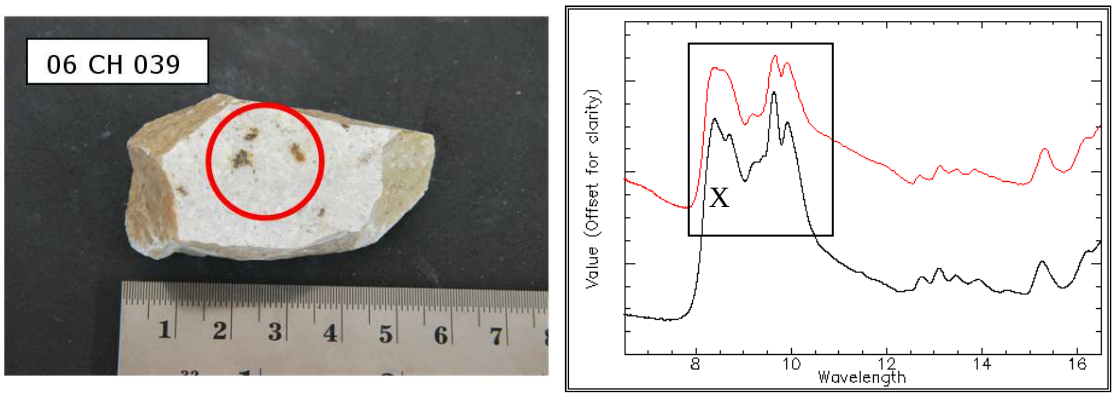

a **b**

Figure 5-29(a) Rock sample 06 CH 039 photograph with red circle indicating the measurement boundary, (b) spectral analysis of 06 CH 39 (black) matched with spectra of albite (red)

Figure 5-28b shows that the spectral measurement result from rock sample 06 CH 034 matches with spectral reference from andesine mineral. There is a good match between the rock sample spectra and the spectral reference. In the range 7.5- 10.5 µm and 11.5- 13.5 µm wavelengths, the rock sample spectral features were matched with the andesine spectral feature (Figure 5-28x and y).

The spectral measurement result from rock sample 06 CH 039 matched with spectral reference from albite (Figure 5-29b). From the shape and the position of the features was showing a good match between sample spectra and the reference spectra. We can see from the figure 529b, that in the range 8.5- 11 µm wavelengths, the rock sample spectrum was matched with albite spectral features (Figure 5-29x).

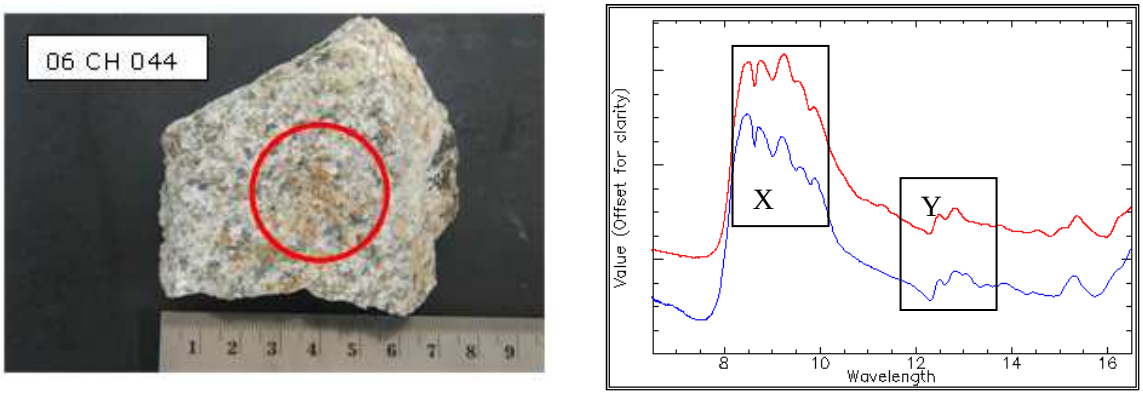

a b

Figure 5-30 (a) Rock sample 06 CH 044 photograph with red circle indicating the measurement boundary, (b) spectral measurement of 06 CH 044 (red) matched with spectral reference of andesine(blue)

From Figure 5-30b, it is shown that the spectral measurement result from rock sample 06 CH 044 matches the sample spectra with spectral reference from andesine mineral. In the range 7.5- 10.5 µm and 11.5- 13.5 µm wavelengths, the rock sample spectral features were matched with the andesine spectral feature (Figure 5-30x and y).

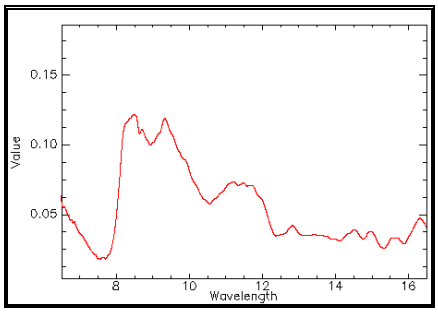

Figure 5-31 Unknown mineral spectra of 06 CH 057

From Figure 5-31, it is seen that the spectral measurement result from rock sample 06 CH 057, the sample spectra was try to be match visually with spectral mineral reference. The analysis does not fit with any spectra in the reference. Therefore, this kind of spectra is categorized as unknown mineral spectra.

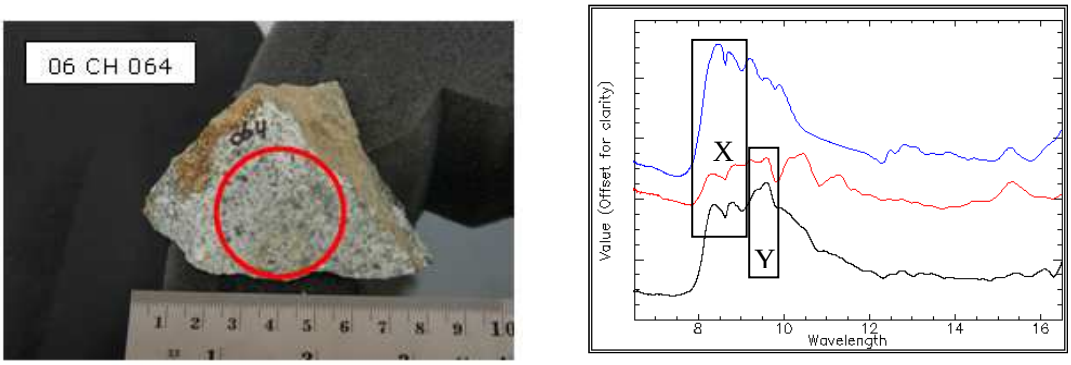

a b

Figure 5-32 (a) Rock sample 06 CH 064 photograph with red circle indicating the measurement boundary, (b) spectral measurement of 06 CH 064 (black) matched with spectral reference of andesine (blue) and epidote (red).

The spectral measurement from rock sample 06 CH 064 matched with spectral reference and andesine and epidote minerals (Figure 5-32b). We can see from the figure, that in the range 7.5-9.5 µm wavelengths, the rock sample spectrum was matched with peak and absorption features from the andesine mineral spectral feature (Figure 5-32x). In the range of 9.5-10 µm the rock sample spectral peak was matched with the peak from epidote peak feature (Figure 5-32y).

5.4. Alteration zones

In this part, the spectral measurements from the rock samples are plotted over the existing alteration mineral maps (Figure 5-16). There are three feldspar members that identified from rock samples in the study area and it was distributed along the alteration zones. . There are several alteration zones made by Enaudi (1995) such as K-silicate; propylitic; sodic-calcic and weak sericitic.

The results from the rock samples measurement was compared with the information from the literature, related to the alteration zones that were present in the study area. To build a better understanding about this relationship, the results from the rock samples TIR spectra was presented as a map and summarize as a table. From the map and the figure it was shown that the analysis is poorly correlated. The table that was summarized from Enaudi (1995) shows information about the present mineral in the alteration zones. The result did not fully match with the available information . However, the feldspars was present feldspar is matched with several alteration zones. In the pottasic zones, it was mention that the present plagioclase feldspar was changes to K-feldspar and in the spectral measurement shows that plagioclase feldspar are present. The present of plagioclase feldspar was shows by the present of albite and andesine. In this zone, andesine represent the changes from plagioclase feldspars to potassic feldspar.

In the next alteration zones, the sodic-calcic alteration zone shows the presence of potassium feldspar was changes into oligoclase. In these zones the result from the rock samples TIR spectra measurement show the present of albite. This result does not match with information that was built in the alteration zones map. Albite is categorized as plagioclase feldspar. It is not match with the information that shows in this alteration zones should be occupied by the alkali feldspar group.

The propylitic alteration zones show in the table 5-3 the presence of Oligoclase, K-feldspar and albite. The results from the rock samples TIR analysis shows the presence of andesine. This information also didn’t match with the information of mineral that exist in this alteration zones. From the table 5-3 also mention the feldspar mineral are present are close to the alkali feldspar. The result shows the presence of andesine in this alteration zone. This also shows a low correlation of the spectral measurement and the existing alteration zones information.

The presence of albite was shown in the sericitic alteration zones. The information in this alteration zones mentioned that feldspar was not present in this zone. This was unmatched with the result with the samples TIR measurement.

Table 5-3 Cross table between alteration zones and the mineral are present in the alteration zones.

Alteration Zones	**Important Mineral changes**	**Field samples measurement**
Potassic	• Hornblende and biotite→ Plogophyte • **Plagioclase→ K-feldspar**	• **Andesine** • **Albite**
sodic-calcic	• Hornblende & biotite → Actinolite • **K-Feldspar → oligoclase**	• **Albite**
Propylitic	• **Oligoclase, K-Feldspar**, Hornblende, biotite, Magnetite and sphene are remain • New mineral occur are actinolite, biotite, **albite**, epidote, Hematite, sericite , rutile, Pyrite, Tourmaline (chalcopyrite).	• **Andesine**
Sericitic	• Chalcopyrite is remain • Sericitic and quartz • **No feldspar**	• **Albite**

6. Discussion and Conclusion

6.1. Discussion

This study aimed at revealing the feldspar mineralogy and mineral chemistry using the thermal infrared wavelength range. Feldspar minerals are one of the useful parameter in the mineral exploration. It was related to the gold and base metal deposits. The spectral data for these mineral groups can help on revealing the mineralogy and mineral chemistry information, especially in the infrared wavelengths range. These mineral groups generally were sub dived into two subgroups; namely plagioclase and alkali feldspars.

The analysis to reveal wavelength facilitating feldspars identification used the latest spectral data from the USGS mineral spectral library. In this research, we have to consider this analysis in order to differentiate and classified the members of the feldspar groups in the spectral data respectively.

The rock samples were obtained from the Yerington area, Nevada states, USA. There are 51 samples. The samples were measured in the TIR wavelength with FT-IR spectrometer in order to get the spectral information from each of the samples. The mixture of mineral was influenced the spectra that was obtained from the measurement. However, the spectrum was able to recognize. For some spectra that cannot match with the reference spectral library, it was named unknown.

This following section contains answers to the research questions:

Which wavelengths do diagnostic absorption features in feldspar TIR spectra?

Characterization for plagioclase feldspar spectra in TIR wavelengths was shown in the range of 8- 10 microns (figure 6-1A). In this range, there are variation of spectrum used as a guide to classified feldspars. In plagioclase group, albite and andesine were showing spectral features in 12 to 16 µm wavelengths range. The plagioclase group was influenced by the changes in the chemical composition. The spectra difference for each member in plagioclase group were calculated, the result from reflectance minima position is resulting a pattern of changes due to the increasing of the percentage anorthite. The reflectance spectra minima were shifted towards the longer wavelengths when the percentages of anorthite were increasing However, there is an anomaly for andesine. Andesine was showing shifting position towards the shorter wavelength range.

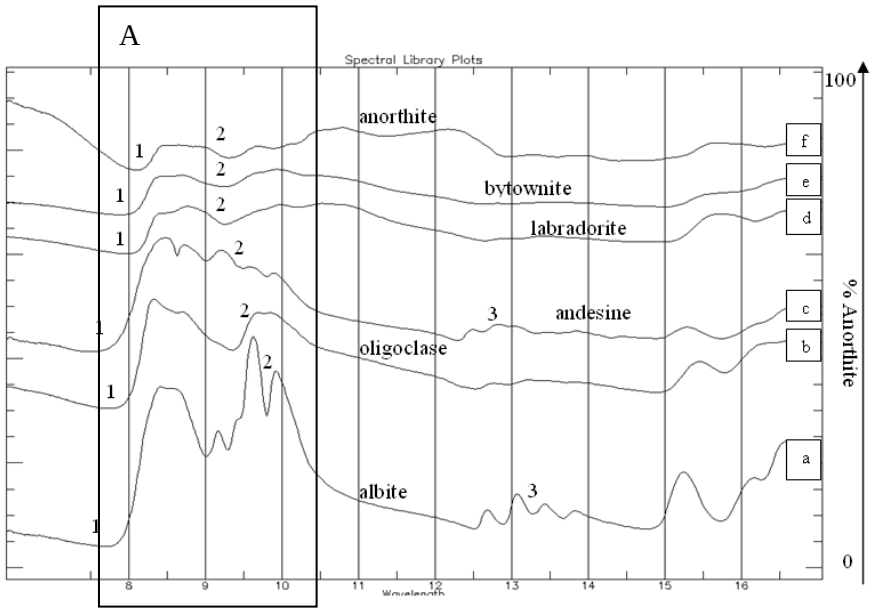

Figure 6-1 Plagioclase feldspar spectra library result

In the alkali feldspar group, the 8- 10 microns are important wavelengths regions to discriminate between its members (figure 6-1A). This group were calculated for the spectral difference as well as plagioclase group. The calculation was useful to show pattern changes for each member in this group, is the absorption band depth calculation. In this case, it was calculated using the emissivity spectra. The pattern was showing the decreasing of spectral absorption band depth from Ca rich feldspar to K-rich feldspar in alkali feldspars group.

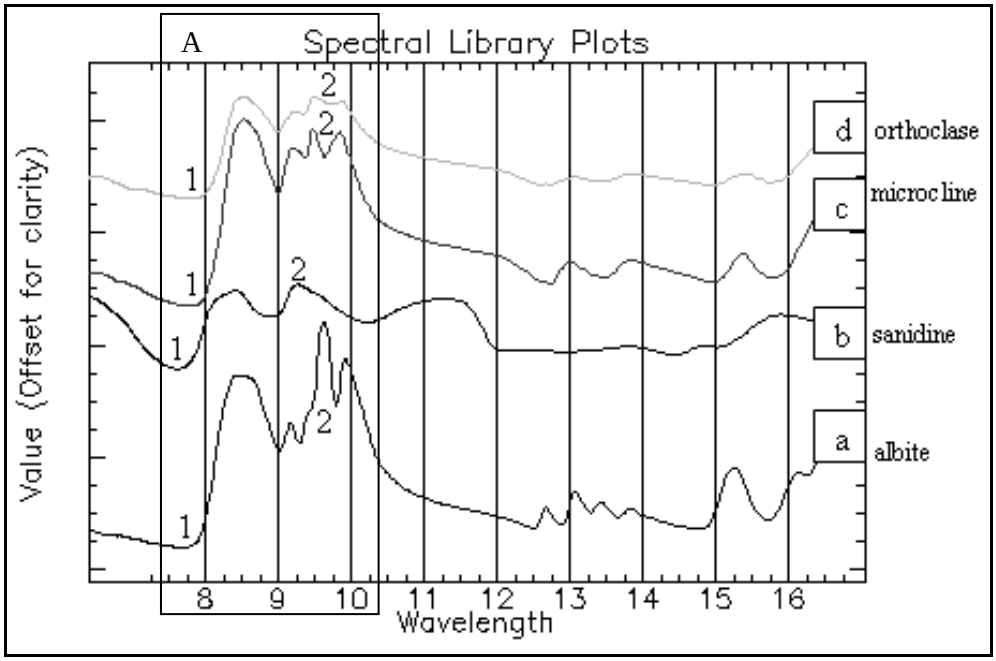

Figure 6-2 Alkali feldspar spectral library

In this observation the spectra data also was varying in grain size in the measured samples. . It is different when we compare it with the result from (Nash and Salisbury, 1991); their observations were showing a systematical pattern in the reflectance minima position for plagioclase members. In their observation they used the same powdered grain size samples.

Can feldspars mineralogy of field samples of Yerington area be determined using TIR spectroscopy?

Analysis of field samples reveals classification of mineralogy in the study area. Three members of feldspar resulted from 51 samples that were measured in TIR wavelengths, namely: albite, andesine and sanidine. Albite can be classified as alkali and plagioclase feldspars. Sanidine is alkali feldspar member and andesine is a plagioclase group member.

Several feldspars member were present in the various alteration zones. The alteration zones are based on the previous researcher work. The sampling points were plotted overlaid on the alteration map zones. There are 4 four alteration zones were filled with feldspars mineral. In this alteration zones, the presents of feldspars are not match with the information from the alteration reference zones.

The feldspar mineralogy was determined from the field samples measurement; however, the results do not match with the existing information about the presence of minerals for each alteration zones. This could caused mineralogy that were resulting from the TIR should be combined with other method, such as SWIR wavelength analysis, microprobe and XRD analysis. These results are summarized in table 5-3.

6.2. Conclusions

- The thermal infrared wavelength range was suitable for identifying the spectra of feldspar minerals. With the variation of absorption features and peaks are vary and visible for observation in this wavelength region.

- The differences of grain size in the samples can influence the spectral result. It is shown in the several spectra with fine grain size was showing a hilly shape in the 10-12µm wavelength region.

- The ordered and disordered albite polymorph types are visible in the albite spectral data, the different shape of albite spectra and the spectral reflectance value showed it.

- The reflectance minima position or known as the Christiansen frequency was useful for determining the members of plagioclase feldspar group.

- Determination of spectral width in the range of 7-9 µm helps to determine the mineralogy of alkali feldspar.

- The rock samples spectra measurement in TIR wavelengths region are poorly correlated with the existing alteration zones map.

6.3. Recomendations

- SWIR wavelength analysis should be conducted, in order to help for unmixed the mineral spectra determination in the rock samples.

- Origin, presence of impurity, physical properties of mineral and degree of weathering should be taken into account in order to get clear understanding of pure feldspar spectra characteristic

- X ray diffraction and microprobe analysis should be conducted, in order for comparison in mineralogical identification of the rock samples from the study area.

- Further study should be carried out to get spatial distribution of alteration zones of the study area using the spectral characteristic that were identified in this research.

Reference

Clark, R.N., Swayze, G.A., Wise, R., Livo, E., Hoefen, T., Kokaly, R., and Sutley, S., 2007, **USGS Digital Spectral Library splib06a** U.S. Geological Survey.

Cudahy, T.J., Hewson, R., Roache, A., Caccetta, M., Yang, K., Whitbourn, L., Connor, P., Coward, D., and Mason, P., submitted, Drill Core Logging of Feldspar Composition and Other Minerals Associated with Archaean Gold Mineralisation at Kambalda, Western Australia, Using a Bi-Directional Thermal Infrared Reflectance System, P2007/19, CSIRO Exploration & Mining.

Cudahy, T.J., Okada, K., Yamato, Y., Cornelius, A., and Hewson, R., 2001a, Mapping tha Skarn-Porphyry-Epithermal alteration system at Yeringtin, Nevada, Using VNIR-SWIR-TIR remotely sensed data, 1121R, CSIRO Exploration and Mining.

Cudahy, T.J., Wilson, J., Hewson, R., Linton, P., Harris, P., Sears, M., Okada, K., and Hackwell, J.A., 2001b, Mapping Variations in Plagioclase Felspar Mineralogy Using Airborne Hyperspectral TIR Imaging Data.

Deer, W.A., Howie, R.A., and Zussman, J., 1966, introduction to the rock - forming minerals: London, Longman, 528 p.

—, 2001, Framework silicates : Feldspars: London, Geological Society of London, 972 p.

Dilles, J.H., Enaudi, M.T., Proffett, J., and Barton, M.D., 2001, Overview of the Yerington Porphyry Copper District: Magmatic and nonmagmatic sources of Hydrothermal Fluids: Their Flow paths and alteration effects on rocks and Cu-Mo-Fe-Au Ores.

Enaudi, M.T., 1994, 6-km Vertical Cross Section Through Porphyry Copper Depposits, Yerrington District, Nevada :Multiple Intrusions, Fluids, and Metal Sources Society of Economic Geologist international exchange lecture.

Hecker, C.A., 2006, Geologic Surface Compositional Mapping from Thermal Infrared SEBASS Data.

Nash, D.B., and Salisbury, J.W., 1991, Infrared reflectance spectra of plagioclase feldspars: geophysical research letters, v. 18, p. 1551-1154.

Pirajno, F., 1992, Hydrothermal mineral deposits : principles and fundamental concepts for the exploration geologist: Berlin etc., Springer-Verlag, 709 p.

Smith, J.V., and Brown, W.L., 1988, Feldspar minerals : Vol. 1. Crystal structures, physical, chemical, and microtextural properties: Berlin etc., Springer-Verlag, 828 p.

Stuart, B.H., 2004, Infrared spectroscopy : fundamentals and applications: Chichester etc., Wiley & Sons, 224 p.

Appendices

Appendix 1. Technical information for bruker vertex 70 TIR measurement

BASIC

Experiment	:	Sphere_MCT_wardhana_Msc.XPM
Operator name	:	Administrator
Sample description	:	06CH032
Sample form	:	Sample form
Path	:	D:\wardhana
File name	:	06CH032

ADVANCED

Experiment	:	Sphere_MCT_wardhana_Msc.XPM
File name	:	<@Snm>
Path	:	D:\wardhana
Resolution	:	8 cm^{-1}
Sample scan time	:	4096 scans
Background scan time	:	4096 scans
Save data file from	:	7000 cm^{-1} to 500 cm^{-1}
Result spectrum	:	Reflectance

Data to be saved			
V	Reflectance	v	Phase spectrum
v	Single channel	v	Background
v	Sample interferogram	v	Background interferogram

OPTIC

External synchronization	:	Off
Source setting	:	Backward input
Beam splitter	:	KBr
Optical filter setting	:	Open
Aperture setting	:	8 mm
Accessory	:	Any
Measurement channel	:	Right front exit
Background measurement channel	:	Right front exit
Detector setting	:	MCT on sphere (external)
Scanner velocity	:	40 KHz
Sample signal gain	:	Automatic
Background signal gain	:	Automatic
Delay after device change	:	0
Delay before measurement	:	0
Optical bench reag	:	Off

ACQUISITION

Wanted high frequencies limit	:	15,000 : 15796.97 cm-1
Wanted low frequencies limit	:	0 : 0.00 cm-1
Laser wave number	:	1576.97
Interverogram size	:	14216 points
FT sizer	:	16K
High pass filter	:	Open
Low pass filter	:	40 KHz
Acquisition mode	:	Double sided; forward backward
Correlation mode	:	Off
External analog signals	:	No analog value

FT

Phase resolution	:	32
Phase interferogram points	:	1777
Phase correction mode	:	Mertz
Apodization function	:	Happ-Genzel
Zero filling factor	:	1

sample number	**Mineral**
06CH 001	Epidote + quartz
06CH 003	Epidote + sanidine
06CH 039	Quartz + albite
06CH 004	Quartz + andesine
06CH 005	Andesine + illite
06CH 006-1	Montmorilonite
06CH 006	Montmorilonite
06CH 007	Quartz
06CH 008	Andesine + heulandite .+ quartz
06CH 009	glauchophane
06CH 010	Antigorite +chrysocolla + epidote
06CH 011	Albite + quartz
06CH 12-1	Andesine + quartz
06CH 12-2	Andesine
06CH 12-3	Andesine + quartz
06CH 12	Andesine + quartz
06CH 013-1	Albite + amphibole
06CH 013	Quartz + sanidine
06CH 014-1	Unknown

sample number	Mineral
06CH 014	Unknown
06CH 015	Andesine
06CH 022	Unknown
06CH 023	Andesine
06CH 028	Quartz + illite
06CH 028b-2	Unknown
06CH 028b1	Unknown
06CH 029	Andesine + quartz
06CH 029b-1	Andesine + quartz
06CH 029b	Unknown
06CH 032	Andesine
06CH 033-1	Labradorite
06CH 033	Andesine
06CH 034	Andesine
06CH 035	Andesine
06CH 037	Andesine
06CH 038	Andesine
06CH 043	Andesine
06CH 044-1	Andesine
06CH 044	Andesine
06CH 046	Andesine
06CH 047	Unknown
06CH 049	Andesine
06CH 051	Andesine
06CH 057	Unknown
06CH 058	Epidote
06CH 060	Andesine
06CH 62-1	Unknown
06CH 062	Unknown
06CH 064	Andesine + epidote
06CH 066-1	Unknown
06CH 066	albite
06CH 068	Andesine + epidote
06CH 069	Quartz + andesine
06CH 070-1	Unknown
06CH 070	Andesine + epidote
06CH 072-1	Andesine
06CH 072	Andesine
06CH 074	Unknown
06CH 075	Unknown
06CH 076	Unknown
06CH 077-1	Unknown

sample number	Mineral
06CH 077	Unknown
06CH 078	Unknown
06CH 080	Unknown
06CH 081-1	Quartz
06CH 081	Quartz

Appendix 2 Fields samples photograph

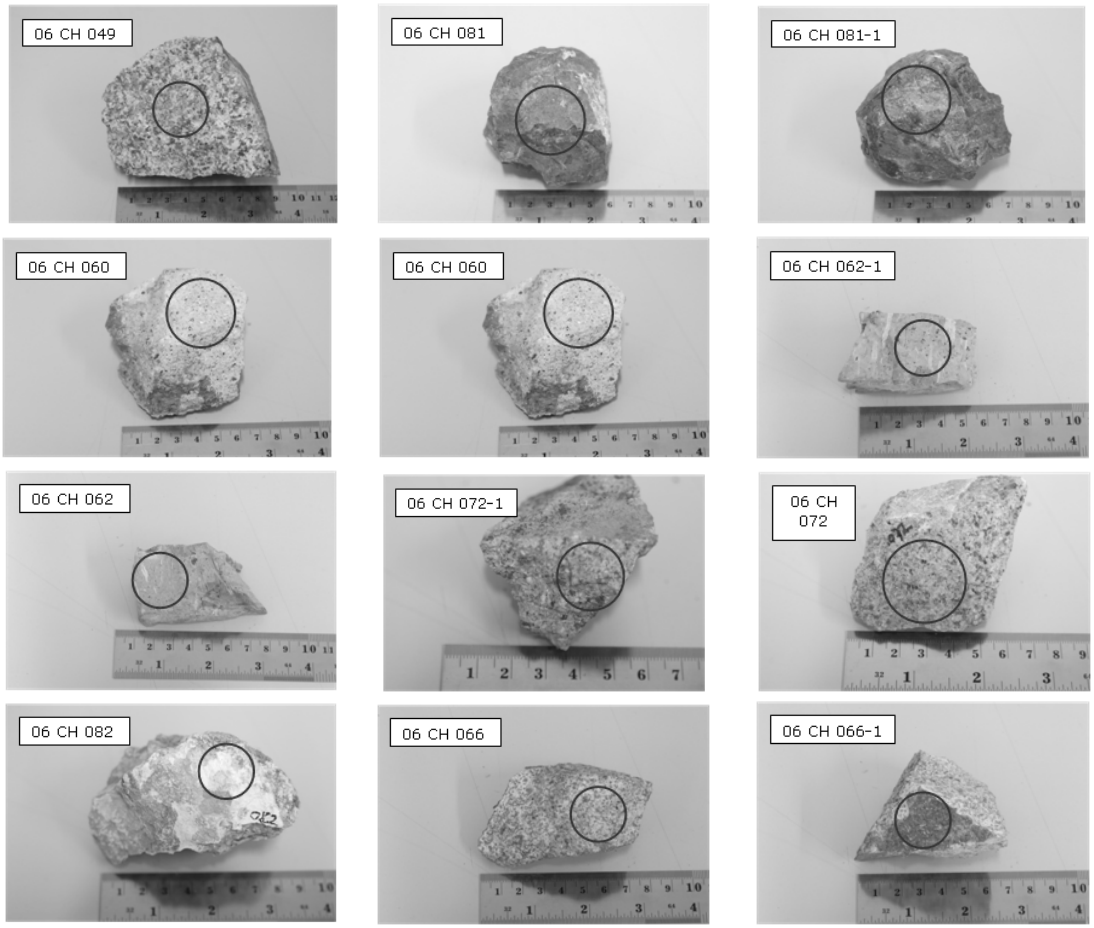

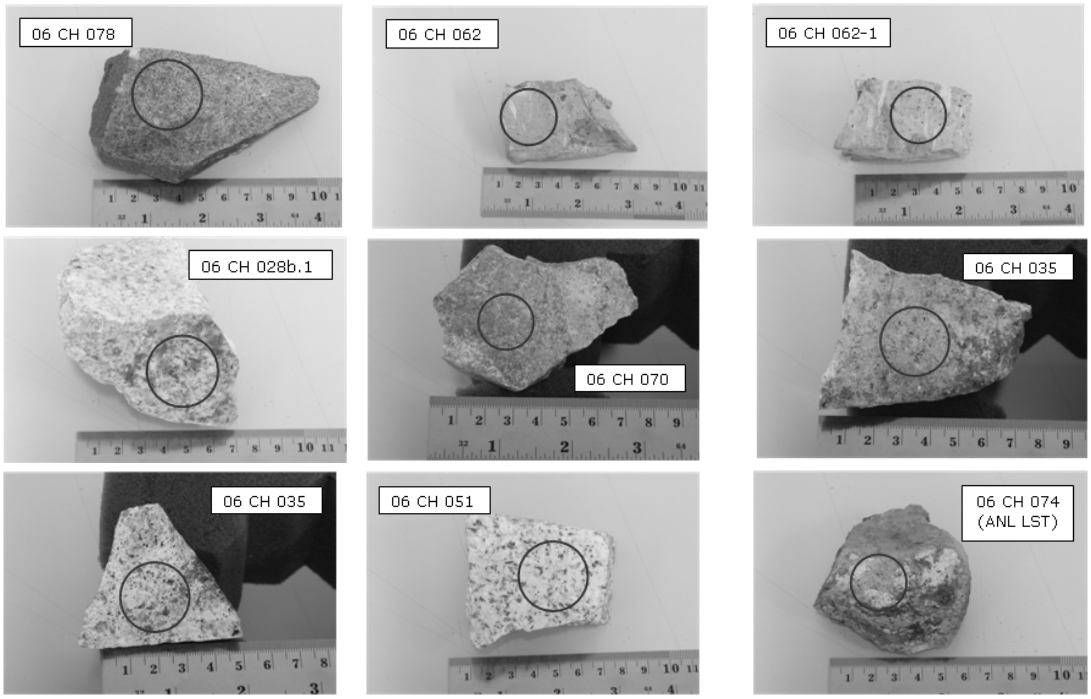
06 CH 078
06 CH 062
06 CH 062-1
06 CH 028b.1
06 CH 070
06 CH 035
06 CH 035
06 CH 051
06 CH 074
(ANL LST)

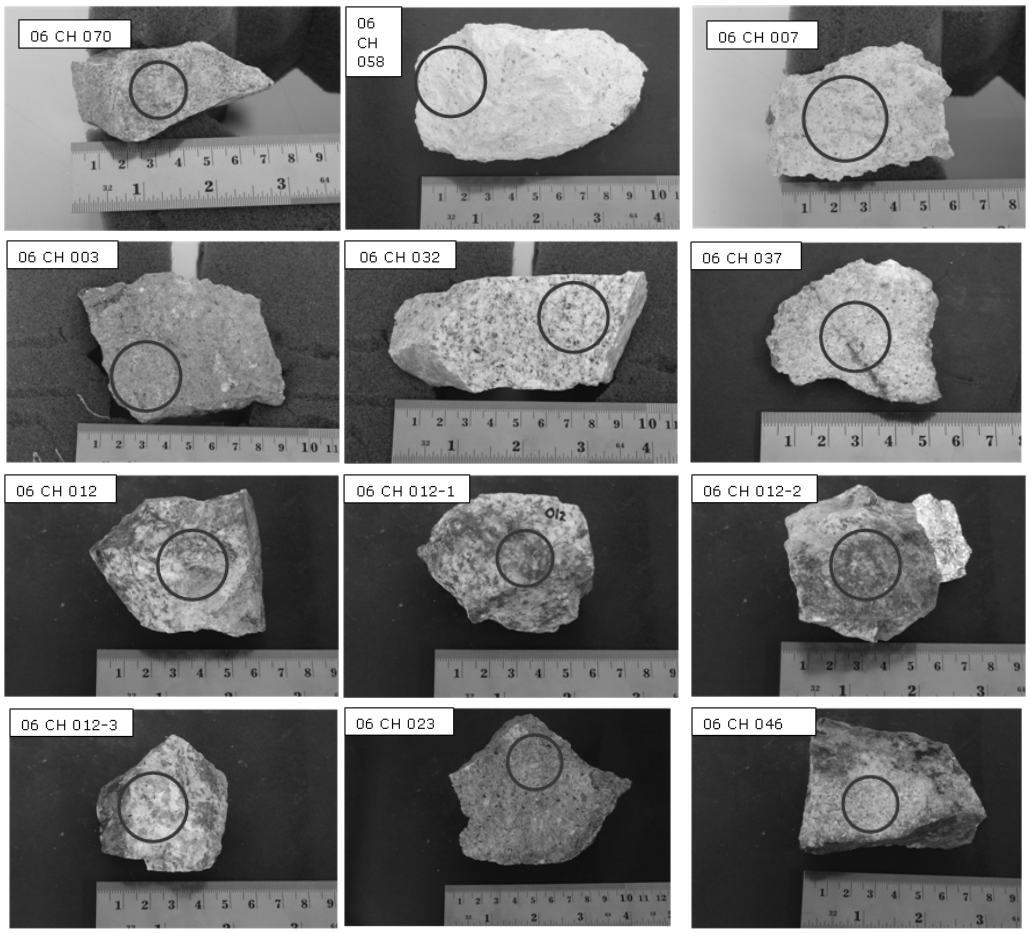
06 CH 070
06
CH
058
06 CH 007
06 CH 003
06 CH 032
06 CH 037
06 CH 012
06 CH 012-1
06 CH 012-2
06 CH 012-3
06 CH 023
06 CH 046

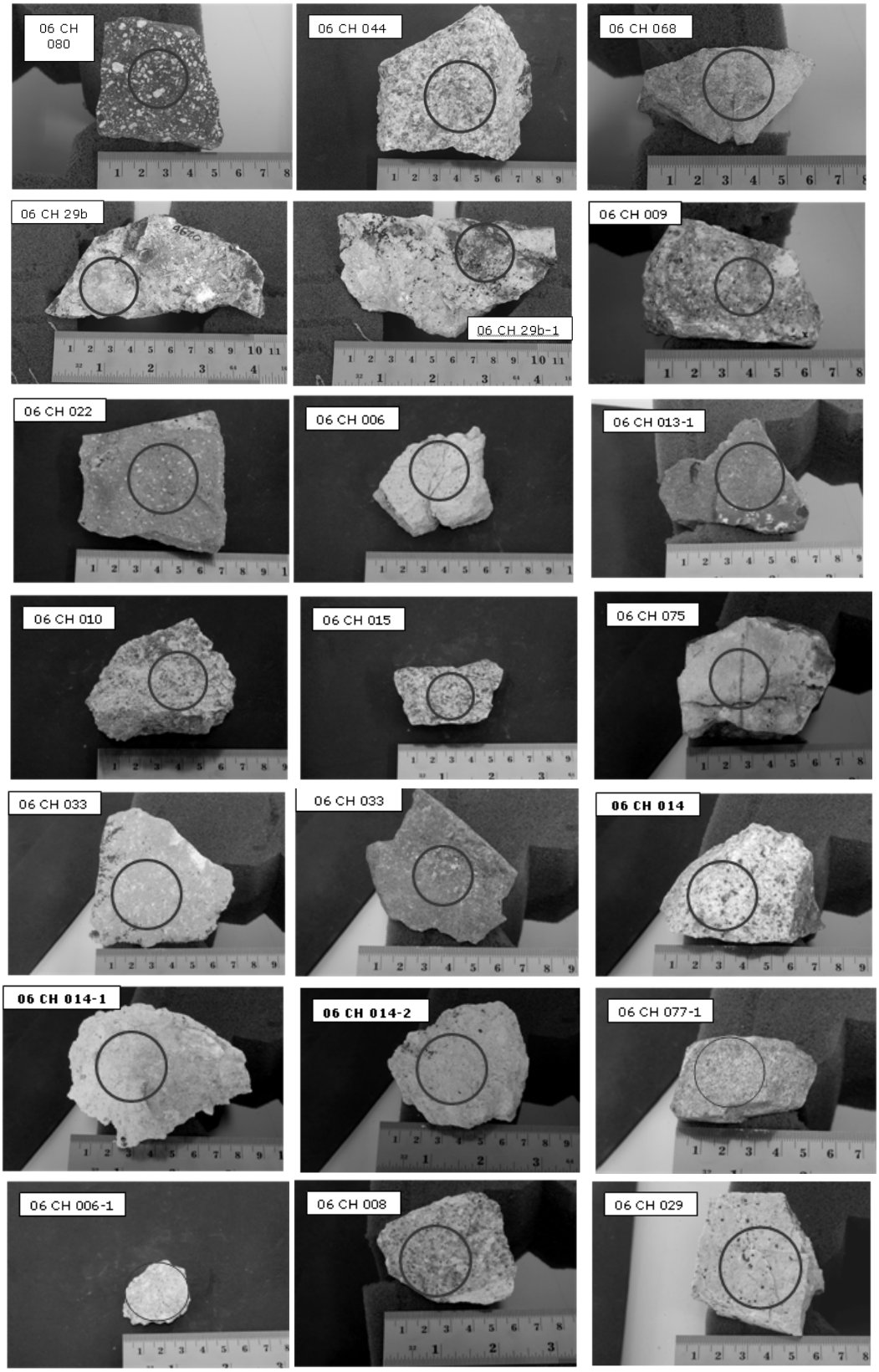
06 CH 080
06 CH 044
06 CH 068
06 CH 29b
06 CH 29b-1
06 CH 009
06 CH 022
06 CH 006
06 CH 013-1
06 CH 010
06 CH 015
06 CH 075
06 CH 033
06 CH 033
06 CH 014
06 CH 014-1
06 CH 014-2
06 CH 077-1
06 CH 006-1
06 CH 008
06 CH 029

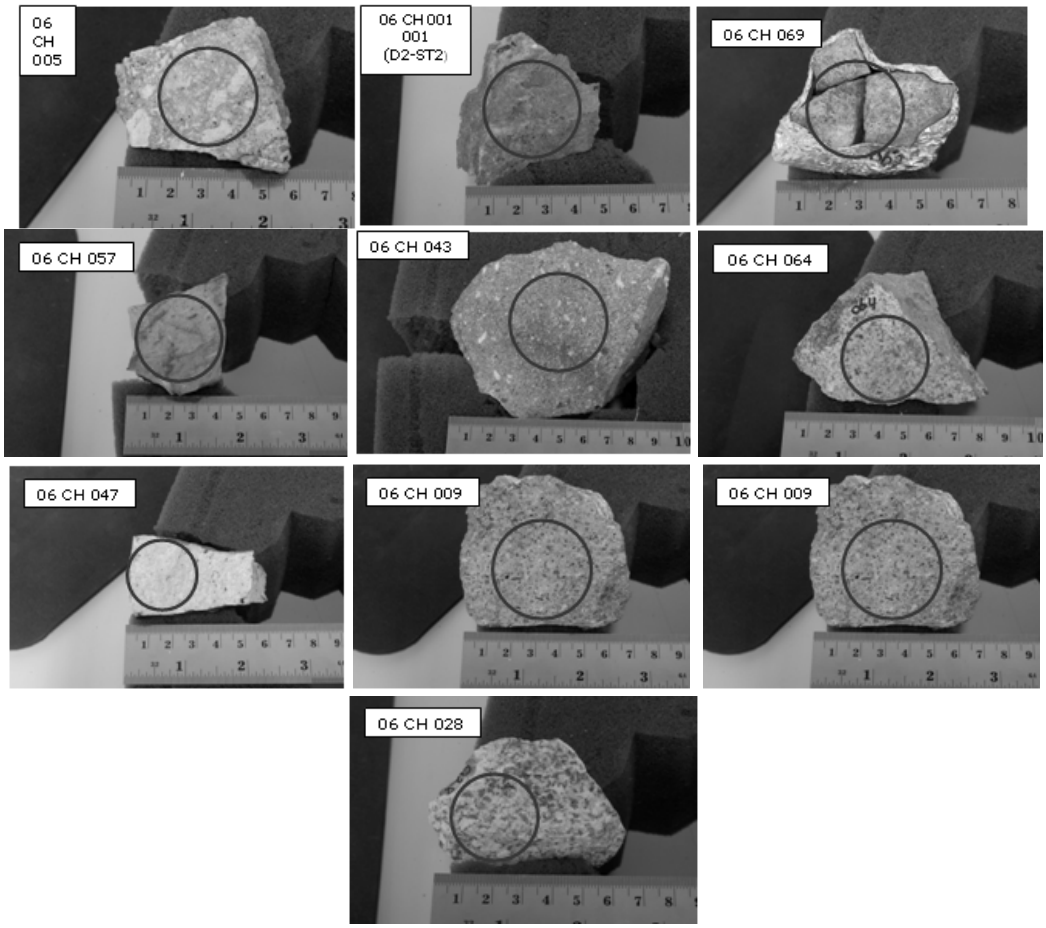
06
CH
005
06 CH 001
001
(D2-ST2)
06 CH 069
06 CH 057
06 CH 043
06 CH 064
06 CH 047
06 CH 009
06 CH 009
06 CH 028

Appendix 3 rock samples TIR spectra

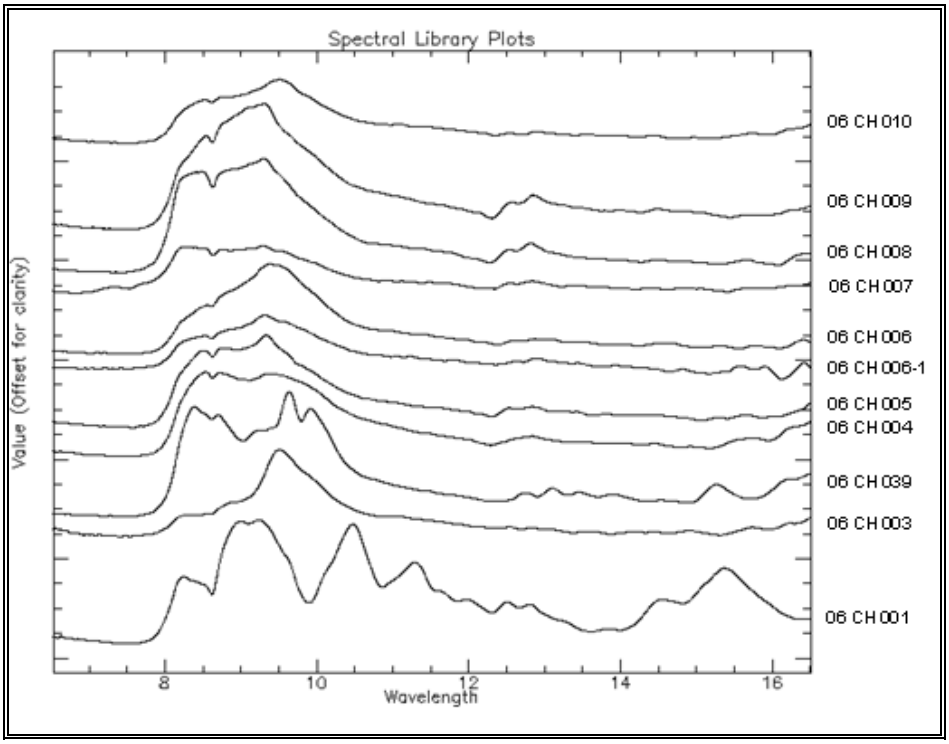

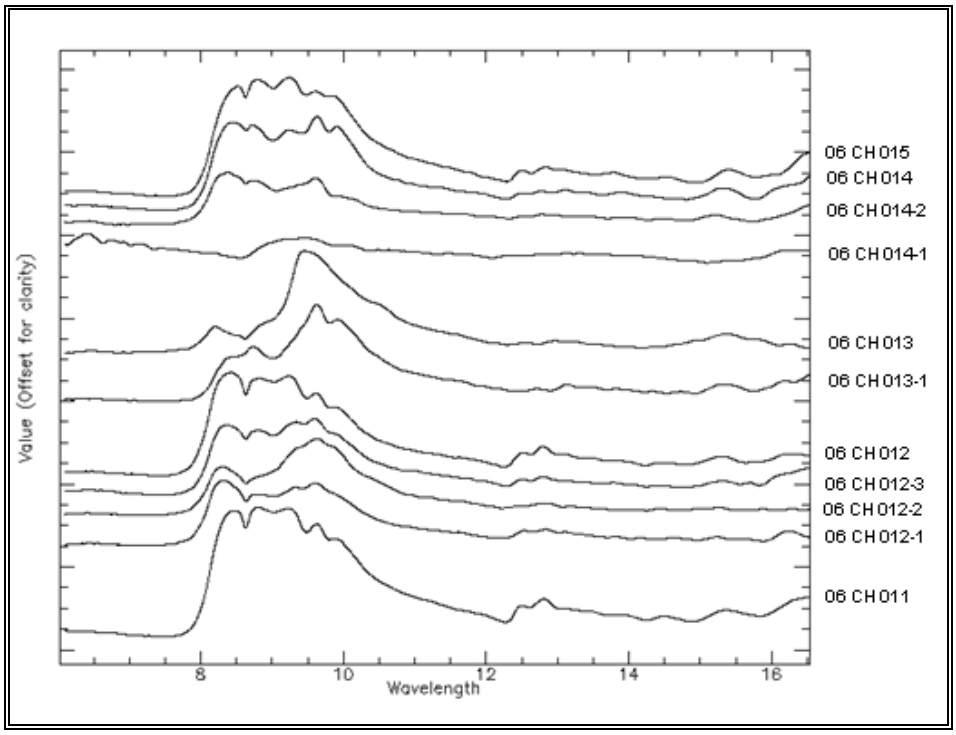

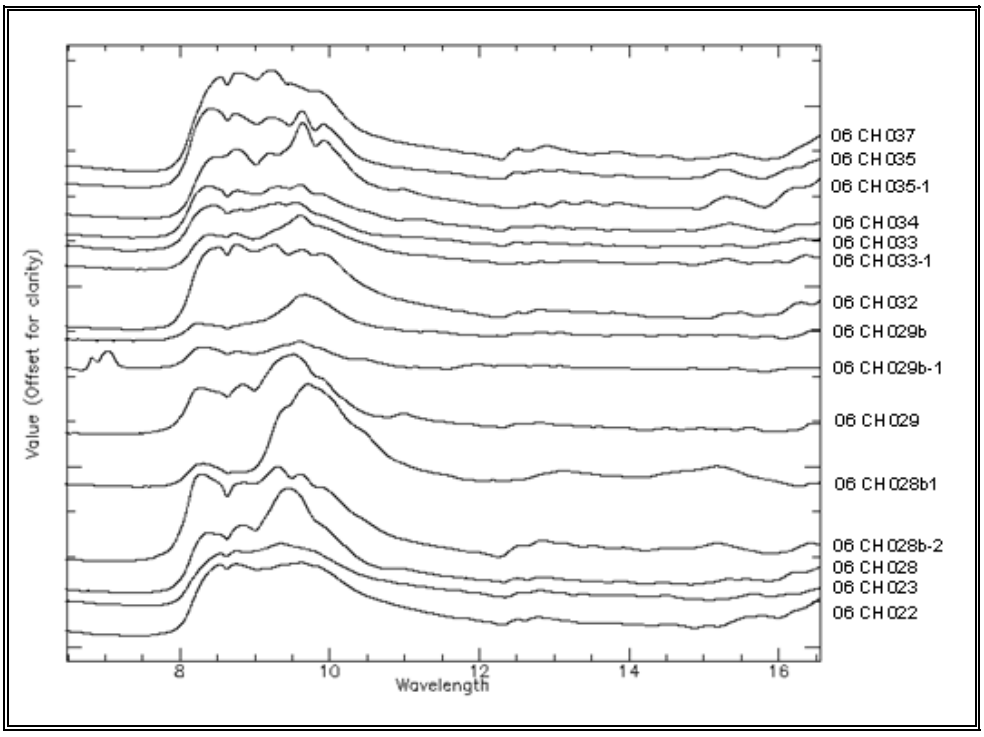
Value (Offset for clarity)
Wavelength
8
10
12
14
16
06 CH 037
06 CH 035
06 CH 035-1
06 CH 034
06 CH 033
06 CH 033-1
06 CH 032
06 CH 029b
06 CH 029b-1
06 CH 029
06 CH 028b1
06 CH 028b-2
06 CH 028
06 CH 023
06 CH 022

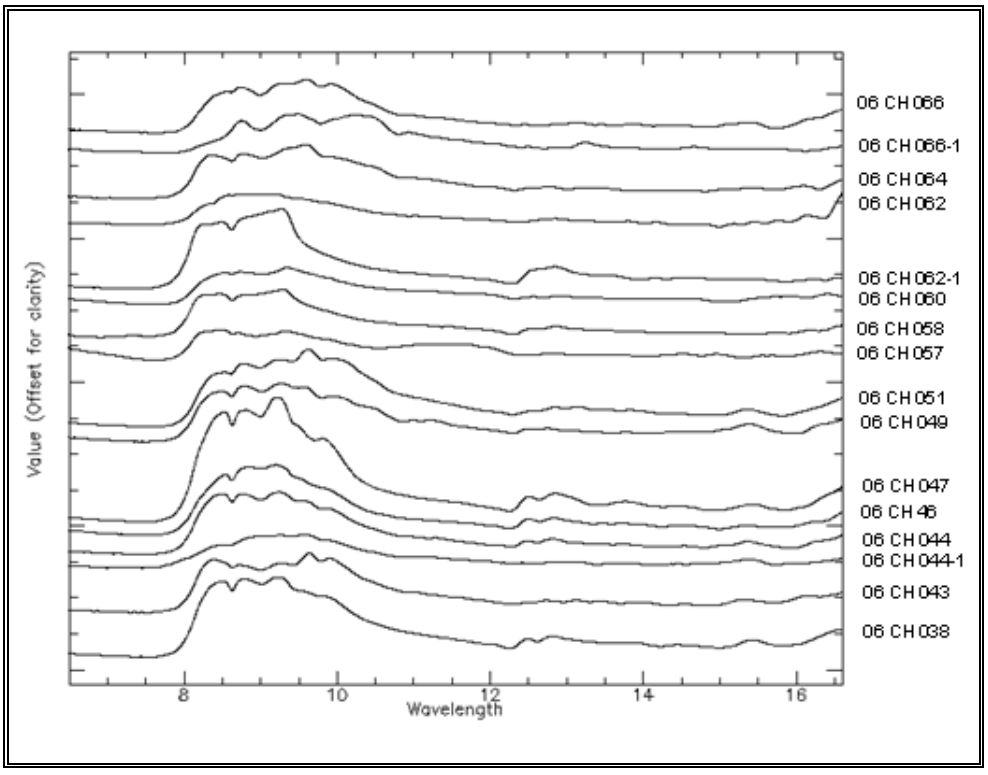
Value (Offset for clarity)
Wavelength
8
10
12
14
16
06 CH 066
06 CH 066-1
06 CH 064
06 CH 062
06 CH 062-1
06 CH 060
06 CH 058
06 CH 057
06 CH 051
06 CH 049
06 CH 047
06 CH 46
06 CH 044
06 CH 044-1
06 CH 043
06 CH 038

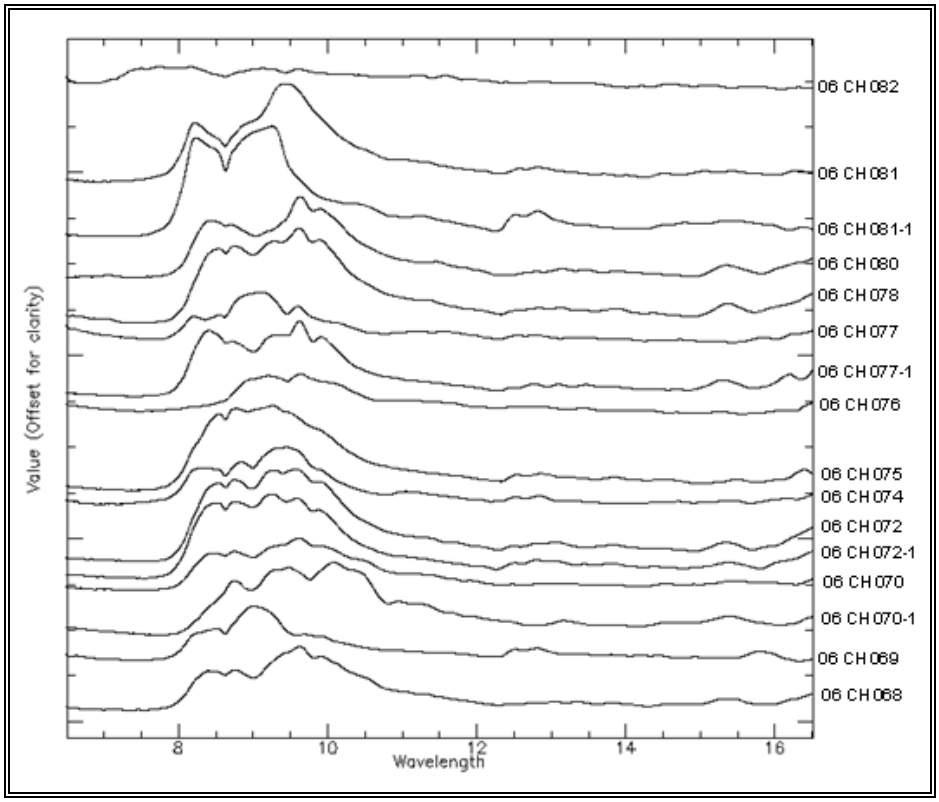

Appendix 4 dispec calculation result

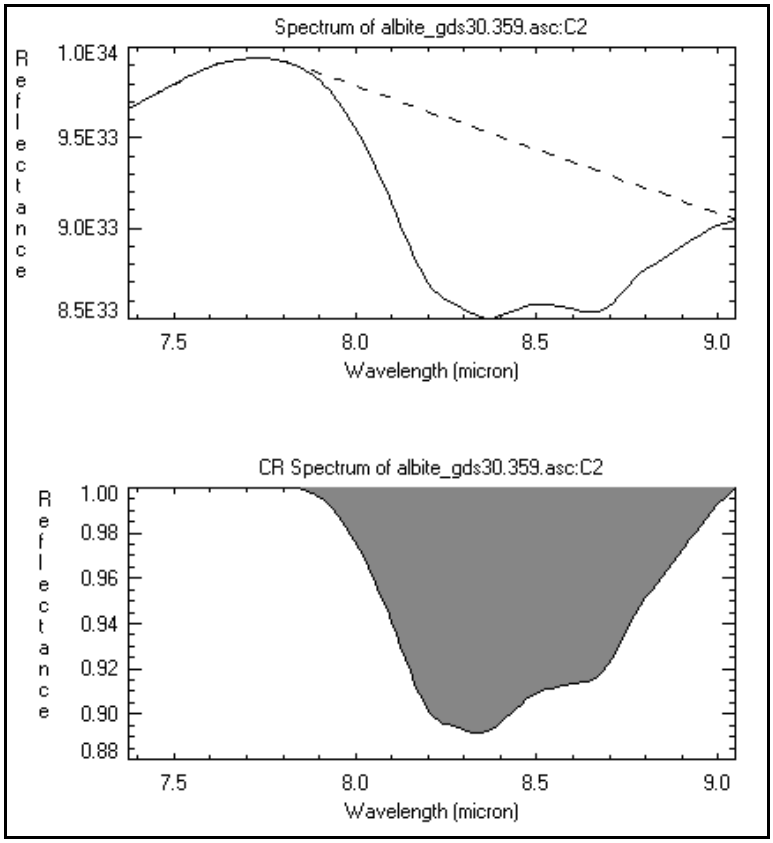

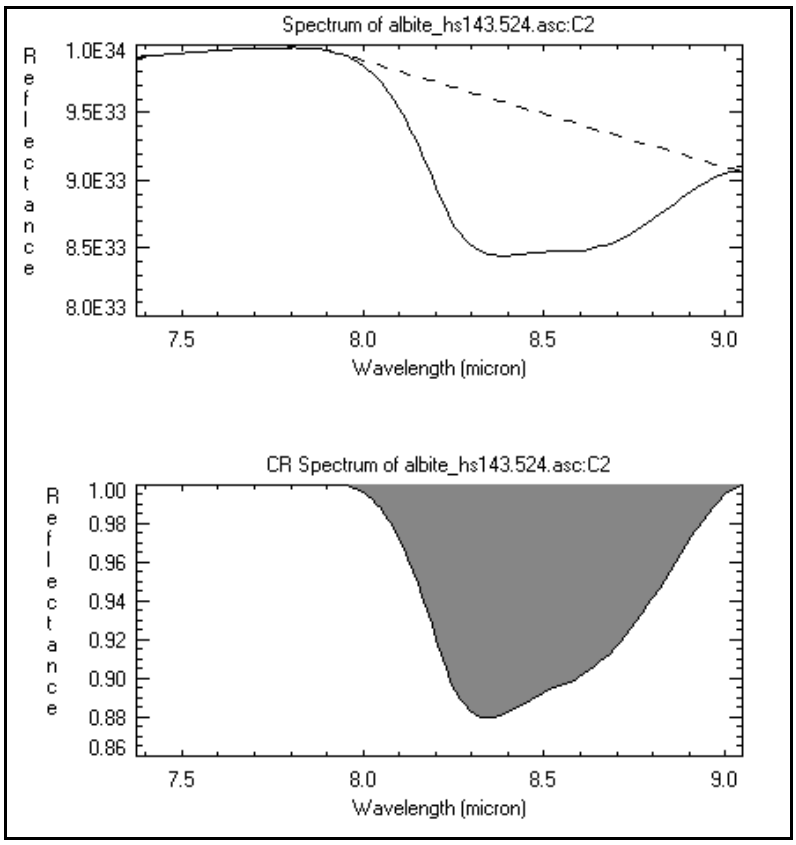
Spectrum of albite_hs143.524.asc:C2
Reflectance
1.0E34
9.5E33
9.0E33
8.5E33
8.0E33
7.5
8.0
8.5
9.0
Wavelength (micron)
CR Spectrum of albite_hs143.524.asc:C2
Reflectance
1.00
0.98
0.96
0.94
0.92
0.90
0.88
0.86
7.5
8.0
8.5
9.0
Wavelength (micron)

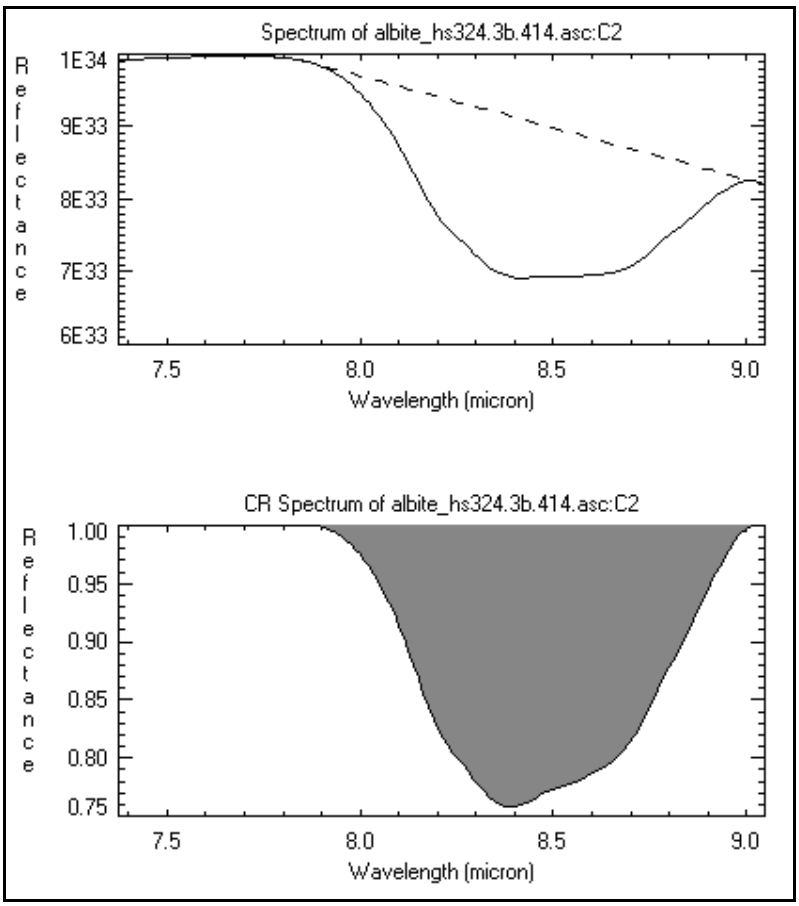
Spectrum of albite_hs324.3b.414.asc:C2
Reflectance
1E34
9E33
8E33
7E33
6E33
7.5
8.0
8.5
9.0
Wavelength (micron)
CR Spectrum of albite_hs324.3b.414.asc:C2
Reflectance
1.00
0.95
0.90
0.85
0.80
0.75
7.5
8.0
8.5
9.0
Wavelength (micron)

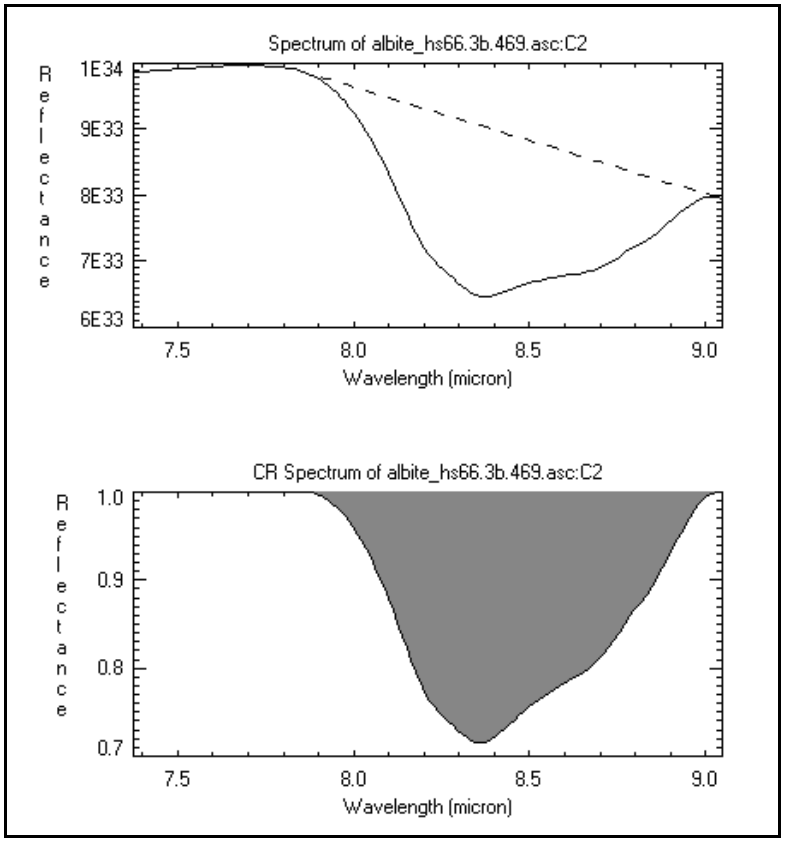
Spectrum of albite_hs66.3b.469.asc:C2
Reflectance
1E34
9E33
8E33
7E33
6E33
7.5
8.0
8.5
9.0
Wavelength (micron)
CR Spectrum of albite_hs66.3b.469.asc:C2
Reflectance
1.0
0.9
0.8
0.7
7.5
8.0
8.5
9.0
Wavelength (micron)

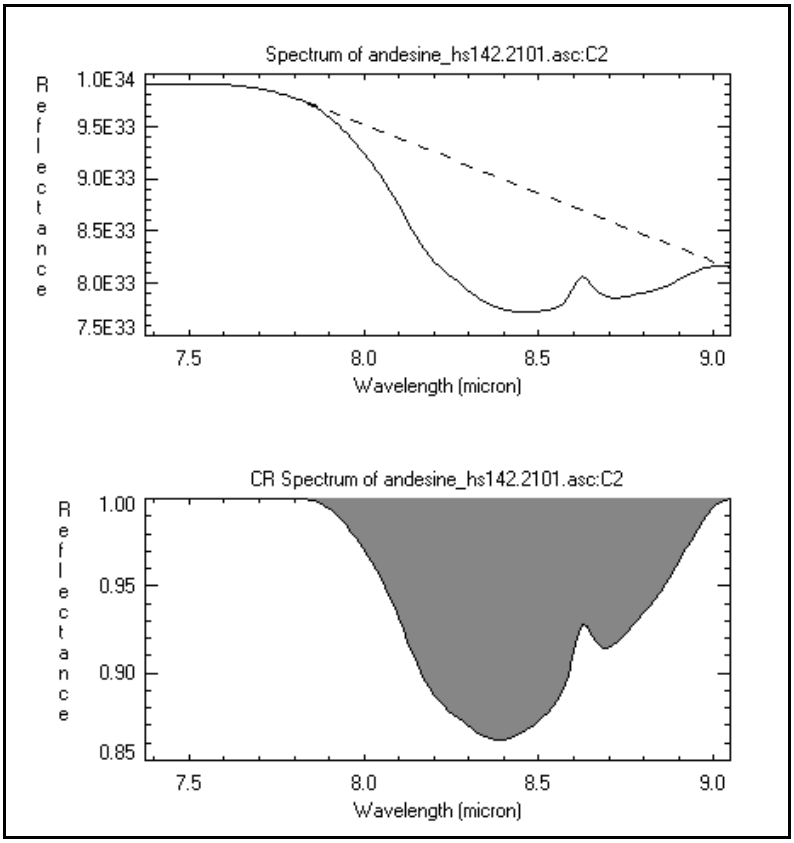
Spectrum of andesine_hs142.2101.asc:C2
Reflectance
1.0E34
9.5E33
9.0E33
8.5E33
8.0E33
7.5E33
7.5
8.0
8.5
9.0
Wavelength (micron)
CR Spectrum of andesine_hs142.2101.asc:C2
Reflectance
1.00
0.95
0.90
0.85
7.5
8.0
8.5
9.0
Wavelength (micron)

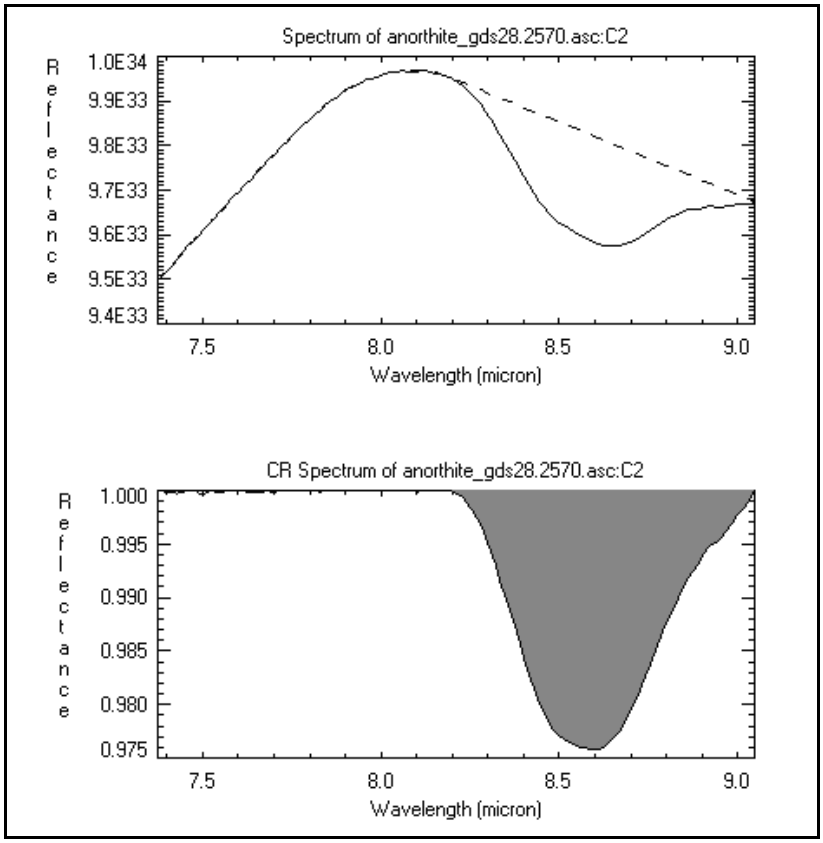
Spectrum of anorthite_gds28.2570.asc:C2
Reflectance
1.0E34
9.9E33
9.8E33
9.7E33
9.6E33
9.5E33
9.4E33
7.5
8.0
8.5
9.0
Wavelength (micron)
CR Spectrum of anorthite_gds28.2570.asc:C2
Reflectance
1.000
0.995
0.990
0.985
0.980
0.975
7.5
8.0
8.5
9.0
Wavelength (micron)

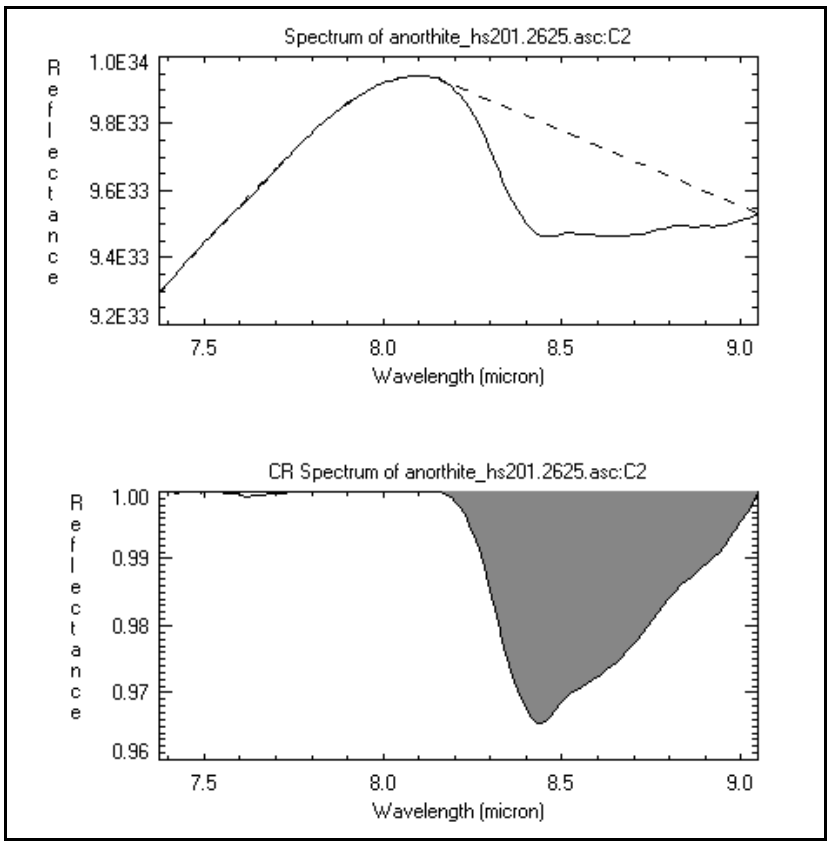
Spectrum of anorthite_hs201.2625.asc:C2
Reflectance
1.0E34
9.8E33
9.6E33
9.4E33
9.2E33
7.5
8.0
8.5
9.0
Wavelength (micron)
CR Spectrum of anorthite_hs201.2625.asc:C2
Reflectance
1.00
0.99
0.98
0.97
0.96
7.5
8.0
8.5
9.0
Wavelength (micron)

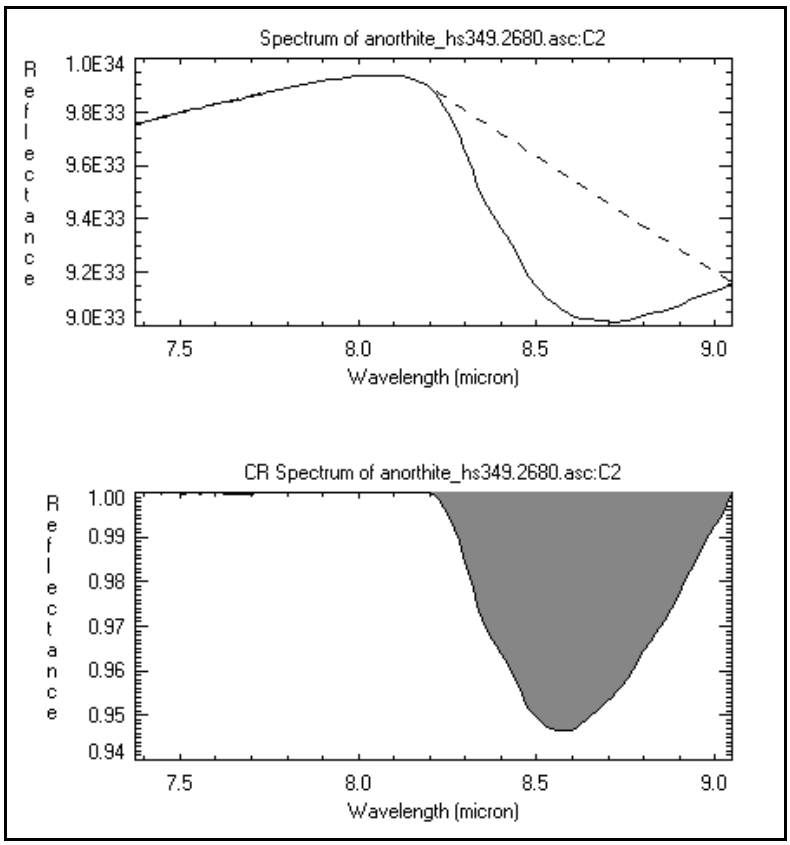
Spectrum of anorthite_hs349.2680.asc:C2
Reflectance
1.0E34
9.8E33
9.6E33
9.4E33
9.2E33
9.0E33
7.5
8.0
8.5
9.0
Wavelength (micron)
CR Spectrum of anorthite_hs349.2680.asc:C2
Reflectance
1.00
0.99
0.98
0.97
0.96
0.95
0.94
7.5
8.0
8.5
9.0
Wavelength (micron)

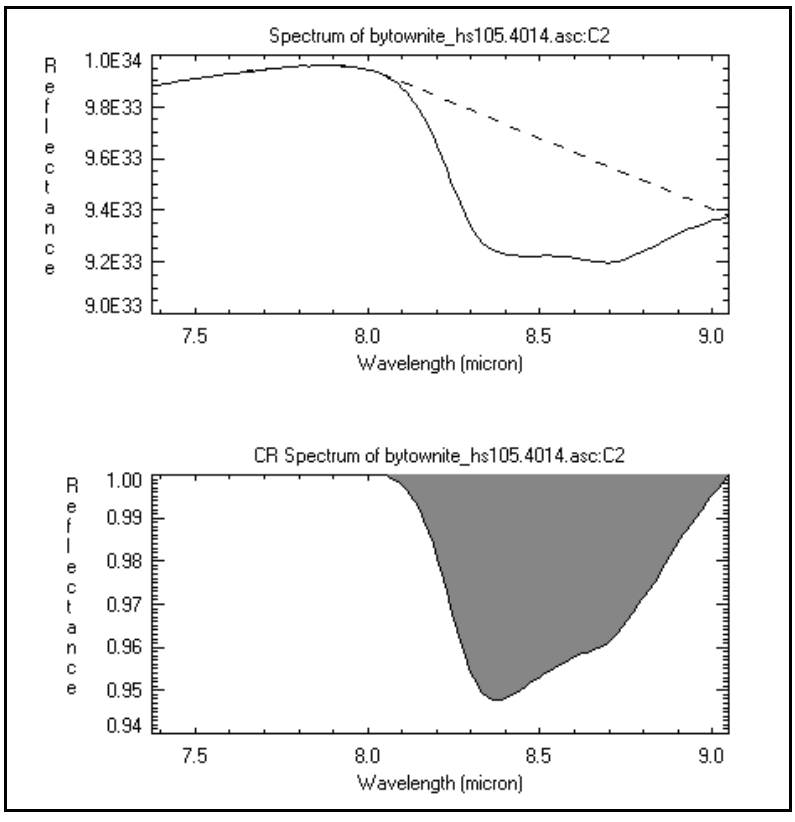
Spectrum of bytownite_hs105.4014.asc:C2
Reflectance
1.0E34
9.8E33
9.6E33
9.4E33
9.2E33
9.0E33
7.5
8.0
8.5
9.0
Wavelength (micron)
CR Spectrum of bytownite_hs105.4014.asc:C2
Reflectance
1.00
0.99
0.98
0.97
0.96
0.95
0.94
7.5
8.0
8.5
9.0
Wavelength (micron)

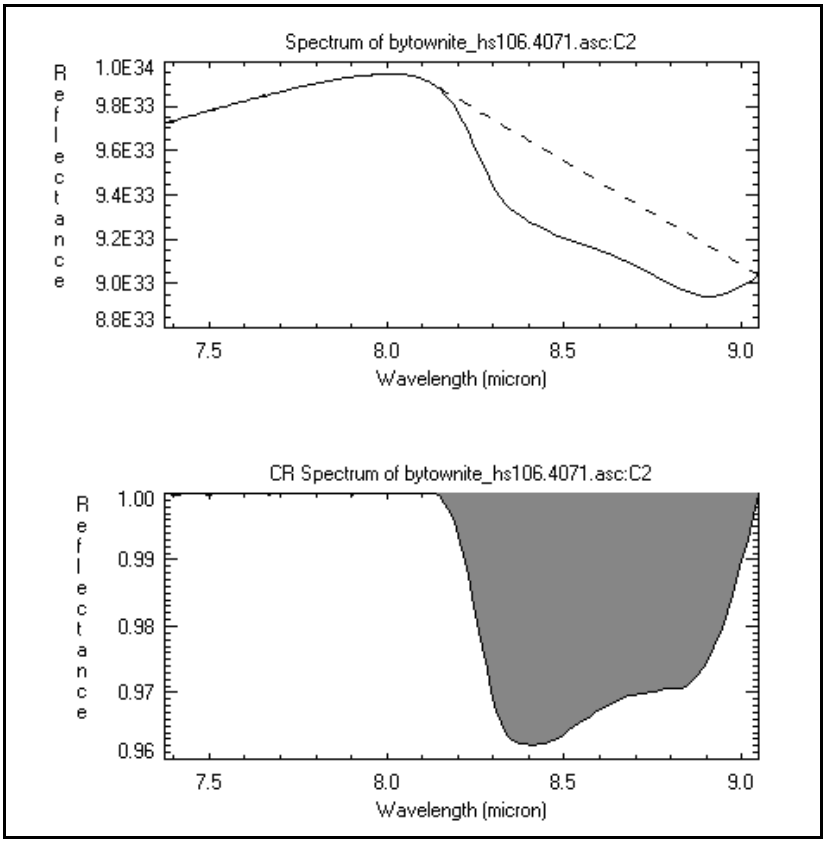
Spectrum of bytownite_hs106.4071.asc:C2
Reflectance
1.0E34
9.8E33
9.6E33
9.4E33
9.2E33
9.0E33
8.8E33
7.5
8.0
8.5
9.0
Wavelength (micron)
CR Spectrum of bytownite_hs106.4071.asc:C2
Reflectance
1.00
0.99
0.98
0.97
0.96
7.5
8.0
8.5
9.0
Wavelength (micron)

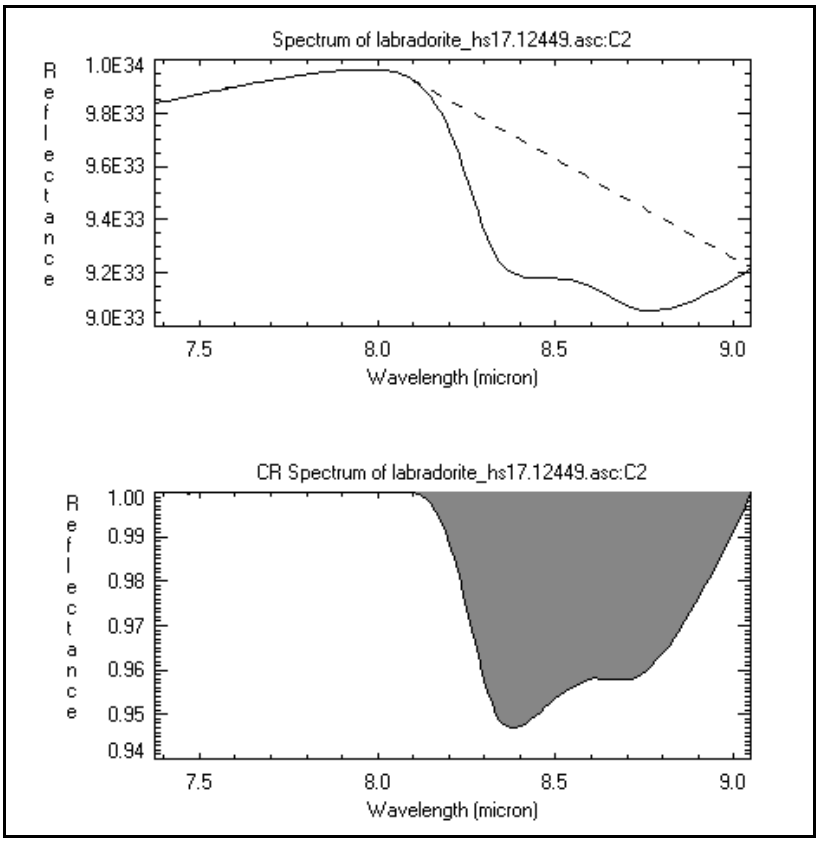
Spectrum of labradorite_hs17.12449.asc:C2
Reflectance
1.0E34
9.8E33
9.6E33
9.4E33
9.2E33
9.0E33
7.5
8.0
8.5
9.0
Wavelength (micron)
CR Spectrum of labradorite_hs17.12449.asc:C2
Reflectance
1.00
0.99
0.98
0.97
0.96
0.95
0.94
7.5
8.0
8.5
9.0
Wavelength (micron)

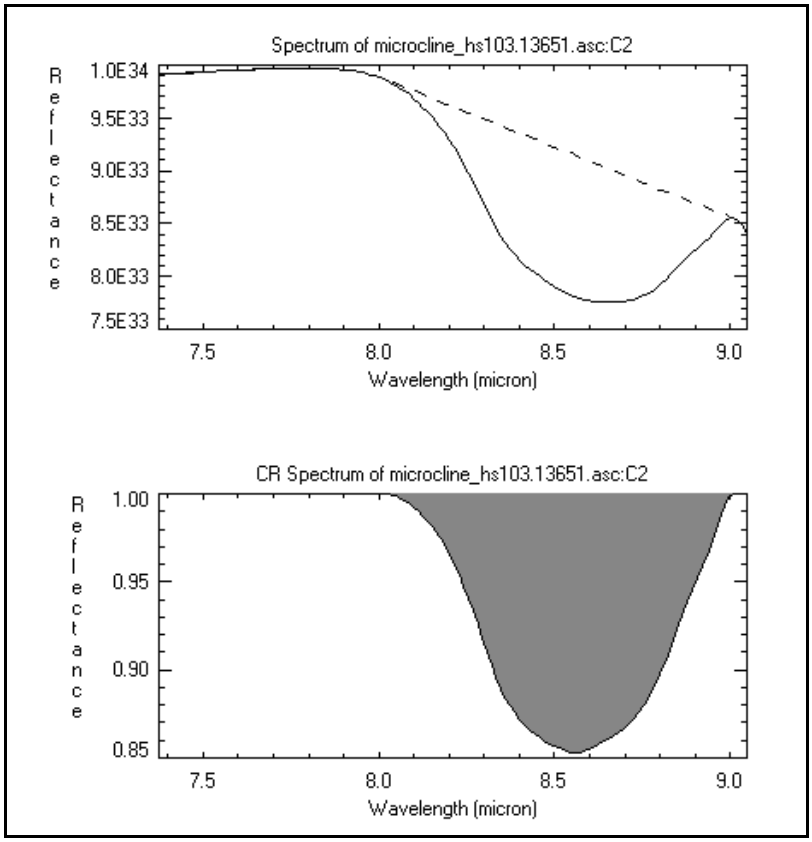
Spectrum of microcline_hs103.13651.asc:C2
Reflectance
1.0E34
9.5E33
9.0E33
8.5E33
8.0E33
7.5E33
7.5
8.0
8.5
9.0
Wavelength (micron)
CR Spectrum of microcline_hs103.13651.asc:C2
Reflectance
1.00
0.95
0.90
0.85
7.5
8.0
8.5
9.0
Wavelength (micron)

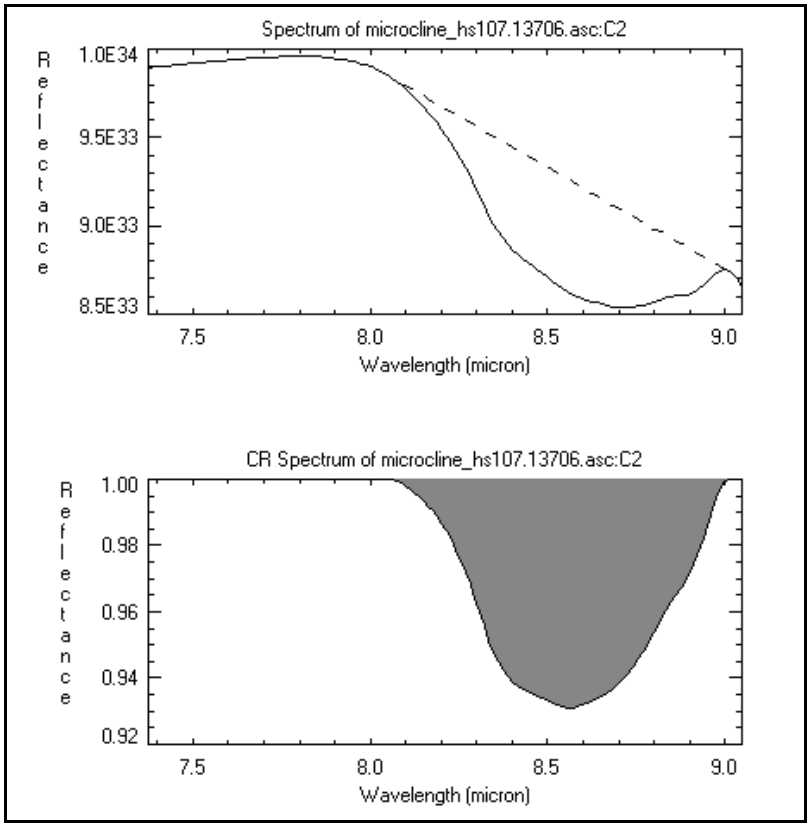
Spectrum of microcline_hs107.13706.asc:C2
Reflectance
1.0E34
9.5E33
9.0E33
8.5E33
7.5
8.0
8.5
9.0
Wavelength (micron)
CR Spectrum of microcline_hs107.13706.asc:C2
Reflectance
1.00
0.98
0.96
0.94
0.92
7.5
8.0
8.5
9.0
Wavelength (micron)

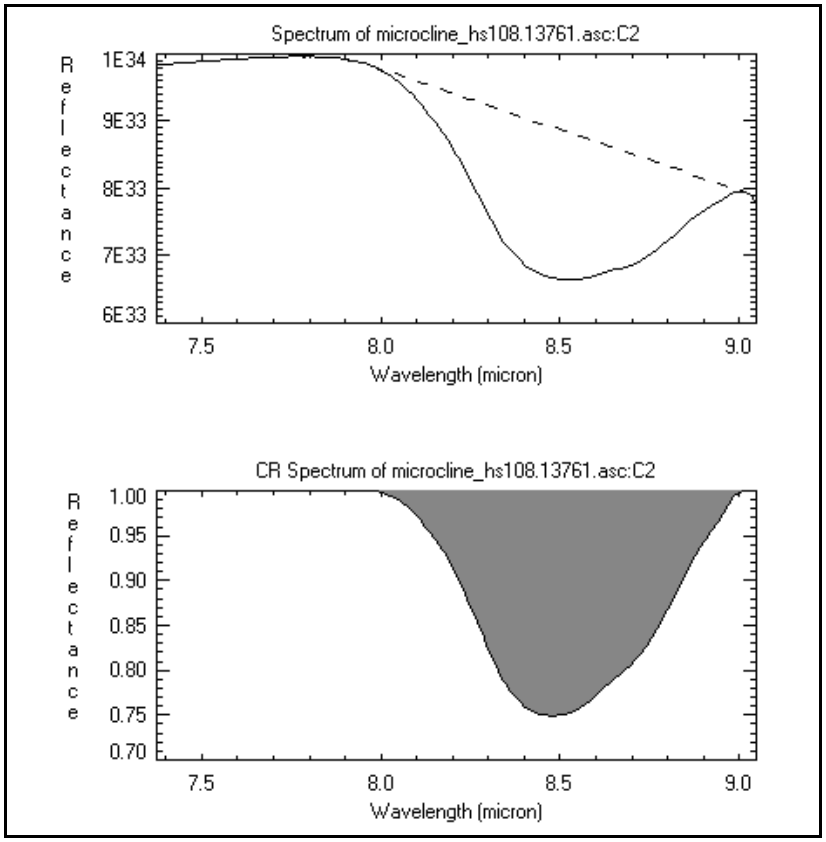
Spectrum of microcline_hs108.13761.asc:C2
Reflectance
1E34
9E33
8E33
7E33
6E33
7.5
8.0
8.5
9.0
Wavelength (micron)
CR Spectrum of microcline_hs108.13761.asc:C2
Reflectance
1.00
0.95
0.90
0.85
0.80
0.75
0.70
7.5
8.0
8.5
9.0
Wavelength (micron)

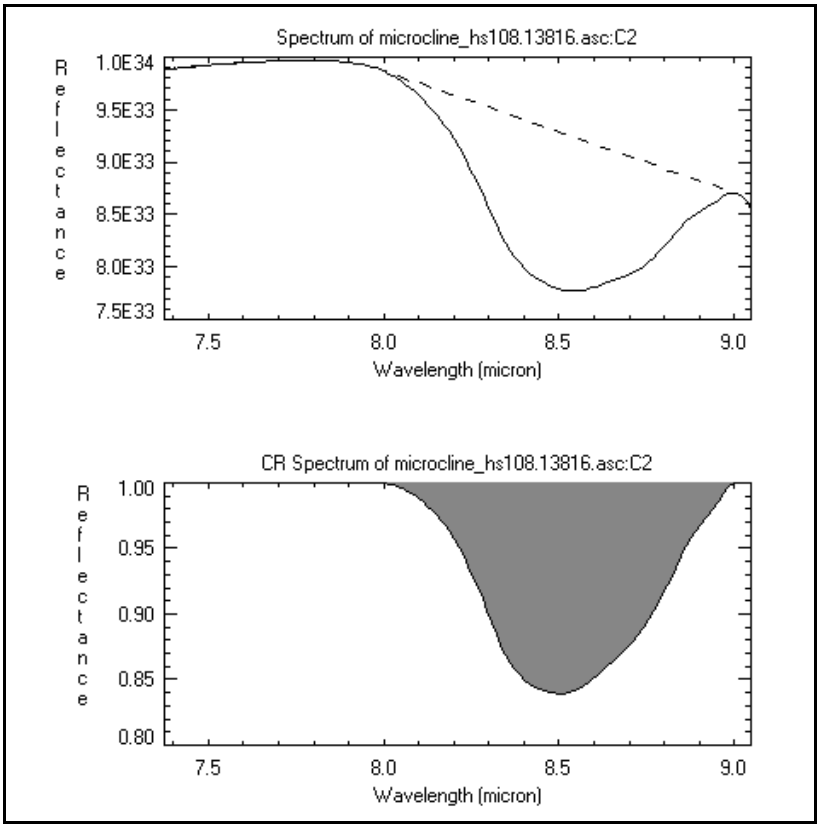
Spectrum of microcline_hs108.13816.asc:C2
Reflectance
1.0E34
9.5E33
9.0E33
8.5E33
8.0E33
7.5E33
7.5
8.0
8.5
9.0
Wavelength (micron)
CR Spectrum of microcline_hs108.13816.asc:C2
Reflectance
1.00
0.95
0.90
0.85
0.80
7.5
8.0
8.5
9.0
Wavelength (micron)

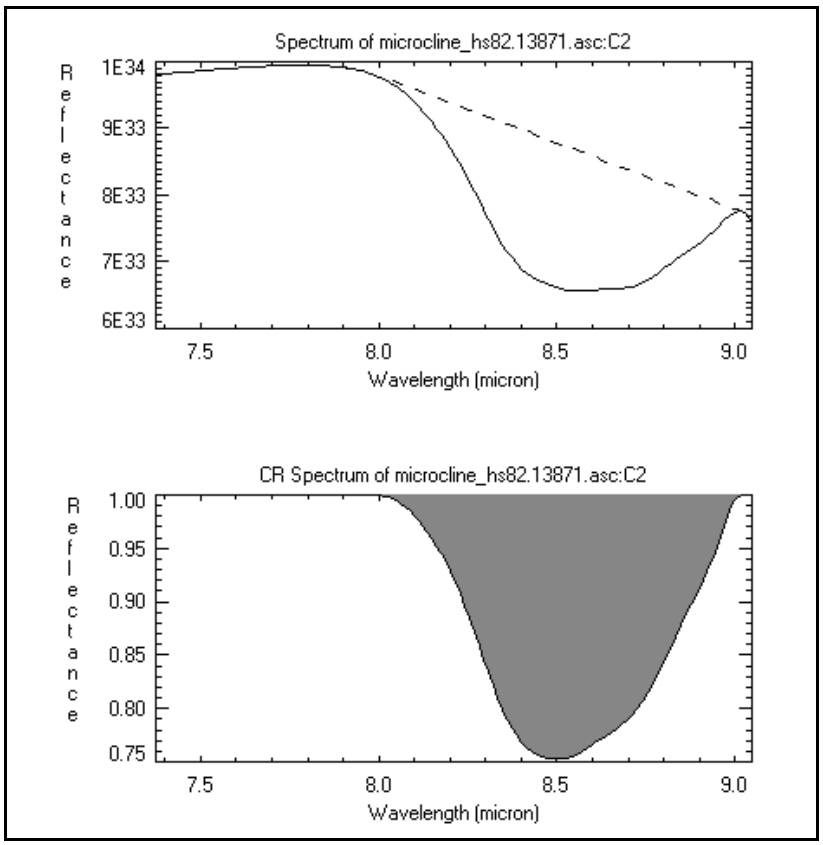
Spectrum of microcline_hs82.13871.asc:C2
Reflectance
1E34
9E33
8E33
7E33
6E33
7.5
8.0
8.5
9.0
Wavelength (micron)
CR Spectrum of microcline_hs82.13871.asc:C2
Reflectance
1.00
0.95
0.90
0.85
0.80
0.75
7.5
8.0
8.5
9.0
Wavelength (micron)

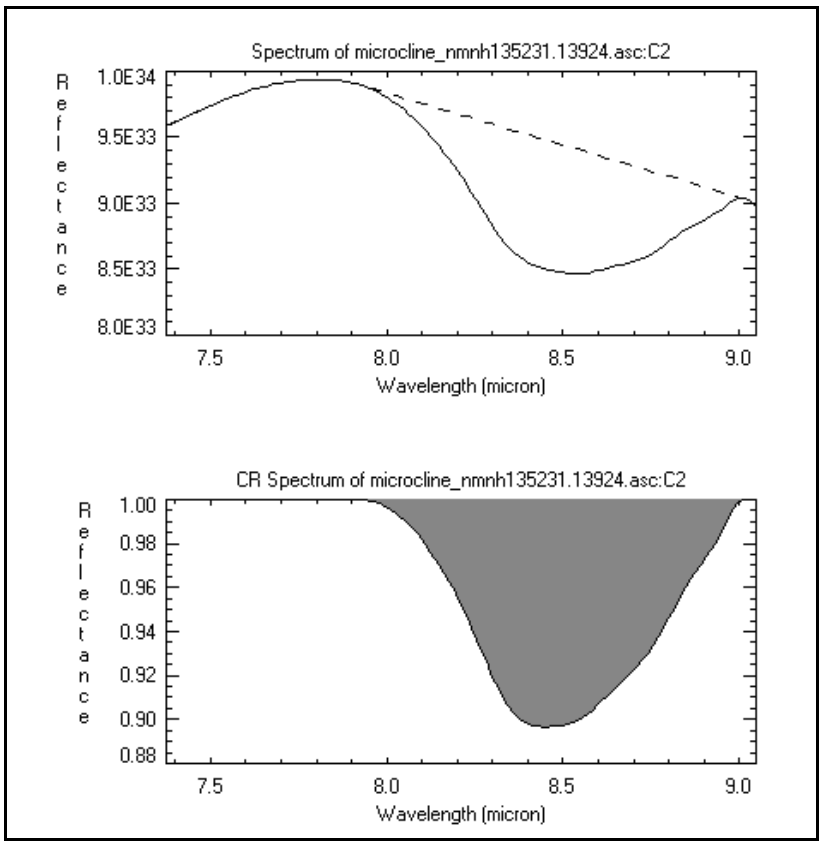
Spectrum of microcline_nmnh135231.13924.asc:C2
Reflectance
1.0E34
9.5E33
9.0E33
8.5E33
8.0E33
7.5
8.0
8.5
9.0
Wavelength (micron)
CR Spectrum of microcline_nmnh135231.13924.asc:C2
Reflectance
1.00
0.98
0.96
0.94
0.92
0.90
0.88
7.5
8.0
8.5
9.0
Wavelength (micron)

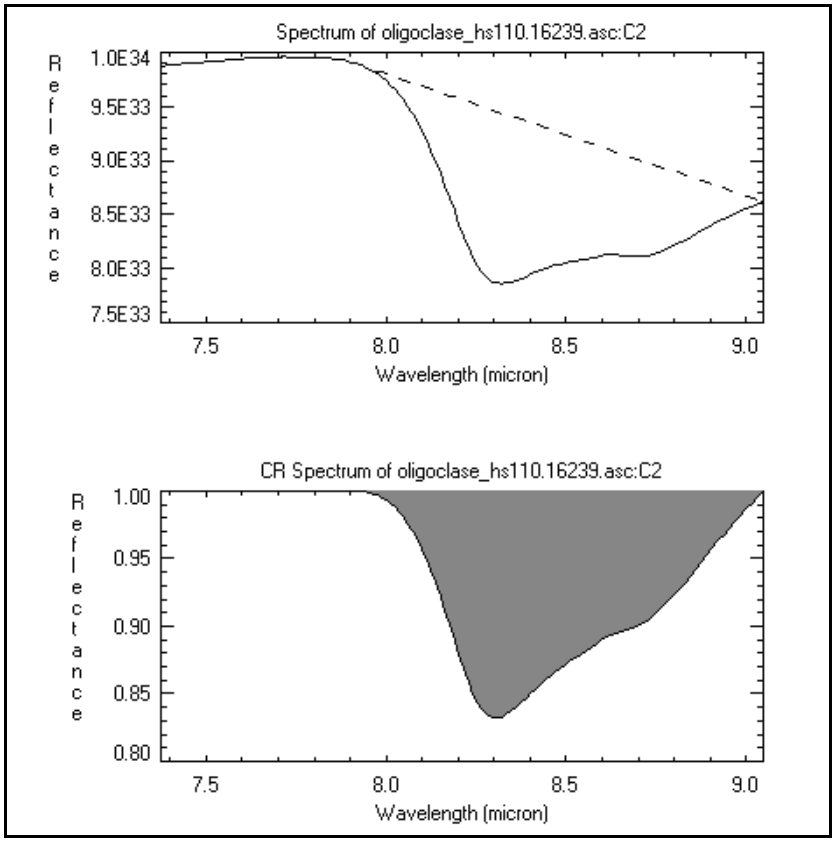
Spectrum of oligoclase_hs110.16239.asc:C2
Reflectance
1.0E34
9.5E33
9.0E33
8.5E33
8.0E33
7.5E33
7.5
8.0
8.5
9.0
Wavelength (micron)
CR Spectrum of oligoclase_hs110.16239.asc:C2
Reflectance
1.00
0.95
0.90
0.85
0.80
7.5
8.0
8.5
9.0
Wavelength (micron)

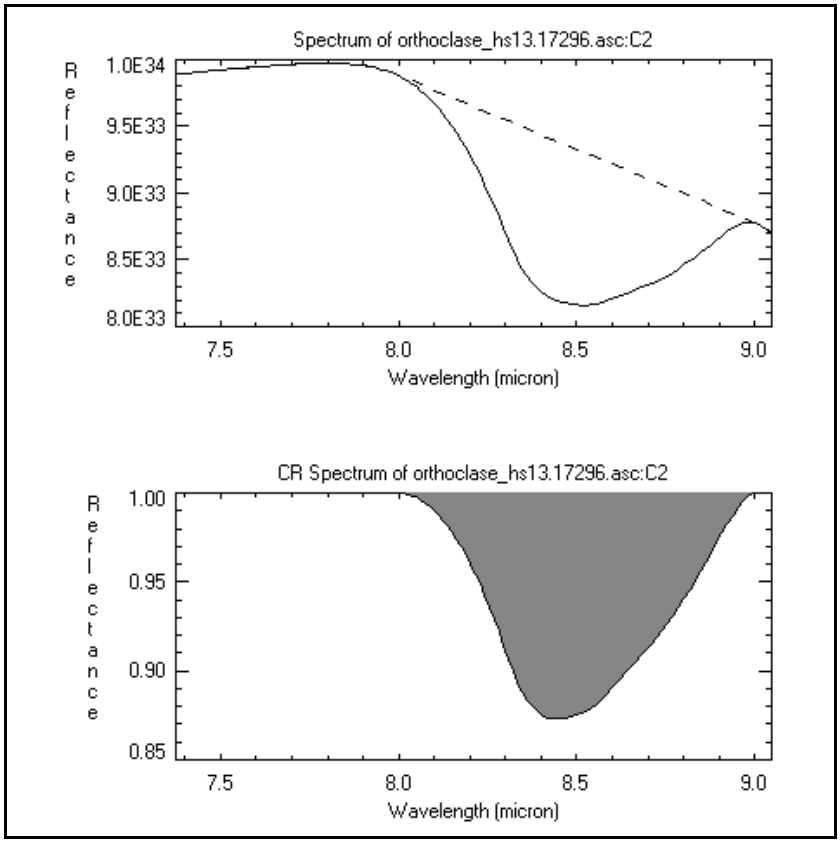
Spectrum of orthoclase_hs13.17296.asc:C2
Reflectance
1.0E34
9.5E33
9.0E33
8.5E33
8.0E33
7.5
8.0
8.5
9.0
Wavelength (micron)
CR Spectrum of orthoclase_hs13.17296.asc:C2
Reflectance
1.00
0.95
0.90
0.85
7.5
8.0
8.5
9.0
Wavelength (micron)

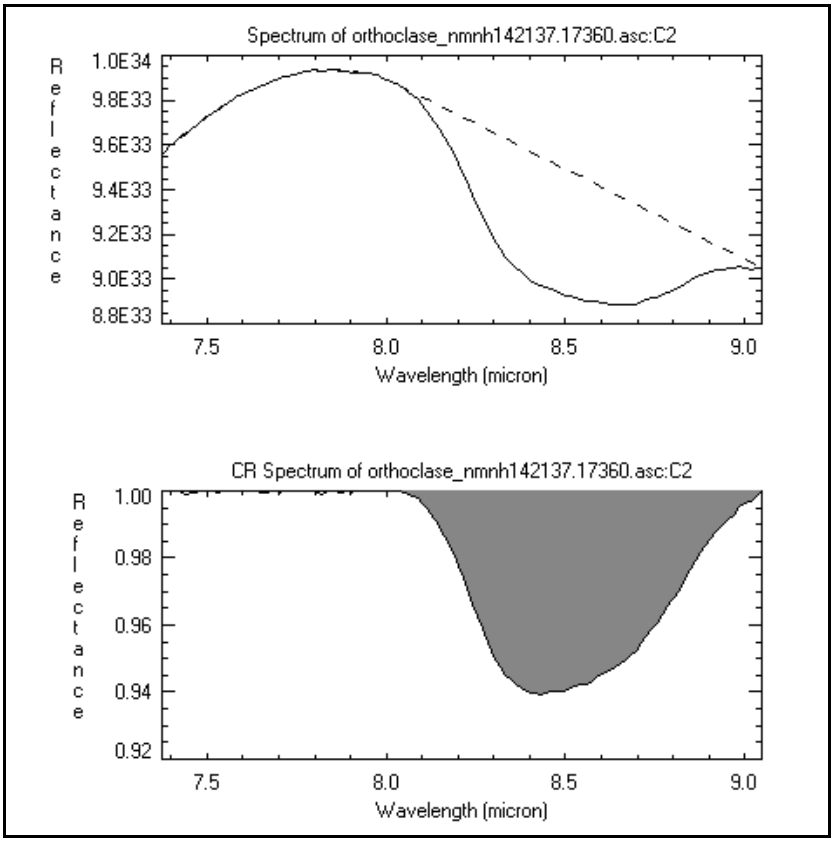
Spectrum of orthoclase_nmnh142137.17360.asc:C2
Reflectance
1.0E34
9.8E33
9.6E33
9.4E33
9.2E33
9.0E33
8.8E33
7.5
8.0
8.5
9.0
Wavelength (micron)
CR Spectrum of orthoclase_nmnh142137.17360.asc:C2
Reflectance
1.00
0.98
0.96
0.94
0.92
7.5
8.0
8.5
9.0
Wavelength (micron)

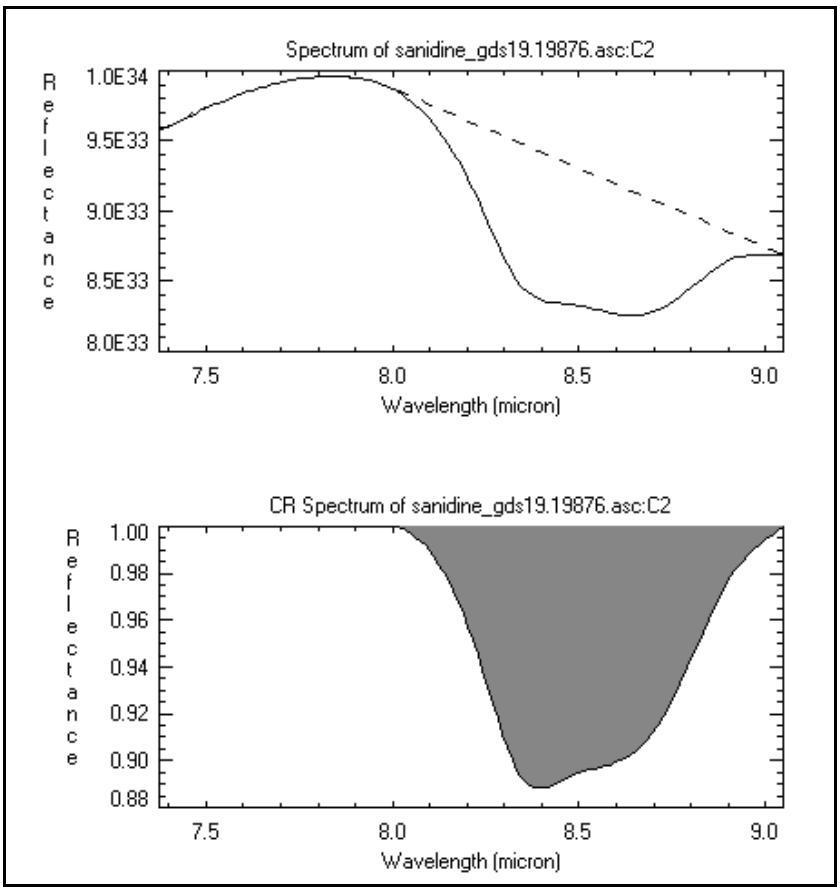
Spectrum of sanidine_gds19.19876.asc:C2
Reflectance
1.0E34
9.5E33
9.0E33
8.5E33
8.0E33
7.5
8.0
8.5
9.0
Wavelength (micron)
CR Spectrum of sanidine_gds19.19876.asc:C2
Reflectance
1.00
0.98
0.96
0.94
0.92
0.90
0.88
7.5
8.0
8.5
9.0
Wavelength (micron)

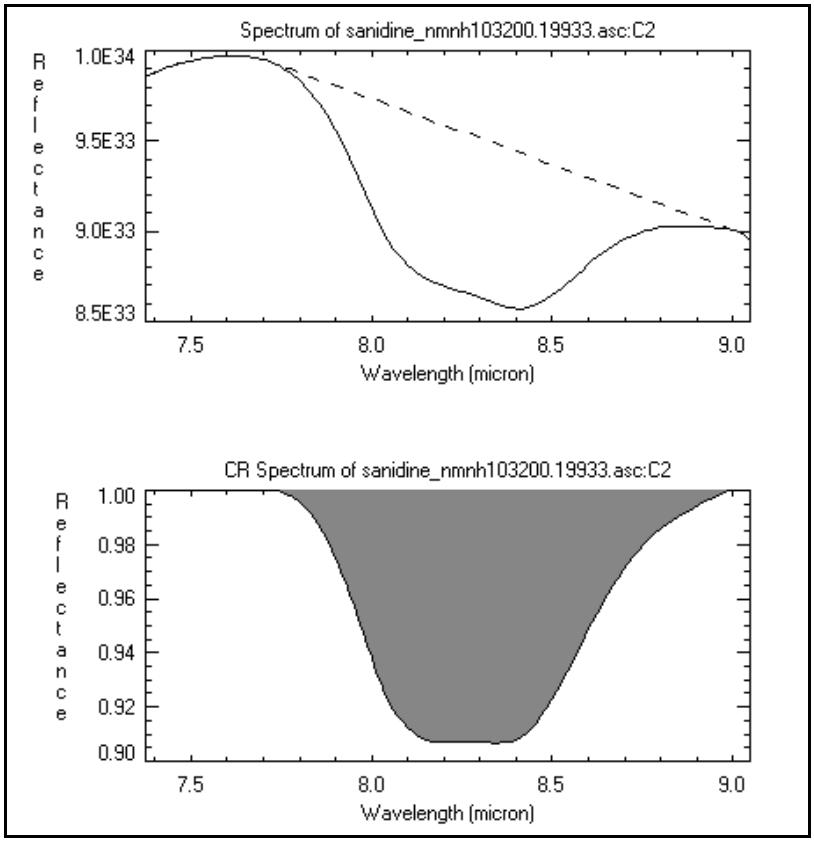
Spectrum of sanidine_nmnh103200.19933.asc:C2
Reflectance
1.0E34
9.5E33
9.0E33
8.5E33
7.5
8.0
8.5
9.0
Wavelength (micron)
CR Spectrum of sanidine_nmnh103200.19933.asc:C2
Reflectance
1.00
0.98
0.96
0.94
0.92
0.90
7.5
8.0
8.5
9.0
Wavelength (micron)